SOLID STATE ABSTRACTS

an abstract journal devoted to the theory, production and use of solid state materials and devices

VOLUME 1 NUMBER 3

PHYSICS

METALLURGY

ELECTRONICS

METALS

SEMICONDUCTORS

SUPERCONDUCTORS

PHOSPHORS

MAGNETICS

DIELECTRICS

SOLID STATE ABSTRACTS

VOLUME 1, NUMBER 3

December, 1960

Abstracts 6620–6927

TABLE OF CONTENTS

Abstracts of the Solid State Literature

Metallurgy and Chemistry of Solids

Alloys . . . 107
Crystal Structure . . . 108
Crystal Growth . . . 111
Crystal Surfaces and Preparation . . . 112
Environmental Effects . . . 113

Solid State Physics

Crystal Physics . . . 114
Electrical Properties
General . . . 114
Dielectric Properties . . . 114
Carrier Properties . . . 115
Conductivity . . . 116
Superconductivity . . . 117
Galvanomagnetic Properties . . . 118
Other Electrical Properties . . . 118
Magnetic Properties . . . 119
Optical Properties . . . 121
Thermal Properties . . . 122
Mechanical Properties . . . 122

Solid State Devices

Semiconductor Diodes – General . . . 123
Point Contact Diodes . . . 123
Junction Diodes . . . 123
Transistors – General . . . 127
Junction Transistors . . . 129
Surface Barrier Transistors . . . 130
Analog Transistors . . . 130
Functional Units . . . 130
Other Conductive Devices . . . 130
Photodevices . . . 131
Thermistors . . . 132
Magnetic Devices . . . 132
Dielectric Devices . . . 135
Superconductive Devices . . . 135
Piezoelectric Devices . . . 136

Solid State Device Measurements . . . 136

Basic Solid State Device Circuits

General . . . 137
Amplifiers . . . 137
Oscillators . . . 139
Switching Circuits . . . 140
Signal Converters . . . 140
Other . . . 140

Applications of Solid State Devices

General (Medical, Aeronautical, etc.) . . . 141
Radio . . . 142
Television . . . 142
Telephony . . . 143
Microwaves . . . 143
Other Communication Type Applications . . . 143
Computers, etc. . . . 144
Power . . . 147
Control . . . 148
Instrumentation . . . 148

New Products . . . 150

Subject Index . . . 152

Author Index . . . 159

Editor: GEOFFREY KNIGHT, JR.

Assistant Editor: MYRON A. COHEN

PUBLISHED MONTHLY BY

Cambridge Communications Corporation, 238 Main Street, Cambridge 42, Massachusetts, Tel. Klrkland 7-1997

Subscription Rate: $25.00 per year. Single Copies and Back Issues: $2.50. Advertising Rates on Request.

Cambridge Communications Corp. is not prepared to furnish copies of the articles abstracted. However, there are many libraries throughout the country which maintain photocopying services.

SYMBOLS USED IN THE ABSTRACTS

L: Letter to the Editor. A: Only an abstract is given in the reference. R: Only a review is given in the reference. E: Erratum.

The reference numbers in the indices are the abstract numbers, not the page numbers.

Copyright 1960 by Cambridge Communications Corp. Printed in the U.S.A. by the University Press, Inc.

Second-class mail privileges applied for at Boston, Massachusetts.

ABSTRACTS OF THE SOLID STATE LITERATURE

METALLURGY AND CHEMISTRY OF SOLIDS

ALLOYS

6620 CALCULATION OF THE HEAT OF SOLUTION OF COPPER IN GERMANIUM FROM DIFFUSION MEASUREMENTS by M. Tanenbaum (Bell Labs.); J. Chem. Phys., Vol. 32, pp. 1126-1127, Apr. 1960

The diffusion of substitutional copper in germanium below 700°C is explained by a dissociation mechanism proposed by Frank and Turnbull. It is shown that this mechanism provides a means for estimating the heat of solution of copper in germanium by measuring the activation energies for substitutional copper diffusion and for self-diffusion in germanium.

6621 SOLUBILITY ENHANCEMENT IN GaP-Si ALLOYS by E. E. Loebner and I. J. Hegyi (RCA Labs.); J. Electrochem. Soc., Vol. 107, p. 198C (A), Aug. 1960

The growth of single mixed crystals of a sphalerite structure which contain GaP and Si in amounts varying from 0 to 100 mole percent was discussed. The crystals could be grown provided they were also heavily zinc doped. Zinc appears to function as a differential charge compensator. It seems necessary since the amphoteric silicon self-compensates in GaP only incompletely while the solubility of P in Si somewhat exceeds that of the partly compensating Ga. Evidence for complex compound formation was discussed.

6622 METASTABLE SOLID SOLUTIONS IN THE GALLIUM ANTIMONIDE-GERMANIUM PSEUDO-BINARY SYSTEM by P. Duwez, R. H. Willens, and W. Klement, Jr. (Cal. Inst. Tech.); J. Appl. Phys., Vol. 31, p. 1500 (L), Aug. 1960

An x-ray diffraction study of a series of alloys prepared from stoichiometric gallium antimonide and zone refined germanium is discussed. A single phase with the disordered zincblende structure was found in all the alloys and no significant or systematic deviation from Vegard's law was found. These results are consistent with the covalent bonding of the zincblende structure of gallium antimonide and the diamond structure of germanium.

6623 PREPARATION AND PROPERTIES OF AlSb-GaSb SOLID SOLUTION ALLOYS by J. F. Miller, H. L. Goering and R. C. Himes (Battelle); J. Electrochem. Soc., Vol. 107, pp. 527-533, June 1960

Studies made of ingots of the quasi-binary GaSb-AlSb alloy prepared by progressive casting and zone casting at various rates of crystallization are discussed. With the possible exception of a narrow composition range between 10 and 30 mole percent AlSb, which was not investigated, solid solution prevails in the system. Vegard's law was found to be at least roughly applicable; with lattice constants for the alloys ranging between values of 6.0963A for pure GaSb and 6.1361A for pure AlSb. Optical energy gaps determined for alloy specimens increased regularly with cell size from a value of 0.68 ev for GaSb to a value of 1.74ev for AlSb. Values of electrical resistivity and hole mobility for the relatively impure alloy specimens were also intermediate between those for the compounds in a like state of purity. Liquidus data for the system are also presented.

6624 SOLID SOLUTION IN $A^{II}B^{VI}$ TELLURIDES by J. C. Woolley and B. Ray (U. Nottingham); J. Phys. Chem. Solids, Vol. 13, pp. 151-153, May 1960

Alloys prepared in the three systems CdTe-HgTe, CdTe-ZnTe, and HgTe-ZnTe are discussed. Solid solution occurs at all compositions in each system and the variation of lattice parameter with composition has been determined in each case. The form of the solidus curve in the HgTe-ZnTe system has been obtained by x-ray methods.

Solid Solutions of $Pb_2Ta_2O_6$ with Nb, Ba, and Sr - See 6679

Lead Titanate Solid Solution Ceramics Containing Nb or Ta - See 6678

Vapor Pressure of III-V Compounds - See 6626

6625 THE STANDARD FREE ENERGY OF FORMATION OF SILICON CARBIDE by J. Smiltens (Air Force Cambridge Res. Center); J. Phys. Chem., Vol. 64, pp. 368-369, Mar. 1960

The standard free energy ΔF^0 of formation of silicon carbide (solid) from graphite and liquid silicon is reported to be -11.3kcal at 1855°C. This corresponds to a room-temperature heat of formation (from solid silicon) of -18.2kcal. The increment ΔF^0 is determined from the relationship $P_{ij}' / P_{ij}'' = \exp[(j-i)\Delta F^0/RT]$, where P_{ij}' is the partial pressure of the species C_iSi_j in the vapor above silicon carbide + graphite and P_{ij}'' is the partial pressure of the same species in the vapor above silicon carbide + liquid silicon. For numerical determination of ΔF^0 the mass spectroscope data of Drowart, De Maria, and Inghram [see abstract 3468] and of Drowart and De Maria have been used.

6626 THERMODYNAMIC DATA AND VAPOR PRESSURES OF THE MOST IMPORTANT III-V COMPOUNDS [in German] by T. Renner (Siemens); Solid-State Electronics, Vol. 1, pp. 39-45, Mar. 1960

Tables of the enthalpy of formation, free energy of formation, and entropy for the most important III-V compounds, prepared from data collected from various sources, are presented. Vapor pressure data for As over InAs, As over GaAs, and P over InP are also given.

CRYSTAL STRUCTURE
(including imperfections and impurities)

6627 LATTICE VACANCIES IN NEUTRON IRRADIATED GERMANIUM by M. C. Wittels (Oak Ridge National Lab.); Bull. Am. Phys. Soc., Ser. II, Vol. 5, p. 375 (A), June 15, 1960

Defects produced in 40 ohm-cm p-type Ge single crystals as a result of exposure at approximately 85°C to fast neutron fluxes of up to 4×10^{20} neutrons/cm^2 are discussed. X-ray diffraction and hydrostatic weighing measurements indicate that at these dosages and temperatures sufficient defects are trapped so that density reductions as high as 5×10^{-3} develop. In addition, a pronounced variation in the densities as determined by unit cell measurements and those obtained from hydrostatic weighing reveals that the predominant defects stable at room temperature are vacancies.

6628 OPTICAL DETECTION OF VACANCIES CREATED BY HIGH-ENERGY RADIATION IN SODIUM CHLORIDE by H. W. Etzel and J. G. Allard (U.S. Naval Res. Labs.); Phys. Rev., Vol. 116, pp. 885-887, Nov. 15, 1959

The detection of vacancies created by high-energy radiation in sodium chloride single crystals by comparing the F-center coloration produced by ultraviolet light after irradiation and optical bleaching to that obtained before irradiation is reported. The behavior of the F-center coloration as a function of time or irradiation under ultraviolet light after exposure of the crystals to high-energy radiation is different for synthetic and natural sodium chloride. This difference is attributed to the presence of hydroxyl ions in the synthetic crystals which are inadvertently introduced into the lattice during the growth of the crystals in air. The results obtained are the same whether 40-kvp x-rays, 2-Mev electrons, or $Co^{60}\gamma$ rays are used to create the F centers.

6629 ELECTRICAL AND OPTICAL INVESTIGATION OF ABSORPTION CENTERS IN RUTILE SINGLE CRYSTALS by K. G. Srivastava (MIT); Phys. Rev., Vol. 119, pp. 516-520, July 15, 1960

A study of the production of absorption centers in single crystals of rutile by thermal quenching or optical irradiation at the edge of the characteristic absorption region (4200 A) is discussed. The centers cause relaxation spectra in the low-frequency range and are observed only when the a-c field is applied parallel to the optic axis. The temperature dependence of the main dispersion peak indicates an activation energy of 0.18 ev. Introduction of silver or copper by thermal diffusion did not produce low-frequency absorption maxima.

6630 OBSERVATION OF DISLOCATIONS IN SILICON BY THE ANOMALOUS TRANSMISSION OF X-RAYS [in French] by A. Authier (Faculté des Sciences, Paris); J. Phys. Radium, Vol. 21, pp. 655-659, Aug.-Sept. 1960

A photographic study of dislocations in nearly perfect Si single crystals which utilized the anomalous transmission of X-rays is discussed. A crystallographic study of the observed dislocations is given. The dislocations are observed as black and white fine double streaks.

6631 DISLOCATIONS IN SILICON CARBIDE BY S. Amelinckx and G. Strumane (Geologisch Inst., Ghent) and W. W. Webb (Union Carbide); J. Appl. Phys., Vol. 31, pp. 1359-1370, Aug. 1960

A study of the dislocation structure of type 6H hexagonal silicon carbide by etching combined with optical microscopy and by x-ray diffraction microscopy is discussed. The validity of the conventional etching technique for identification of the sites of the intersection of dislocations with (0001) surfaces has been established. However, high densities of dislocations lying in (0001) planes and hence heretofore undetected by etching techniques were often observed by diffraction microscopy. Dislocations with $[11\bar{2}0]$ vectors have now been found with evidence for slip both on basal planes and on a "puckered" pyramidal plane. Pileups formed by slip and dislocation walls formed by climb were also observed. Silicon carbide shows many of the characteristics of more conventional plastically deformable materials.

6632 DISLOCATION CLIMB IN PLASTICALLY DEFORMED InSb by J. J. Duga and R. E. Maringer (Batelle Mem. Inst.); Bull. Am. Phys. Soc., Ser. II, Vol. 5, p. 375 (A), June 15, 1960

Metallographic observations on plastically deformed single crystal InSb were discussed. It was found that dislocation climb occurs only under certain specialized conditions. For example, specimens deformed by uniaxial compression exhibited no tendency toward polygonization either during deformation at 300°C or during subsequent annealing at temperatures around 500°C. On the other hand, some degree of polygonization is observed during plastic bending, although subsequent annealing at 500°C results only in motion in the glide plane. From analysis of electrical properties in deformed specimens, the nature of the deformation-induced defects has been established. The relation between these defects and etch-pit patterns was discussed. These data are consistent with the three criteria for polygonization: (1) the dislocations must have the edge-orientation, (2) there must be present a sufficiently high density of vacancies, and (3) the strain field associated with the dislocations must be large enough to promote migration of vacancies toward the

dislocation core. It is suggested that the presence of Lomer-Cottrell barriers is not the only factor limiting polygonization when intersecting slip systems are activated.

6633 DISLOCATIONS IN GRAPHITE SINGLE CRYSTALS by R. Bacon and R. Sprague (Natl. Carbon); J. Appl. Phys., Vol. 31, pp. 1831-1832 (A), Oct. 1960

Electron microscopic observations of dislocations in natural graphite single crystals were discussed. The crystals were cleaved in such a way as to produce very small amounts of mechanical deformation. Well-defined dislocation lines were observed lying in the (0001) basal planes. A jerky motion of dislocations along a (0001) slip plane frequently was observed as the result of stresses induced by beam heating. Dislocation motion was seen to be impeded by interaction with other dislocations or with a foreign particle. Very regular dislocation networks were observed with spacings varying from about 4000 to 15,000 A. Frequent splitting of dislocations into partials separated by a distance of 1000 to 2000 A indicates a very low stacking fault energy for graphite.

6634 SEMICONDUCTOR TYPE AND LOCAL DOPING DETERMINED THROUGH THE USE OF INFRARED RADIATION by N. J. Harrick (Philips Lab.); Solid-State Electronics, Vol. 1, pp. 234-244, July 1960

Infrared techniques for determining semiconductor type and local doping are discussed and examples of measurements as applied to inhomogeneities in germanium are given. The techniques outlined are generally most sensitive in doping ranges where standard techniques are insensitive. Semiconductor type is determined from the direction of drift of an added carrier packet, thus the minority carrier is determined. Firstly, a measure of the infrared absorption of the sample gives the equilibrium carrier density from which the doping density can be computed; secondly, a determination of the maximum extraction level can be used to calculate the local sample doping level; thirdly, since any inhomogeneities in a sample act like junctions, local injection-extraction effects occur if a current is passed through the sample, and from observation of these effects the nature of the local doping can be deduced. The first approach for determining sample doping and homogeneity is more useful for heavily doped samples while the latter two are more useful for near-intrinsic samples. The advantages of these techniques are that sample preparation is particularly simple, sample parameters are not masked by the surface, and information about the nature of the sample deep within the bulk can be obtained without dissecting the sample.

Dissociation Mechanism for the Diffusion of Substitutional Cu in Ge - See 6620

6635 CALCULATION OF CONCENTRATION PROFILES AND SURFACE CONCENTRATION FROM SHEET-CONDUCTANCE MEASUREMENTS OF DIFFUSED LAYERS by M. F. Lamorte (Westinghouse); Solid-State Electronics, Vol. 1, pp. 164-171, July 1960

The ohmic contact method for obtaining the sheet-conductance profile of a diffused layer is described and equations from which the concentration profile may be obtained from sheet-conductance measurements are presented. For three impurity-concentration distributions, equations for surface concentration which necessitate the measurements of sheet conductance, junction penetration, and the background conductivity are presented. If the sheet conductance is much greater than the product of the background conductivity and the junction penetration, only the sheet conductance need be measured in order to determine the surface concentration.

Measurement of Diffusion Constants by Ion Drift - See 6753

6636 INFLUENCE OF SURFACE PHENOMENA ON THE RATE OF IMPURITY DIFFUSION IN SILICON [in French] by G. Feuillade and S. Marette (Centre National d'Etudes des Telecommun.); J. Chim Phys., Vol. 57, pp. 228-247, Mar. 1960

The thermodynamic conditions for the formation of a superficial impurity source of the impurities B, P, Ga, and Al during the prediffusion of silicon are examined in detail. Several suitable methods for demonstrating its aggregate properties (geometry, electric and elastic properties) are considered.

6637 DIFFUSION OF BORON INTO SILICON by A. D. Kurtz and R. Yee (Minneapolis-Honeywell Regulator); J. Appl. Phys., Vol. 31, pp. 303-305, Feb. 1960

An investigation of the diffusion of boron into silicon over a temperature range of 1050°C to 1350°C by means of an open-tube vapor-solid diffusion technique at atmospheric pressure is discussed. A p-n junction method of measuring the diffused layer was used to determine the diffusion constant. Lower diffusivities and a somewhat lower activation energy, ($\Delta H = 81$ kcal) were obtained than those reported previously. The difference is attributed to variation of diffusivity with surface concentration and is discussed on the basis of field-aided diffusion theory.

6638 DIFFUSION OF Li IN Si AT HIGH T AND THE ISOTOPE EFFECT by E. M. Pell (GE Res. Labs.); Phys. Rev., Vol. 119, pp. 1014-1021, Aug. 1, 1960

A reinvestigation of the diffusion rate of Li in Si at high temperatures using an outdiffusion technique is discussed. The resulting D for Li^7 is $(2.21 \pm 0.07) \times 10^{-6} cm^2/sec$ at $(800 \pm 5)^\circ C$ and $2.4 \times 10^{-5} cm^2/sec$ at $(1350 \pm 5)^\circ C$. If these results are combined with ion drift results, the diffusion constant can be described by $D = (2.5 \pm 0.2) \times 10^{-3} \exp[-(0.655 \pm 0.01)e/kT]$. The isotopic effect upon the diffusion has been investigated using Li^6 and Li^7. At 800°C, the value for D_{Li^6}/D_{Li^7} is $1.07_5 \pm 0.02$, in accordance with the expected inverse dependence on the square root of the mass. The ionic charge of the Li and the atomic mechanism for Li diffusion is discussed in the light of these and other results.

6639 DIFFUSION OF CADMIUM IN PURE AND CADMIUM DOPED AgBr by J. E. Hanlon (U. Chicago); J. Chem. Phys., Vol. 32, pp. 1492-1500, May 1960

Measurement of the diffusion of Cd in pure AgBr and dilute $AgBr-CdBr_2$ solid solutions by a tracer technique using carrier-free Cd^{109} is discussed. The data support Lidiard's theory for the diffusion of divalent impurities in monovalent ionic crystals From the diffusion rates in the pure material, it is possible to calculate the association energy ΔG of $Cd^{++}Ag$ vacancy complexes. The value of ΔG extrapolated to $0^\circ K$ is estimated to be 0.21 ± 0.04 ev. The observed concentration dependence of Cd diffusion in doped samples can be explained only if the mobility of complexes is assumed to have a strong concentration dependence.

6640 RADIOTRACER STUDIES OF THE INCORPORATION OF IODINE INTO VAPOR-GROWN Ge by W. E. Baker and D. M. J. Compton (IBM); IBM J. Res. and Dev., Vol. 4, pp. 269-274, July 1960

Measurements of the incorporation of iodine into single crystals of Ge grown by the disproportionation of GeI_2 made using I^{131} as a radioactive tracer are discussed. The results show that I is not likely to be a hindrance to device use of this material since the amount incorporated is moderately low and does not appear to be correlated with electrical effects. It does not diffuse appreciably and no excess is found at an all-deposited p-n junction. The concentration of I appears to decrease with increasing temperature, to be independent of growth rate on a (111) orientation of the seed, but to vary by a factor of up to 50 from one orientation to another. It is deduced that the I is incorporated by a mechanism intimately connected with the crystal growth.

6641 INCORPORATION OF As INTO VAPOR-GROWN Ge by W. E. Baker and D. M. J. Compton (IBM); IBM J. Res. and Dev., Vol. 4, pp. 275-279, July 1960

A study of the incorporation of arsenic into single crystal germanium grown by the disproportionation of GeI_2 carried out using As^{76} as a radioactive tracer and Hall effect measurements is described. The deposition was carried out in a sealed tube using as source material a single crystal of Ge doped to 2.5×10^{19} atoms/cm^3 with As. It was found that all the As incorporated into the vapor-grown Ge was electrically active, at least for material grown on a (211) Ge seed. The concentration of As in the deposited Ge was lower than that in the source, and appeared to depend on the crystallographic orientation of the growing face.

Introduction of Impurities During Epitaxial Vapor Growth of Ge - See also 6651

6642 DETERMINATION OF SMALL STOICHIOMETRIC DEVIATION IN OXIDE MONOCRYSTALS by H. B. Sachse (Keystone Carbon); Analyt. Chem. Vol. 32, pp. 529-530, Apr. 1960

Determination of the oxygen surplus in monocrystals of manganese (II) oxide, cobalt (II) oxide, and nickel (II) oxide by a modified Bunsen method is discussed. The method permits the measurement of deviations down to 1 milliatom of oxygen per molecule of monoxide with an accuracy on the order of ±10 percent or better. The detection of still smaller stoichiometric deviations is possible, however, with increased error.

Non-Stoichiometry of $PbNb_2O_6$-Type Compounds - See 6676

6643 EFFECT OF THERMAL HISTORY ON THE DISLOCATION SUBSTRUCTURE NEAR THE SURFACES OF A LITHIUM FLUORIDE CRYSTAL by J. M. Schultz and J. Washburn (U. Calif.); J. Appl. Phys., Vol. 31, pp. 1800-1801, Oct. 1960

A series of x-ray and etchpit experiments performed to determine some of the effects of temperature on the perfection of surface layers in LiF are discussed. It was found that the perfection of a cleaved surface is substantially increased at temperatures near the melting point, that rearrangement and annihilation of dislocations takes place at much lower temperatures, and that rapid cooling promotes the formation of shallow dislocation loops.

6644 ORIGIN OF THE "FIRST-ORDER STRUCTURE" OF CP4-ETCHED Ge SURFACES by G. Bonfiglioli, A. Ferro, and A. Mojoni (Inst. Elettrotec. Nazionale, Torino); J. Appl. Phys., Vol. 31, pp. 684-686, Apr. 1960

The origin of the so-called "1st-order structure" observed on micrographs of CP4-etched germanium surfaces is discussed. It is shown that while etching proceeds the ending points of some dislocations are reached or some of them become passivated. In both cases, the etch pits no longer grow and their traces given rise to the 1st-order structure.

6645 X-RAY STUDIES OF AMORPHOUS CARBON FROM SILICON CARBIDE by E. R. Czerlinsky and F. Euler (U. S. Air Force Cambridge Res. Ctr.); Proc. Conf. Silicon Carbide, Pergamon Press, 1960, pp. 155-161

The high-temperature reaction of SiC single crystals with chlorine is discussed. The reaction leaves a carbon residue that maintains the size and shape of the original crystals. The structure of this residue does not show any relationship to that of SiC, and X-ray analysis proves that the residual carbon is amorphous. A few spotty lines in the diffraction pattern are attributed to unreacted SiC, the presence of which is corroborated by spectroscopic analysis.

6646 NEW SYNTHETIC GARNETS by S. Geller, C. E. Miller, and R. G. Treuting (Bell Labs.); Acta Cryst., Vol. 13, pp. 179-186, Mar. 1960

Twenty-three new synthetic garnets with formulae $M^{2+}R_2^{3+}Mn_2Ge_3O_{12}$, $M^{2+}R_2^{3+}M_2^{2+}Ge_3O_{12}$, $R_3^{3+}M_2^{2+}GaGe_2O_{12}$ and $Ca_3M^{4+}M^{2+}Ge_3O_{12}$ are reported. In these, M^{4+} is a tetravalent metal ion of Zr, Sn or Ti; R^{3+} is an yttrium or gadolinium ion; M^{2+} is one of a variety of divalent metal ions, not all of which go into all the types. It is probable that R^{3+} could be almost any trivalent rare earth ion. Three other garnets, $Mn_3NbZnFeGe_2O_{12}$; one of probable formula $Ca_3ZrFeGe_{2.8}O_{12}$, in which Fe has an average valence of 2.9, and $Y_2Mn_2FeGe_{2.8}O_{12}$, in which Fe has an average valence of 2.8 are also reported. The latter two are defect structures. The distribution of ions in the new garnets is discussed.

Crystal Structure of Ferroelectric Lead Metatantalate - See 6679

Crystal Structure of $PbNb_2O_6$ Compounds - See 6676

CRYSTAL GROWTH

6647 LIQUID-SOLID INTERFACE SHAPE OBSERVED IN SILICON CRYSTALS GROWN BY THE CZOCHRALSKI METHOD by W. D. Edwards (Def. Res. Board, Ottawa); Can. J. Phys., Vol. 38, pp. 439-443, Mar. 1960

A study made of the macroscopic structure of the liquid-solid interface which exists during growth of silicon crystals by the Czochralski method is discussed. In two crystals the interface was seen to contain a (111) facet. The development of such facets is discussed with reference to current crystal growth theories.

6648 CROSS-SECTIONAL RESISTIVITY VARIATIONS IN GERMANIUM SINGLE CRYSTALS by J. A. M. Dikhoff (N. V. Philips); Solid-State Electronics, Vol. 1, pp. 202-210, July 1960

An investigation of the dependence of the cross-sectional resistivity variations which occur frequently in germanium single crystals upon crystal orientation and upon the shape of the solid-liquid interface during crystal growth is discussed. A direct relationship exists between the crystal orientation, the shape of the growth interface, and the occurrence of persistent cross-sectional resistivity variations. The origin of these variations is closely related to the presence of a flat facet which coincides with a {111} plane on the otherwise curved growth interface. The segregation constants of several impurities appear to be different for the flat part and for the curved part of the growth interface, thus causing cross-sectional variations of the impurity concentration. Methods for preventing these variations are discussed.

6649 EPITAXIAL GROWTH OF GERMANIUM AND SILICON SINGLE CRYSTAL FILMS FROM THE VAPOR PHASE by G. Russell (Motorola); 1960 Electron Dev. Mtg.

Single crystal films of germanium and silicon grown on suitably prepared substrates by the hydrogen reduction of the respective tetrachlorides were discussed. The problem of obtaining single crystal growth was shown to be a major function of substrate surface preparation, temperature of substrate, and of the tetrachlorides. Measurement techniques and factors affecting conductivity type, resistivity, and film thickness were discussed. Current limiters and other devices made utilizing the single crystal films were discussed and results presented.

Growth of Ge by Disproportionation of GeI_2 - See 6640, 6641

6650 VAPOR DEPOSITION OF SILICON by N. P. Sandler, S. A. Prussin, and A. Stevenson (Pacific Semicon.); 1960 Electron Dev. Mtg.

Single crystal silicon deposits on a heated silicon substrate obtained from the reduction of trichlorosilane by hydrogen were discussed. Commercially available trichlorosilane can be used without further purification to get n-type silicon deposits as high as 40 ohm cm. Surface preparation to get good epitaxy involves chemical etching followed by hydrogen reduction of native oxide immediately prior to introduction of $HSiCl_3$ into the hydrogen flow. Good silicon deposition rates thus far encountered are optimal at 40 - 80 microns per hour, but can be increased by minimizing gas turbulence. Techniques of the process, including consideration of controlled doping were discussed.

6651 EPITAXIAL VAPOR GROWTH OF Ge SINGLE CRYSTALS IN A CLOSED-CYCLE PROCESS by J. C. Marinace (IBM); IBM J. Res. and Dev., Vol. 4, pp. 248-255, July 1960

The Ge-I_2 disproportionation reaction in a sealed tube is discussed. The reaction will deposit Ge epitaxially upon Ge seeds at a typical rate of 10 μ/hr at a typical temperature of 400°C. Dislocations are of the same kind and approximate concentrations as observed in ordinary melt-grown Ge. Chemical purity is comparable to the best melt-grown Ge. The fraction of donors transferred from the source material to the deposited material is nearly unity over a wide range of concentrations, while the fraction of acceptors transferred is considerably less than unity. However, either n-type or p-type Ge can be deposited, and by using two sources within the same tube alternating layers can be obtained.

6652 HIGH VACUUM EVAPORATOR FOR RADIOACTIVE MATERIALS by H. Widmer and J. Kirsch (Columbia U.); Rev. Sci. Instr., Vol. 31, pp. 791-793, July 1960

An evaporator for the deposition of radioactive germanium on germanium substrates is described. The apparatus, which was built for use in an experimental study of self diffusion, has the following features: (a) The apparatus can be outgassed at 300-400°C above its operating temperature. (b) After bakeout the crucible can be charged in vacuum. (c) The germanium substrate can be rotated during evaporation to deposit uniform films on all faces and can be heated before and during evaporation at temperatures up to the melting point to encourage epitaxy. (d) The evaporator can be easily dismantled and cleaned.

6653 THE VACUUM EVAPORATION OF SINGLE CRYSTAL THIN FILMS OF SILICON by A. P. Hale and B. D. James (Fairchild); 1960 Electron Dev. Mtg.

Single crystal silicon films evaporated onto a silicon substrate in a vacuum of about 10^{-6} mm Hg were discussed. Source and substrate temperatures and the rate of deposition are critical parameters in attaining epitaxy with the substrate. Where the source silicon is heated in a crucible, the crucible material is important. Physical imperfections, doping, and electrical characteristics of the films and devices made from them were discussed.

6654 PRODUCTION AND PROPERTIES OF THIN LAYERS OF INDIUM ANTIMONIDE by G. Bate and K. N. R. Taylor (U. British Columbia); J. Appl. Phys., Vol. 31, pp. 991-994, June 1960

A new method of producing thin layers of indium antimonide is described. This consists of suddenly squashing a drop of molten indium antimonide between two optical flats and allowing it to cool. Large area, self-supporting specimens of 10-μ thickness have been prepared in this way and their properties examined. Although these layers are polycrystalline, their electrical and

optical properties are in good agreement with the single-crystal materials from which they were obtained.

6655 THIN FERROMAGNETIC FILMS by A. C. Moore (RRE); IRE Trans., Vol. CP-7, pp. 3-14, Mar. 1960

An account of the work at the Royal Radar Establishment on the preparation and properties of thin ferromagnetic films is presented. The work provides the prospect of a computer store in which a million bits would occupy less than an eighteen-inch cube, and which would possess a switching time faster than twenty μsec. The store would be cheap and easily constructed.

6656 PROPAGATION MECHANISM OF GERMANIUM DENDRITES by D. R. Hamilton and R. G. Seidensticker (Westinghouse Res. Labs.); J. Appl. Phys., Vol. 31, pp. 1165-1168, July 1960

The role of the twin planes in the rapid dendritic propagation of germanium crystals is examined on the basis of corner nucleation. A model is proposed and it is shown that at least two twin planes must be present for continued easy propagation in <211> directions, in good agreement with experimental observations. The absence of the dendrite with only one twin is explained.

6657 GALLIUM ARSENIDE DENDRITES by R. H. Moss and H. C. Nicholson (Westinghouse Elec.); J. Electrochem. Soc., Vol. 107, p. 198C (A), Aug. 1960

Sustained and controlled dendritic growth in gallium arsenide was discussed. Dendrites have been reproducibly pulled from the melt using a syringe-type furnace in which the composition of the melt is determined by means of a controlled vapor pressure. Under both macroscopic and microscopic examination, the gallium arsenide dendrites have the salient characteristics of dendrites as reported by Longini, Bennet, et al.

Growth of GaP-Si Single Crystals - See 6621

6658 PRODUCTION OF ALKALI HALIDE SINGLE CRYSTAL FILAMENTS AND POINTS by J. McNulty, M. Silver, and R. S. Witte (U. Notre Dame); Rev. Sci. Instr., Vol. 31, pp. 904-905, Aug. 1960

The controlled dissolution of a parallelepiped-shaped alkali halide single crystal in an aqueous solution to form a single crystal filament or point is described. The crystal, with its lower face painted with Glyptal to prevent dissolution, is lowered into a bath of distilled water. By varying the depth of immersion and the time of dissolution, a 3mm x 3mm x 1 cm parallelepiped can be shaped to a filament about 10μ in diameter and 1 cm in length. With further etching points having tip radius of 1 to 5μ can be obtained. Photomicrographs of a single crystal of KCl in various stages of the process are shown. With modification the technique can also be used with other materials.

CRYSTAL SURFACES AND PREPARATION (including contacts)

6659 ADSORPTION AND BONDING PROPERTIES OF CLEAVAGE SURFACES OF BISMUTH TELLURIDE by D. Haneman (Brown U.); Phys. Rev., Vol. 119, pp. 567-569, July 15, 1960

Electron diffraction measurements of the adsorption of oxygen, ozone, nitrogen, carbon monoxide, and water vapor at room temperature on clean (0001) surfaces of bismuth telluride are discussed. It was found that there was no measurable adsorption of the gasses and that water vapor had a very low sticking coefficient of the order of 10^{-5}. The results are discussed in terms of the chemical bonding of bismuth telluride. It is concluded that the atoms on cleavage faces are in a saturated-bond condition.

6660 SURFACE DAMAGE IN III-V COMPOUNDS: {111} SURFACES by E. P. Warekois, M. C. Lavine, and H. C. Gatos (Lincoln Lab.); J. Electrochem. Soc., Vol. 107, p. 199C (A), Aug. 1960

The observation that for a given cold-working treatment the depth of damage in the GaAs and InSb {111} surfaces terminating with group V atoms is greater than the corresponding depth of damage in the {111} surfaces terminating with group III atoms was discussed. In the absence of cold-work, the group V surfaces exhibit a somewhat greater degree of perfection than the group III surfaces. The experimental methods included etching and x-ray diffraction techniques.

6661 ELECTROLYTIC ETCHING OF SEMICONDUCTORS by D. R. Turner (Bell Labs.); Surface Chem. Metals and Semicon., (J. Wiley and Sons), 1960, pp. 285-310

The electrolytic etching of germanium, silicon, and some intermetallic compounds is reviewed. Anodic dissolution reactions at semiconductor electrodes require electron holes. If the hole concentration in the semiconductor is relatively low, as in low resistivity n-type germanium or silicon, the available holes in the surface region are used up at low current densities and the etch rate is slow. The anodic current under these conditions can be increased by providing additional holes at the surface. Holes produced as a result of illuminating the semiconductor give uniform electrolytic etching on n-type semiconductors. Germanium is electrolytically etched in several electrolytes while silicon can only be dissolved anodically in fluoride solutions. A thick film of amorphous silicon forms on silicon anodes in acid fluoride solutions below a critical current density.

6662 EFFECT OF Cu PRECIPITATION ON DISLOCATION ETCH PITS IN Ge by H. Savage (Air Force Cambridge Res. Ctr.); J. Appl. Phys., Vol. 31, pp. 1472-1473, Aug. 1960

Quenching and annealing heat treatments performed on n-type germanium single crystals containing measured quantities of copper introduced by diffusion are discussed. The effect on etch pit sizes and resistivity was recorded. It is shown that

saturation with copper does not inhibit completely the formation of etch pits, although they are altered in size.

6663 ETCH PITS IN PYROLYTIC GRAPHITE by A. Tarpinian and G. E. Gazza (Watertown Arsenal Labs.); J. Appl. Phys., Vol. 31, pp. 1657-1658, Sept. 1960

The observation of etch pits in pyrolytic graphite after ion-bombardment etching is described and their similarity to dislocation etch pits is discussed. Evidence of etch-pit multiplication in the form of slip-line segments and low-angle tilt boundaries is presented.

6664 ETCH PITS ON DENDRITIC GERMANIUM. A CLARIFICATION by P. J. Holmes (Assoc. Elec. Ind.); Phys. Rev., Vol. 119, pp. 131-132, July 1, 1960

The discrepancy between the reports of Billig and Holmes and Bennett and Longini [see abstract 4547] on the orientations of etch pits on the main faces of germanium dendrites is discussed. It is shown that this discrepancy arose because the orientation of equilateral pits on {111} surfaces depends on the etchant used. A check on the earlier work confirms that there is in fact no contradiction: ferricyanide and WAg etches produce pits which point upwards on "perfect" faces grown in a "G direction," while superoxol and similar etchants give pits pointing downwards

Effect of Chemical Etches on Fast Ge Surface States - See 6670

Effect of Etching on Surface Structure - See 6644

6665 SILICON ETCHING IN THE HNO_3-RICH PHASE OF THE HF-HNO_3 SYSTEM by D. L. Klein and D. J. D'Stefan (Bell Labs.); J. Electrochem. Soc., Vol. 107, p. 198C (A), Aug. 1960

A study of the etching rate of single crystal silicon in HF-HNO_3 as a function of the ratio of the concentrated acids, stirring rate, and temperature was discussed. Over the ranges studied, the rates were proportional to these functions. For n, p,- and junction samples, ranging in resistivity from 0.05 to 78 ohm-cm, no difference in etch rate was observed. Etch rate appears to be dependent on diffusion of the fluoride ion to the silicon surface for HF-HNO_3 <1.

6666 ELECTROLESS PLATED CONTACTS TO SILICON CARBIDE by R. L. Raybold (NBS); Rev. Sci. Instr., Vol. 31, pp. 781-782, July 1960

A technique for applying electroless nickel contacts to SiC and BP crystals is described. The crystals are (1) electrolytically etched in HF, (2) rinsed well (in distilled water), (3) sensitized by dipping in a bath of about 10% stannous chloride, (4) rinsed well, (5) dipped in a palladium chloride solution (~0.2%), (6) rinsed again, (7) dried in a blast of dry nitrogen, and (8) immersed, preferably for 1 minute, in a plating solution consisting of 30 g/liter $NiCl_2 \cdot 6H_2O$, 10 g/liter $NaH_2PO_2 \cdot H_2O$, and 50 g/liter $NaC_2H_3O_3$ at a temperature of 90°C. The contact area can be defined by means of a mask or the entire crystal can be plated and the unwanted material removed mechanically. For crystals which resist plating by this process, steps (6) and (7) are eliminated. The contacts have a lower resistance on SiC than other low temperature contacts and can be soldered with indium and DIVCO 335 or a similar flux immediately after plating. Heat treatment does not improve the characteristics of contacts on smooth SiC surfaces.

6667 TRANSPARENT INDIUM CONTACTS TO CdS by Y. T. Sihvonen and D. R. Boyd (GM); Rev. Sci. Instr., Vol. 31, pp. 992-994, Sept. 1960

Diffusion and sputtering techniques for applying low resistance, highly transparent, antireflecting contacts to CdS are described. The diffusion process entails heating CdS for several minutes in the presence of indium vapor. The resulting crystal surface resistance has been adjusted to range as low as 12 ohms/square without any observable crystal discoloration. In the sputtering process an 82-18% indium-tin alloy is placed onto the crystal surface using oxygen as the sputtering atmosphere. The resulting film is Sn-doped In_2O_3, measuring 100-150 ohms/square, and showing 80-100% transmittance from 4600 to 20,000 A.

6668 HARD GALLIUM ALLOYS FOR USE AS LOW CONTACT RESISTANCE ELECTRODES AND FOR BONDING THERMOCOUPLES INTO SAMPLES by G. G. Harman (NBS); Rev. Sci. Instr., Vol. 31, pp. 717-720, July 1960

Hard alloys of gallium, prepared at room temperature in a manner similar to that of dental amalgams are discussed. They may be packed into cavities in semiconductors or in some cases applied to a flat surface and allowed to harden under pressure. The maximum operating temperatures range from 250° to about 900°C for various alloys. The electrical characteristics, when used on ferrites and controlled valency semiconductors, are similar to those of the frequently used semiliquid indium-mercury and indium-gallium electrodes.

ENVIRONMENTAL EFFECTS
(Heat Treatment and Radiation)

6669 HEAT TREATMENT OF GALLIUM ARSENIDE by J. T. Edmond (SERL); J. Appl. Phys., Vol. 31, pp. 1428-1430, Aug. 1960

The conversion of n-type GaAs to p-type or less strongly n-type as a result of heat treatment is discussed. The heat treatment was carried out in small quartz tubes of two grades of purity. The magnitude of the changes was much less in high-purity quartz. The effect in ordinary quartz was shown to be due in part to copper contamination, the copper originating in the quartz. The changes could be reduced by annealing.

Radiation-Created Vacancies in NaCl - See 6628

Stability of Neutron Bombardment Damage in Ge - See 6672

Lattice Vacancies in Neutron Irradiated Ge - See 6627

SOLID STATE PHYSICS

CRYSTAL PHYSICS (including Energy Band Structure)

6670 EFFECT OF CHEMICAL ETCHES ON THE FAST GERMANIUM SURFACE STATES by Y. Margoninski (Hebrew U.); J. Chem. Phys., Vol. 32, pp. 1791-1795, June 1960

Simultaneous measurements of surface recombination velocity and added trapped charge density in the fast states as a function of surface potential carried out on the same n-type filament which was subjected to three different etches (CP-4A, concentrated HNO_3 and HF) are discussed. Most measurements were performed at various temperatures. It was found that (a) the reproducibility of surface state parameters after successive treatments with CP-4A was excellent; (b) the influence of the different etches was surprisingly small, with one exception: the average capture probability c_p for holes was found to undergo a more than three-fold increase after treatment with HF; (c) the energy of the recombination center did not always decrease with increasing temperature, contrary to all previously reported measurements.

6671 FUNDAMENTAL LATTICE DISPERSION FREQUENCIES OF NaCl AND KCl at 82°K by M. Hass (U.S. Naval Res. Lab.); Phys. Rev., Vol. 119, pp. 633-635, July 15, 1960

Infrared dispersion frequencies of NaCl and KCl at 82°K measured by infrared absorption of thin films are discussed. Values of $170 \pm 2\,cm^{-1}$ and $149 \pm 2\,cm^{-1}$, respectively were found. Good agreement seems to be obtained between these values and those predicted by the Szigeti formula or a combination of the Lundqvist and Odelevski formulas at low temperatures where anharmonic effects are small.

ELECTRICAL PROPERTIES GENERAL

6672 TRANSITORY ELECTRICAL PROPERTIES OF N-TYPE GERMANIUM AFTER A NEUTRON PULSE by H. J. Stein (Sandia); J. Appl. Phys., Vol. 31, pp. 1309-1313, Aug. 1960

An investigation of the stability of neutron bombardment damage in Sb-doped Ge is discussed. Continuous measurements of the electrical conductivity and Hall mobility following a neutron pulse were made in the temperature range from 77° to 308°K with a time resolution of 1 sec. At temperatures near 195°K an initial decrease in conductivity and mobility was followed by an additional decrease which exhibited nearly second-order kinetics. At 273°K and above an initial decrease in conductivity and mobility was followed by a recovery consistent with an activation energy of 0.68 ev. The void region model of Gossick and Crawford is employed to explain the initial decrease in mobility and a major portion of the initial decrease in conductivity.

DIELECTRIC PROPERTIES (including Ferroelectric and Piezoelectric Properties)

6673 CONTACT ELECTRIFICATION OF SEMICONDUCTORS by W. R. Harper; Brit. J. Appl. Phys., Vol. 11, pp. 324-331, Aug. 1960

Recently published experimental findings on the electrification of rutile powder by sliding down a metal chute are explained by an extension of the author's theory of the separation electrification of metals. The mechanism of the electrification of insulators must, in most cases, be quite different.

6674 MEASUREMENTS OF THE DIELECTRIC CONSTANT OF $BaTiO_3$ SINGLE CRYSTALS IN THE PARAELECTRIC REGION AT X BAND by A. Lurio and E. Stern (IBM Watson Lab.); J. Appl. Phys., Vol. 31, pp. 1805-1809, Oct. 1960

Measurement of the dielectric constant and loss tangent of single crystals of $BaTiO_3$ as a function of temperature in the frequency range of 8.2 to 12.4 kMc is discussed. The technique consists of looking for transmission resonances through the crystal whenever its thickness became $\lambda/2$ (where λ is the wavelength in the material). From the Curie-Weiss behavior of the dielectric constant in the paraelectric region, the A constant was determined to be $3.77 \times 10^{-5\,0}C^{-1}$.

6675 METHOD FOR MEASURING THE DIELECTRIC CONSTANT OF FERROELECTRIC CERAMICS AT S-BAND FREQUENCIES by C. B. Sharpe and C. G. Brockus (U. Michigan); J. Am. Ceram. Soc., Vol. 43, pp. 302-305, June 1960

A method for measuring the complex dielectric constant of ferroelectric ceramics at microwave frequencies is discussed. The method employs a disk-shaped sample in a radial-line configuration at the end of a coaxial-line structure. An equivalent circuit, established by admittance measurements, is used to relate the radial admittance at the sample face to the measured admittance on the slotted line preceding the coaxial sample holder. The nonuniform variation of electric field over the face of the sample is taken into account by means of a continued fraction expansion of $x J_1(x)/J_0(x)$ in terms of $x = k'a$, where k' is the wave number in the ferroelectric sample and a is its radius. Representative data on the variation of the complex dielectric constant with temperature at 3 kMc are given for two samples of $BaTiO_3$ fired under atmospheric pressure and 5000 lb/in^2. The frequency spectrum of hot-pressed $Cd_2Nb_2O_7$ in the range 1.8 to 4.0 kMc is also presented.

6676 NONSTOICHIOMETRY AND FERROELECTRIC PROPERTIES OF $PbNb_2O_6$-TYPE COMPOUNDS by E. C. Subbarao and G. Shirane (Westinghouse Res. Labs.); J. Chem. Phys., Vol. 32, pp. 1846-1851, June 1960

The crystal structure of $PbNb_2O_6$ consists of a framework of

NbO_6 octahedra linked through corners. The Pb^{2+} ions occupy 5 out of the 6 available interstitial sites in this framework. Single-phase compositions have been prepared by solid-state reactions to yield nonstoichiometric compounds of the form $A_{1+x}B_2O_6$ where A and B may consist of two ions of different valency and x has values between −0.08 and 0.15. In these materials, the number of unfilled interstitial sites inherently present in $PbNb_2O_6$ lattice has been varied. Lattice parameter and x-ray intensity data confirm that the additional ions introduced occupy the same sites as Pb^{2+} ions. The ferroelectric Curie temperature has been studied as a function of the composition of these dielectric solids. For compositions with $x>0$, the Curie temperature is not very sensitive to composition. As the number of unfilled interstitial sites increases ($x<0$), the Curie temperature decreases sharply.

6677 TEMPERATURE DEPENDENCE OF THE VELOCITY OF SIDEWISE 180° DOMAIN-WALL MOTION IN $BaTiO_3$ by A. Savage and R. C. Miller (Bell Labs.); J. Appl. Phys., Vol. 31, pp. 1546-1549, Sept. 1960

Measurement of the velocity of the sidewise 180° domain-wall motion in single-crystal $BaTiO_3$ over the temperature range 25° to 100°C as a function of the applied electric field is discussed. The velocity, described by $v=v_\infty \exp(-\delta/E)$, where δ is the activation field, E the applied electric field, and v_∞ the extrapolated wall velocity for $E=\infty$, increases by about four orders of magnitude over this temperature range. The temperature dependence lies primarily in δ. The magnitude of δ as a function of temperature, impurity concentration, and crystal thickness is discussed.

6678 STUDIES ON LEAD TITANATE CERAMICS CONTAINING NIOBIUM OR TANTALUM by E. C. Subbarao (Westinghouse Res. Labs.); J. Am. Ceram. Soc., Vol. 43, pp. 119-122, Mar. 1960

Dielectric, lattice constant, and thermal-expansion measurements made on solid solution ceramics in the systems $PbTiO_3$–$Pb_{0.5}NbO_3$, and $PbTiO_3$-$Pb_{0.5}TaO_3$ are discussed. The ferroelectric Curie temperature is lowered to 465°C at the solubility limit (2 to 5% Nb or Ta). Replacement of Ti^{4+} by Nb^{5+} or Ta^{5+} In these perovskite-type solid solutions is accompanied by the creation of cation vacancies. These vacancies seem to facilitate material transport and aid sintering. Thus ceramics with up to 91% of theoretical density were obtained. These compositions have peak dielectric constants of the order of 10,000 with tan δ less than 0.1 in the interval 25° to 525°C.

6679 X-RAY, DIELECTRIC, AND OPTICAL STUDY OF FERROELECTRIC LEAD METATANTALATE AND RELATED COMPOUNDS by E. C. Subbarao, G. Shirane and F. Jona (Westinghouse Res. Labs.); Acta Cryst., Vol. 13, pp. 226-231, Mar. 1960

An investigation of the properties of single crystals of ferroelectric lead metatantalate, $PbTa_2O_6$, grown using $Pb_2V_2O_7$ as a flux is discussed. An X-ray and optical study shows that $PbTa_2O_6$ has orthorhombic symmetry with $a_0 = 17.68$, $c_0 = 7.754$ A, $b_0/a_0 = 1.002$ at room temperature. The ferroelectric axis is perpendicular to the 001 direction. Dielectric constant and birefringence along the three directions have been measured as a function of temperature through the Curie point at 265°C. The crystals remain orthorhombic in the paraelectric region. A dielectric and X-ray study of the solid solution systems $Pb(Ta, Nb)_2O_6$, $(Pb, Ba)Nb_2O_6$, and $(Pb, Sr)Ta_2O_6$ shows the existence of a phase boundary in the first two systems, separating different ferroelectric modifications. Besides the ferroelectric modification, $PbTa_2O_6$ has a non-ferroelectric rhombohedral form.

6680 DIELECTRIC POLARIZATION AND PIEZOELECTRIC PROPERTIES ON CERTAIN FERROELECTRIC SOLID SOLUTIONS BASED ON SODIUM NIOBATE by V. A. Isupov and V. I. Kosyakov (Inst. for Semiconductors); Sov. Phys.-Solid State, Vol. 1, No.6, pp. 849-853, Dec. 1959

Dielectric polarization (in weak and strong fields) and piezoelectric properties of solid solutions of barium, strontium, and lead metaniobates in sodium niobate are discussed. Certain compositions in the system sodium niobate-lead metaniobate possess high values of the piezoelectric parameter d_{31}/e which is stable in a wide range of temperatures. Piezoelectric parameters of solid solutions of strontium metaniobate in sodium niobate have low values, but they are stable in a wide range of temperatures. Dielectric hysteresis loops were observed in polycrystalline samples of sodium niobate at -196°C.

CARRIER PROPERTIES

6681 PIEZOELECTRIC AND MAGNETOSTRICTIVE PROPERTIES OF GALLIUM IRON OXIDE SINGLE CRYSTAL RESONATORS by D. L. White (Bell Labs.); Bull. Am. Phys. Soc., Ser. II, Vol. 5, p. 189 (A), Mar. 21, 1960

The man-made mineral gallium iron oxide, $Ga_{2-x}Fe_xO_3$, $(0.6 \leq x \leq 1.4)$ is believed to be the only known material which is simultaneously piezoelectric and ferromagnetic. Small single crystals in the shape of rectangular prisms have been fabricated into resonators which could be driven either piezoelectrically or magnetostrictively. According to the crystal's symmetry class, C_{2v}, there are five piezoelectric constants which need not be zero. By exciting the crystals piezoelectrically in various modes of vibration between 0.5 Mc and 5 Mc, piezoelectric constants have been examined. The d_{23} constant is $1.4 \pm 0.3 \times 10^{-8}$ esu, which is about twice as large as that of quartz. The d_{12} constant is believed to be of similar magnitude. The other three constants d_{22}, d_{15} and d_{36}, are smaller and could not be measured. When the crystal is placed in a fixed magnetic field upon which an rf magnetic field is superimposed, resonant modes can be excited magnetostrictively. It is possible to drive the crystals magnetostrictively and to detect the resonances piezoelectrically. It is also possible to use a piezoelectric drive and magnetostrictive detection. It thus has the properties of a gyrator, viz, an antireciprocal transfer matrix.

6682 ANALYSIS OF THE EFFECTS OF MULTIPLY-CHARGED IMPURITIES IN SEMICONDUCTORS BY THE MASS ACTION LAW by N. H. Saunders (Assoc. Electr. Ind.); J. Electronics Control, Vol. 8, pp. 91-96, Feb. 1960

The mass action law is used to derive expressions for the equilibrium carrier concentration and net steady-state recombination rate in a semiconductor containing impurities capable of being

multiply-ionized. The results are in agreement with those found by other treatments and can easily be modified to apply to the degenerate case.

6683 DETERMINATION OF NUMBERS OF INJECTED HOLES AND ELECTRONS IN SEMICONDUCTORS by F. van der Maesen (Philips Res. Lab.); Philips Res. Rep., Vol. 15, pp. 107-119, Apr. 1960

In semiconductors, deviations Δn and Δp from the equilibrium numbers n_o and p_o of electrons and holes are unequal in many cases because of trapping. It is shown how measurements of the photo Hall effect and of the photoconduction may give information on the numbers Δn and Δp separately. From the ratio Y of the relative change of the Hall effect and of the photoconductivity, the quantity $K = \Delta n/\Delta p$ can be evaluated. Graphs of Y versus K for some substances are given. It is shown how K occurs in the formulae used in computations of the diffusion-recombination length L from photoelectromagnetic and photoconductive data. If r_n and r_p denote the ratios of the Hall-mobility to drift mobility for electrons and holes respectively, r_n/r_p can be evaluated from the measurements where $K = 1$. In this way the value of r_n/r_p at room temperature is found to be 0.54 ± 0.05 for germanium and 0.78 ± 0.04 for silicon.

6684 MEASUREMENT OF DECAY TIMES OF EXCESS CARRIERS IN SEMICONDUCTORS, EXCITED BY X-RAY PULSES by J. A. W. van der Does de Bye (N. V. Philips); Philips Res. Rep., Vol. 15, pp. 275-289, June 1960

A method for the measurement of transient decay times of x-ray-excited excess carrier concentrations in homogeneous semiconductors is described. Two pulse generators which can deliver short pulses of 80 kv and of 150 kv are used. These two voltages imply two different effective linear x-ray attenuation coefficients for every substance. For Ge they are about $20\,cm^{-1}$ and $8\,cm^{-1}$. Thus the bulk can be excited without much disturbance by surface recombination. Excitation, dissipation, sample geometry, and noise set a minimum to the resistivity of the sample for the production of a clearly visible decay curve on the oscilloscope. For Ge this is between 0.1 and 1 ohm-cm. The measuring apparatus comprises an exponential time base and a decay-curve simulator for the measurements of decay time constants, down to 0.1 μsec. Measurements performed on copper-doped Ge yield decay times which are also found with chopped light. Some measurements on CdTe are also described.

Recombination in a Semiconductor containing Multiply-Ionizable Impurities - See 6682

Evaluation of the Ratio of Hall Mobility to Drift Mobility for Electrons and Holes - See 6683

6685 ANOMALOUS RESISTIVITY MEASUREMENTS ON TUNNEL DIODE MATERIALS by B. Selikson (Raytheon); J. Electrochem Soc., Vol. 107, p. 199C (A), Aug. 1960

Four point probe resistivity measurements made on a number of germanium single crystal slices with resistivities ranging from 2 to 0.0006 ohm-cm were discussed. It was observed that while the apparent resistivities rose while the slice was lapped down, the corrected resistivity held constant until a certain thickness was reached. On further reduction of thickness the corrected resistivity started to increase. The percentage increase of resistivity and the thickness at which the increase begins is resistivity dependent.

6686 EFFECT OF P-TYPE GERMANIUM ARSENIDE OCCLUSIONS ON THE RESISTIVITY OF HEAVILY DOPED N-TYPE GERMANIUM by F. A. Trumbore, (Bell Labs.); J. Electrochem. Soc., Vol. 107, p. 198C (A), Aug. 1960

The presence of occlusions of p-type germanium arsenide in low-resistivity arsenic doped germanium, which has been revealed by optical examination and thermal probing was discussed. The presence of such occlusions leads to measured resistivities which are lower than the true resistivity of the bulk germanium. It was postulated that these occlusions are the cause of the difficulties encountered in obtaining material of resistivities lower than 0.0006 - 0.0007 ohm-cm, thus explaining the anomalous results of five different types of crystal growth experiments.

6687 INFLUENCE OF THE FREQUENCY ON THE SEMICONDUCTIVITY OF MANGANESE DIOXIDE DOPED WITH THORIUM [in French] by J.-P. Chevillot and J. Brenet; Comptes Rendus, Vol. 250, pp. 515-517, Jan. 18, 1960

The effect of Th^{4+} doping in MnO_2 on the variations of the resistivity as a function of the applied frequency is examined. The curves obtained are compared to those of β-MnO_2 doped with Li^+. It is found that the rates of the variation of the energy as a function of the frequency are very variable.

Infrared Techniques for Determining Conductivity Types - See 6634

Resistivity Variations in Single Crystals of Ge - See 6648

6688 BOMBARDMENT CONDUCTIVITY IN SYNTHETIC ZINC SULPHIDE CRYSTALS by G.F. Alfrey and K.N.R. Taylor (U. Birmingham); J. Electronics Control, Vol. 8, pp. 301-304, April 1960

Bombardment conductivity pulses observed in crystalline zinc sulphide due to irradiation with 5.3 mev alpha particles are discussed. The counting rate and maximum pulse amplitude have been examined as a function of the applied voltage. The results are interpreted in terms of an exhaustion barrier at the negative electrode and the properties of this barrier obtained.

6689 TRANSIENT CONDUCTIVITY OF BLACK SILICON CARBIDE AGGREGATES by E. A. Fagen (Armour Res. Found); Proc. Conf. Silicon Carbide, Pergamon Press, 1960, pp. 331-346

The measurement, by high voltage pulse techniques, of the transient conductivity of single contacts isolated from granular aggregates of black silicon carbide is discussed. It was found possible to separate the total conductivity into an isothermal conductivity and an excess conductivity due to self-heating of the contact area. The isothermal conductivity obeys a power law over the range 10 to 100 v, in which the exponent of voltage dependence is scattered apparently at random between 1.5 and 2.5 at room temperature, and decreases with increasing temperature. The thermally induced, or excess, conductivity depends strongly on the integrated thermal history of the heating process for voltages exceeding about 32 v. These results are compared with existing theories of the silicon carbide contact and it is shown that field emission is the most likely cause of isothermal nonlinearity.

6690 ORGANIC SEMICONDUCTORS II. THE ELECTRICAL RESISTIVITY OF ORGANIC MOLECULAR COMPLEXES by M. M. Labes, R. Sehr, and M. Bose (Franklin Inst.); J. Chem. Phys., Vol. 33, pp. 868-872, Sept. 1960; Proc. Princeton U. Conf. Semiconduction Molecular Solids, pp. 47-60, 1960

The preparation of thirty molecular complexes involving quinones, halogens, polynitroaromatics, or tetracyanoethylene as electron acceptors and aromatic hydrocarbons or substituted aromatics as electron donors and room temperature electrical resistivity measurements made on compressed microcrystalline material are discussed. A lowering of electrical resistivity is generally associated with complex formation. The results are discussed in terms of crystal structure and charge transfer complex theory.

SUPERCONDUCTIVITY

6691 GAUGE INVARIANT FORMULATION OF THE BARDEEN-COOPER-SCHRIEFFER THEORY OF SUPERCONDUCTIVITY by T. A. Oliphant and W. Tobocman (Rice Inst.); Phys. Rev., Vol. 119, pp. 502-503, July 15, 1960

The Bardeen-Cooper-Schrieffer theory of superconductivity is reformulated in a way which is manifestly gauge invariant. The method used is to pair electrons having equal and opposite angular momentum rather than equal and opposite linear momentum.

6692 THE PROBABLE EXISTENCE OF SUPERCONDUCTORS WITH A VERY LOW TRANSITION TEMPERATURE [in French] by B. B. Goodman (Métal Inst. Fourier); Comptes Rendus, Vol. 250, pp. 683-685, Jan. 25, 1960

The statistical distribution of the Bardeen-Cooper-Schrieffer parameter $N(0)V$ among the superconducting elements is examined. It is concluded that a number of superconductors with extremely low transition temperatures remain to be discovered.

6693 LAW OF CORRESPONDING STATES IN SUPERCONDUCTIVITY by J. C. Swihart (IBM); Phys. Rev., Vol. 116, pp. 346-347, Oct. 15, 1959

It is shown by means of a crude calculation that a refined version of the Bardeen-Cooper-Schrieffer theory of superconductivity in which the energy gap function $\mu(\nu)$ would not be approximated by a constant would give very nearly the same relation between H_0, the critical field at $T=0$; $2\mu(0)$, the energy gap; and $N(0)$, the density of states at the Fermi surface. Agreement between the theory of experiment is found for the cases of Al, Sn, Hg, and Pb although the experimental error is large for Hg. For the case of Pb, this is the first agreement between the theory and experiment with regard to the thermodynamic variables.

6694 SPIN ALIGNMENT IN THE SUPERCONDUCTING STATE by P. W. Anderson and H. Suhl (Bell Labs.); Phys. Rev., Vol. 116, pp. 898-900, Nov. 15, 1959

It is argued that spin alignment can and will occur for ion-core spins in superconductors, but that the alignment is in the form of extremely small domains. Central to the argument is the concept of the nonlocal susceptibility $\chi(r-r')$, which leads to a positive short-range Kittel-Ruderman-Yosida interaction of ion-core spins, but a negative long-range interaction of range ξ_0. Very general arguments suggest that purely ferromagnetic alignment should not be observed in preference to this domain-like "cryptoferromagnetic" alignment.

6695 MILLIMETER WAVE ABSORPTION IN SUPERCONDUCTING ALUMINUM. I. TEMPERATURE DEPENDENCE OF THE ENERGY GAP by M. A. Biondi and M. P. Garfunkel (Westinghouse); Phys. Rev., Vol. 116, pp. 853-861, Nov. 15, 1959

Measurements of the temperature dependence of the microwave absorption in superconducting aluminum in the wavelength region 20 mm to 3 mm are reported. The results, when plotted as isotherms of surface resistance ratio vs photon energy, show that, at a well-defined energy for each temperature, there is a rapid rise in absorption with increasing energy. This has been interpreted as the onset of absorption resulting from direct excitation of electrons across a forbidden energy gap. The isotherms then permit the determination of the temperature dependence of this energy gap. At absolute zero the gap value is found to be $E_g(0) = (3.2 \pm 0.1)\, kT_c$ (where $T_c = 1.178°K$ is the superconducting transition temperature), in reasonable agreement with the theoretical value of $3.52kT_c$ obtained by Bardeen, Cooper, and Schrieffer. Furthermore, the temperature variation of the gap exhibits the same shape as that given by the theory. Finally, reasonable agreement is obtained between theory and experiment concerning the detailed shapes of the surface resistance vs temperature curves over the measured wavelength range, provided that the experimental value $E_g(0)$ is used in the theory.

6696 MILLIMETER WAVE ABSORPTION IN SUPERCONDUCTING ALUMINUM. II. CALCULATION OF THE SKIN DEPTH by M. A. Biondi (Westinghouse) and M. P. Garfunkel (U. of Pittsburgh); Phys. Rev., Vol. 116, pp. 862-867, Nov. 15, 1959

The skin depth in superconducting aluminum is calculated from the measured frequency dependence of the surface resistance through the Kronig-Kramers integral transforms. At absolute zero, it is found that the skin depth δ is independent of frequency at low frequencies but begins to increase at higher frequencies. The maximum rate of increase of δ occurs when the

photon energy equals the gap energy, $h\nu = 3.2kT_c = E_g$; at this point $\delta(h\nu = E_g)/\delta(h\nu = 0) \approx 1.12$. The maximum value of δ occurs at $h\nu \approx 4kT_c$. The superconducting penetration depth λ [i.e., $\delta(h\nu = 0)$] is found to vary approximately as $\lambda(t) = \lambda(0)(1 - t^4)^{-1/2}$, with $\lambda(0) = 5.15 \times 10^{-6}$ cm and $t \equiv T/T_c$. The effects of changes in the skin depth have been eliminated from the determination of the energy gap by calculation of the real part of the complex conductivity, σ_r. The energy gap values deduced from the behavior of σ_r differ only slightly from the results obtained directly from the surface resistance measurements.

6697 TIME DELAYS IN THE SUPERCONDUCTING TRANSITION OF LEAD FILMS by R. F. Broom and E. H. Rhoderick (SERL); Phys. Rev., Vol. 116, pp. 344-345, Oct. 15, 1959

The results of driving strips of lead between 500 A and 1000 A thick, evaporated onto mica substrates, from the superconducting into the normal state by rectangular current pulses of 0.4μ sec duration are discussed. For current amplitudes just above the threshold value, there was an apparent delay of up to 0.4 μsec before resistance began to appear in the strip. A plausible explanation is that a minute portion of the strip in the neighborhood of a flaw is driven normal almost instantaneously, and that the Joule heating of this normal region eventually causes thermal propagation of the interphase boundary. The delay is the time that must elapse before the temperature of the nucleus rises sufficiently to initiate the thermal spreading process. Similar results were obtained with lead-indium alloys, but in the case of tin the delay was less than the instrumental resolution. The relevance of these results to the interpretation of d-c critical currents is discussed.

GALVANOMAGNETIC PROPERTIES

6698 THE HALL EFFECT IN AN INHOMOGENEOUS MAGNETIC FIELD [in German] by J. Brunner (Siemens); Solid-State Electronics, Vol. 1, pp. 172-175, July 1960

The Hall voltage of a Hall generator with a large ratio of length to width in an inhomogeneous magnetic field is calculated for the case when the normal field component varies linearly along the length of the generator. The error in measurement of fields is shown to be negligible in most cases of practical importance if the gradient of the normal component across the generator is approximately constant.

6699 HALL FIELD RELAXATION IN SEMICONDUCTORS AT HIGH FREQUENCY by K. S. Champlin (U. Minn.); J. Appl. Phys., Vol. 31, pp. 1770-1771, Oct. 1960

Using a simple extension of standard magneto-ionic theory, the frequency dependence of the complex Hall field is calculated for samples with rectangular, cylindrical, and spherical geometry. The result has application to "open-circuit" Hall effect measurements on semiconductors at microwave frequencies.

Magneto-Oscillatory Effect in the Electron-Hole Plasma in a Semiconductor - See 6777

OTHER ELECTRICAL PROPERTIES

6700 ELECTRON-ELECTRON SCATTERING IN N-P TUNNELING by E. O. Kane (Hughes Prod.); Bull. Am. Phys. Soc., Ser. II, Vol. 5, p. 160(A), Mar. 21, 1960

The I-V characteristics of p-n junction diodes show large thermionic currents at forward biases where the energy bands have been "uncrossed." This "excess" current implies the existence of significant energy loss mechanisms in or near the junction. A simple model of such a mechanism postulates the perfect crystal band structure modified only by "tunneling" wave functions extending into the gap. Energy is absorbed either by phonons, photons, or another electron. The first two mechanisms are presumably too small to be important. Calculation of the electron mechanism has shown that it also is incapable of explaining the observed current. The electron-electron scattering mechanism was calculated assuming a constant junction field and parabolic energy bands. In the junction region "tunneling" functions written in Bloch space were used. Two electrons tunnel in from the n side. One electron drops into a tunneling hole and gives up its excess energy to the other electron. The semiclassical method of stationary phase, which is a generalization of the familiar WKB method, was employed.

6701 TUNNELING IN InSb. I. PHONON-ASSISTED TRANSITIONS. II. MAGNETIC FIELD EFFECTS by A. G. Chynoweth, R. A. Logan, and D. E. Thomas (Bell Labs.); Bull. Am. Phys. Soc., Ser. II, Vol. 5, p. 374(A), June 15, 1960

Inflections in the differential conductance vs bias curves of narrow InSb p-n junctions at 4°K are well revealed by automatic plotting equipment. The inflection points occur at biases corresponding to the phonon (or phonon-combination) energies involved. The present precision of the experiments allows these energies to be determined to ±10%. In addition to an inflection at 24 Mev (corresponding to the zero momentum transverse optic, TO, phonon previously reported by Hall), inflections occur at 46, 66, and 84 Mev. These are tentatively interpreted as corresponding to the simultaneous emission of 2, 3, and 4 TO phonons, respectively. Other inflections occur at 5, 11, 36, and 58 Mev, but their exact origins are not understood at present. Magnetic fields cause a reduction in the tunnel current but, as the phonon inflection points continue to occur at the same biases, the reduction in current cannot be caused by series magnetoresistance effects. The way in which the tunnel current depends on H can be accounted for by the increase in the energy gap and the increase in the reduced effective mass with H.

6702 MECHANICAL MODEL FOR UNIAXIAL MAGNETIC ANISOTROPY by H. J. Oguey (IBM); Rev. Sci. Instr., Vol. 31, pp. 710-711, July 1960

A mechanical model constructed as a means of understanding certain properties of anisotropic thin films is discussed. The model renders possible direction finding of the magnetization for a given amplitude and direction of the magnetic field vector lying in the plane of the film, provided rotational processes only are considered. The magnetic field is represented by the position of a small knob, and can be set in its amplitude and direction. A pointer then indicates the orientation of the magnetization vector. Jump phenomena can be easily observed, the loci of which form the critical curve for the uniaxial anisotropy.

6703 REDUCTION IN COERCIVE FORCE CAUSED BY A CERTAIN TYPE OF IMPERFECTION by A. Aharoni (Weizmann Inst. Sci.); Phys. Rev., Vol. 119, pp. 127-131, July 1, 1960

As a first approach to the study of the dependence of the coercive force on imperfections in materials which have high magnetocrystalline anisotropy, the following one-dimensional model is treated. A material which is infinite in all directions has an infinite slab of finite width in which the anisotropy is 0. The coercive force is calculated as a function of the slab width. It is found that for relatively small widths there is a considerable reduction in the coercive force with respect to perfect material, but reduction saturates rapidly so that it is never by more than a factor of 4.

Magnetostrictive Properties of Gallium Iron Oxide Single Crystal Resonators - See 6681

6704 MAGNETIC STRUCTURE OF Mn_4N by W. J. Takei, G. Shirane (Westinghouse) and B. C. Frazer (Brookhaven Natl. Lab.); Phys. Rev., Vol. 119, pp. 122-126, July 1, 1960

The magnetic structure of Mn_4N, determined by neutron diffraction from powders, is discussed. The cubic unit cell has Mn at the corner and face centers and N at the body center. Standard diffraction techniques led to four possible models and it was necessary to perform polarized neutron beam experiments to resolve this ambiguity. The structure is ferrimagnetic with a corner moment of $3.5\,\mu_B$ antiparallel to the three face center moments of $0.7_7\,\mu_B$.

6705 THEORY OF FERROMAGNETIC RESONANCE IN RARE EARTH GARNETS. II. LINE WIDTHS by P.G. De Gennes, C. Kittel, and A.M. Portis (U. California); Phys. Rev., Vol. 116, pp. 323-330, Oct. 15, 1959

The spins of rare earth ions in the garnets are coupled strongly both to the lattice phonons and, by an exchange interaction, to the ferric spin lattice. The rare earth spins thus provide a powerful relaxation channel for the ferric lattice. Two contributions to the line width may be distinguished. A coherent process (in which the total magnetic moment of the ferric lattice relaxes without changing the magnitude of the moment) is dominant at temperatures from 0°K up to just below the Curie temperature. Near and above T_c a fluctuation process (in which ferric spins flip locally) is dominant. The theoretical results describe the order of magnitude and the temperature dependence of the observed line widths in the rare earth garnets and in impure yttrium iron garnet, if one assumes in the absence of direct experimental knowledge that the relaxation frequency $1/\tau$ of the relevant rare earth ions is $\sim 10^{-12}$ sec at 400°K. As the temperature is increased from 0°K, the width increases until a maximum is reached when $1/\tau$ becomes comparable with the ferric-rare earth exchange frequency. Above this temperature the width decreases until near T_c, where there is a sharp rise.

6706 GENERATION OF PHONONS IN HIGH-POWER FERROMAGNETIC RESONANCE EXPERIMENTS by E. Schlömann (Raytheon); J. Appl. Phys., Vol. 31, pp. 1647-1656, Sept. 1960

The magnetoelastic energy of ferromagnets leads to a coupling between spin waves and elastic vibrations. Because of this coupling the normal modes are not purely magnetic or purely elastic but contain admixtures of both kinds of excitation, the mixing being strongest when the unperturbed waves have the same frequency and wavelength. It is shown theoretically that under suitable conditions (of frequency, d-c field, and sample shape) coupled magnetoelastic waves with wavelengths of the order of 1 μ or less can be generated in high-power ferromagnetic resonance experiments. The magnetoelastic interaction increases the threshold precession angle of the uniform mode, the fractional increase being proportional to the group velocity times the relaxation time for spin waves divided by the same quantity for transverse phonons.

6707 CRYSTALLOGRAPHY AND DOMAIN WALLS IN ANTIFERROMAGNETIC NiO CRYSTALS by G. A. Slack (GE Res. Lab.); J. Appl. Phys., Vol. 31, pp. 1571-1582, Sept. 1960

The observation of twin-domain walls in large optically-polished, annealed crystals of antiferromagnetic NiO by specular reflection is discussed. These walls can be moved in annealed crystals by small mechanical stresses ($<10^6$ d/cm^2) or by moderate magnetic fields ($<25{,}000$ oe) to yield completely untwinned crystals. The ease with which a twin wall moves appears to be limited by a spin-rotation energy loss. Crystallographic measurements of the rhombohedral distortion agree with the x-ray data, and verify the [111] antiferromagnetic contraction. The anisotropy in the magnetic susceptibility vs field has been measured for untwinned crystals and is compared with earlier work.

6708 EVIDENCE FOR ANTIFERROMAGNETISM IN $CoBr_2 \cdot 6H_2O$ by H. Forstat, G. Taylor, and R. D. Spence (Michigan State U.); Phys. Rev., Vol. 116, pp. 897-898, Nov.15, 1959

An antiferromagnetic-paramagnetic transition has been observed in a single crystal of $CoBr_2 \cdot 6H_2O$ by using the proton resonance technique and by measuring the heat capacity in the temperature range 1.65-5.05°K. The Néel temperature, obtained by the magnetic measurement is 3.08°K while the heat capacity measurement gave 3.07°K. The entropy change associated with the transition was calculated from the heat capacity data and yielded 1.42 cal/mole deg. The contribution to the entropy change above the Néel temperature was approximately 38 percent of the total entropy change, which indicates a rather slow diminution of the short-range ordering of the Co^{++} spins.

6709 MICROWAVE FARADAY ROTATION IN ANTIFERROMAGNETIC MnF_2 by A.M. Portis and D. Teaney (U. California); Phys. Rev., Vol. 116, pp. 838-845, Nov. 15, 1959

Microwave Faraday rotation has been observed in MnF_2 from 30°K up to 300°K. The antiferromagnetic resonance frequency is computed from the rotation measurements below the Néel point. The results are in good agreement with direct observation of the antiferromagnetic resonance and molecular field theory extrapolations except close to the transition where evidence for magnetic clustering is found. The Kramers-Kronig relations are applied to antiferromagnetic media and it is shown that the Faraday rotation depends both on the shift of the resonance with field and on very small field-induced intensity changes which are present. A study of Faraday ellipticity establishes the need for using terms in the equation of motion which relax the magnetization toward the instantaneous field direction.

6710 FINE STRUCTURE IN THE DECLINE OF THE FERROMAGNETIC RESONANCE ABSORPTION WITH INCREASING POWER LEVEL by E. Schlömann (Raytheon); Phys. Rev., Vol. 116, pp. 828-837, Nov. 15, 1959

A theory of ferromagnetic resonance at high signal powers is developed. The stationary response at high power levels is investigated for the case in which the unstable spin waves have the same frequency as the applied signal. It is found that a fine structure should be superimposed on the general decline of the resonance absorption with increasing power level. This fine structure arises from the discrete nature of the spin-wave spectrum. It should be observable even if the frequency separation of adjacent spin-wave modes is much smaller than the inverse of their relaxation times. The fine structure appears as a series of kinks superimposed on the general decline of the resonance absorption with increasing power level. The separation of subsequent kinks increases with decreasing sample volume and increasing exchange field. An interpretation of experimental data along the lines suggested in this paper should yield information about the strength of the exchange coupling.

6711 PASSAGE EFFECTS IN PARAMAGNETIC RESONANCE EXPERIMENTS by M. Weger; Bell Sys. Tech. J., pp. 1013-1112, July 1960

An attempt is made to classify theoretically paramagnetic resonance signals of inhomogeneously broadened lines occurring under various experimental conditions. The theoretical predictions are checked experimentally. Special emphasis is given to cases in which T_1 is long, and to cases in which the adiabatic condition $\gamma H_1^2 \gg dH/dt$ is violated.

6712 TEST OF SPIN HAMILTONIAN FOR IRON^{3+} IN STRONTIUM TITANATE by S. Aisenberg and H. Statz (Raytheon); Phys. Rev., Vol. 116, pp. 811-818, Nov. 15, 1959

The applicability of a conventional spin Hamiltonian to the paramagnetic spectrum of Fe^{3+} in strontium titanate is investigated. The work was inspired by a paper by Müller who finds deviations from a conventional spin Hamiltonian which he attributed to covalent bonding. The spectrum is remeasured and compared with the more general theory of Koster and Statz. It is found that the conventional Hamiltonian describes the spectrum about as well, in this case, as the improved theory. The remaining discrepancies vary from crystal to crystal and are due to random distortions of the Fe^{3+} site. A rather good agreement with theory was obtained for one crystal which apparently was more perfect than the other measured samples. From perturbation theory, it is concluded that the deviations from a conventional Hamiltonian should be about 0.1 Mc/sec if covalency and exchange effects can be neglected. The experimental errors in the present experiments are about 1 to 2 Mc/sec. Even though for the present example it is unnecessary to resort to the improved theory, it is shown that, even in the absence of covalency, measurable deviations from a conventional spin Hamiltonian are expected in substances where the zero-field splittings and the applied magnetic field are large.

6713 ELECTRON PARAMAGNETIC RESONANCE OF Fe^{3+} IN TiO_2 (RUTILE) by D. L. Carter and A. Okaya (Columbia U.); Phys. Rev., Vol. 118, pp. 1485-1490, June 15, 1960

Paramagnetic resonance from 2 to 110 kMc in Fe^{3+}-doped single crystals of rutile at 78°K, 4.2°K, and 1.4°K is discussed. The rather large zero field splittings measured between the three doublets are 43.3±0.1 kMc and 81.3±0.1 kMc. The derived constants for the spin Hamiltonian are given. The average line width is 35 Mc for 2×10^{19} spins per cm^3, and the average spin-lattice relaxation time T_1 at T=1.4°K is 4 msec. T_1 still has a very slow inverse temperature dependence even at T = 78°K. An increase in sensitivity over metal walled cavity spectrometers was achieved by using the pieces of Fe-doped rutile as the microwave resonators.

6714 PARAMAGNETIC RESONANCE SPECTRUM OF MANGANESE IN CORUNDUM by W. Low and J. T. Suss (Hebrew U.); Phys. Rev., Vol. 119, pp. 132-133, July 1, 1960

The paramagnetic resonance spectrum of Mn^{2+} in Al_2O_3 measured at 3 cm is discussed. The spectrum can be expressed in a spin Hamiltonian with trigonal symmetry with the following parameters: $g_{\parallel} = 2.0017 \pm 0.001$, $g_{\perp} = 2.000 \pm 0.002$, $D = +194.2 \pm 1$, $a-F = +21.9 \pm 0.6$, $A = -79.6 \pm 0.5$, $B = -78.8 \pm 0.8$ in units of $10^{-4} cm^{-1}$.

Paramagnetic Properties of Cr^{3+} in TiO_2 - See 6806

6715 THEORY OF DIAMAGNETISM OF GRAPHITE by J. W. McClure (Union Carbide); Phys. Rev., Vol. 119, pp. 606-613, July 15, 1960

The conduction-electron diamagnetism for the three-dimensional band structure of graphite is discussed. The magnetic energy levels are found and the susceptibility is calculated by analytically carrying out the free energy sum. Agreement with experiment is found for values of the band parameters nearly equal to those which give agreement with the de Haas-van Alphen effect and other phenomena. The value of γ_0 is found to be 2.8±0.1 ev. The results indicate that γ_1 is about 0.27 ev and Δ is about 0.025. The other band parameters do not have an important influence upon the value of the susceptibility. The relation to the general treatments of conduction-electron diamagnetism is also discussed.

OPTICAL PROPERTIES

6716 OPTICAL CONSTANTS OF THIN GERMANIUM FILMS by F. Lukes (Brno U.); Czech. J. Phys., Vol. 10B, No. 1, pp. 59-65, 1960

The index of absorption k determined in the wavelength range 0.35 to 0.78μ and the refractive index n determined in the range 0.35 - 2.5μ in thin evaporated Ge films are discussed. The values are compared with those obtained by other investigators in both single crystals and films. It is shown that these values for thin films and single crystals differ slightly quantitatively but agree fairly well qualitatively.

Grain-Boundary Photoresponse - See 6788

Effect of Absorption and Multiple Reflections on the Transmission of Microwave Energy Through a Semiconductor - See 6779

Absorption Centers in Rutile Single Crystals - See 6629

6717 DECREASE OF F-CENTER PHOTOCONDUCTIVITY UPON BLEACHING by F. C. Hardtke, A. B. Scott, and R. E. Woodley (Oregon State Coll.); Phys. Rev., Vol. 119, pp. 544-549, July 15, 1960

A quantitative study of the rapid decrease in photoconductivity accompanying the relatively less rapid bleaching of F centers in additively colored KCl is reported. The experimental observations agree, except during very early stages of bleaching, with an equation for the variation of sensitivity with total light absorbed which is derived upon the assumption that negative-ion vacancies are created and traps of smaller cross section are filled during bleaching. Except during early stages, where several kinds of traps may be present in low concentration, only one kind of trap other than the negative-ion vacancy need be considered. The effects of added divalent ions, both positive and negative, upon photoconductivity are also discussed.

6718 HIGH FIELDS IN SHADOW REGIONS ON PHOTOCONDUCTORS by S. Machlup and J. D. Nixon (Western Reserve U.); Bull. Am. Phys. Soc., Ser. II, Vol. 5, p. 180(A), Mar. 21, 1960

A narrow shadow region separating the anode and cathode portions of a homogeneous high-resistance photoconductor (CdS) may show some of the characteristics of a p-n junction. The anode-cathode asymmetry can be ascribed to the high field in the shadow region and to the large mobility ratio b (electron: hole mobility). When the shadow is rapidly moved a short distance toward the anode, the persistence, for a time $\rho\kappa$, of the field in the newly illuminated region may cause the mobile electrons within it to be swept into the shadow region, lowering its resistance. The characteristic (maximum) width d of the shadow for this effect is $(V\mu\tau)^{1/2}$. An electron of mobility μ travels a distance d in its lifetime τ in a field V/d. The minimum width is the diffusion length $(kT\mu\tau/e)^{1/2}$. Trapping of electrons by surface states will reduce $\mu\tau$, so that it is expected that the conductance anomaly at the shadow may be affected by capacitively applied fields, nonpenetrating background radiation, or surface treatment.

6719 ELECTRICAL PROPERTIES OF ORGANIC SOLIDS. II. EFFECTS OF ADDED ELECTRON ACCEPTOR ON METAL-FREE PHTHALOCYANINE by G. Tollin, D. R. Kearns and M. Calvin (U. California); J. Chem. Phys., Vol. 32, pp. 1020-1025, Apr. 1960

The addition of ortho-chloranil to the surface of films of metal-free phthalocyanine has been found (a) to increase the dark conductivity of such films by as much as 10^7, (b) to increase the steady-state photoconductivity by as much as 10^5, and (c) to result in the formation of unpaired electrons whose concentration decreases reversibly as a result of illumination. These systems exhibit a light-induced polarization, the phthalocyanine layer becoming more positive with respect to the ortho-chloranil layer. Kinetic studies demonstrate that, upon illumination, a single process (time constant = 60 sec) results in the increase in conductivity, the decrease in unpaired spins and the increase in polarization. A scheme with which the results are consistent is given. The overall results of adding a strong electron acceptor to a film of phthalocyanine are (a) the production of charge carriers in the dark, (b) an increase in the quantum yield for production of charge carriers by light, and (c) an increase in charge carrier lifetime.

6720 BECQUEREL PHOTOVOLTAIC EFFECT IN BINARY COMPOUNDS by R. L. Williams (RCA Labs.); J. Chem. Phys., Vol. 32, pp. 1505-1514, May 1960

An experimental study made of photovoltaic effects which occur at semiconductor-electrolyte interfaces is discussed. Single crystal specimens of CdS and several other compounds were used. It was found that in a number of cases the photovoltaic effect results from a chemical reaction of the electrode materials. In such cases the observations may be explained by a simple mechanism which relates the sign of the photo-emf to the conductivity type of the semiconductor and to the chemical reaction which is occurring. The reaction may be predicted using readily available thermodynamic data. A different process occurs when the electrode material is GaAs. It acts as an inert electrode which exchanges electrons with an oxidation-reduction couple in the solution.

6721 PHOTOEMISSION IN THE PHOTOVOLTAIC EFFECT IN CADMIUM SULFIDE CRYSTALS by R. L. Williams and R. H. Bube (RCA); J. Appl. Phys., Vol. 31, pp. 968-978, June 1960

The photovoltaic effect in Cu-CdS cells and related systems, which is associated with undiffused metal-semiconductor junctions, is discussed. The photovoltaic current has been shown to result from the photoemission of electrons from the copper metal into the CdS crystal. Direct evidence for this conclusion is presented, and the conditions required for the photoemission process to occur are demonstrated by several experiments. Important factors contributing to the efficiency of Cu-CdS photovoltaic cells of this type are: (a) the optical properties of copper, (b) the rectifying contact between the metal and CdS, (c) the good conductivity and high optical transparency which can be achieved in CdS crystals, and (d) the favorable relation between the work function of copper and the electron affinity of CdS.

Photovoltaic Effect Derived from the Carnot Cycle - See 6783

6722 PHOTOEMISSION FROM Si INDUCED BY AN INTERNAL ELECTRIC FIELD by R. E. Simon and W. E. Spicer (RCA Labs.); Phys. Rev., Vol. 119, pp. 621-622, July 15, 1960

External photoelectric emission observed from a back biased silicon p-n junction which had received a cesium surface treatment is discussed. The emission has a threshold of response corresponding to the band gap of silicon and is proportional to the intensity of the incident light. The spectral distribution of this field-induced photoemission has been simply related to the spectral distribution of the fundamental absorption of silicon.

6723 OPTICAL PROPERTIES OF A HIGHLY BORON-DOPED SILICON SURFACE by J. F. Hall, Jr. (Bausch and Lomb Optical); J. Opt. Soc. Am., Vol. 50, pp. 717-720, July 1960

The index of refraction and extinction coefficient of a silicon surface highly doped with boron so as to appear as a semimetal are determined from the specular reflection. The classical theory of metals is employed to obtain a relationship between the optical and electrical properties. The results are substantiated by comparing the calculated and measured reflectance of silicon monoxide layers of known optical properties deposited on the doped silicon surface.

6726 APPARATUS FOR THE MEASUREMENT OF THE THERMAL DIFFUSIVITY OF SOLIDS AT HIGH TEMPERATURES by B. Abeles, G. D. Cody, and D. S. Beers (RCA Labs.); J. Appl. Phys., Vol. 31, pp. 1585-1592, Sept. 1960

An apparatus for measuring the thermal diffusivity of solids in the temperature range 30° — 1000°C is described. It employs a method in which the dispersion and the attenuation of a thermal wave, propagated through the solid, are measured. The theory underlying the method is presented and results of measurements on Armco iron and germanium are given.

6727 TEMPERATURE DISTRIBUTION IN MATERIALS WITH POSITIVE TEMPERATURE COEFFICIENTS OF ELECTRICAL CONDUCTIVITY WHEN HEATED BY EDDY CURRENTS by W. W. Buchman (Hughes Aircraft); IRE Trans., Vol. CP-7, pp. 60-65, June 1960

Steady-state digital and analytical solutions are given for the temperature distribution in slabs and cylinders of materials heated by varying magnetic fields. The materials are assumed to have a positive temperature coefficient of electrical conductivity of the type associated with semiconductors. The stability of the temperature distribution is investigated. It is shown that the solutions can be either stable or unstable, depending upon the size of the sample. Some of the practical significance of such heating is discussed in relation to the design of high-power wide-band transformers employing ferrite cores.

THERMAL PROPERTIES

6724 SPECIFIC HEAT AND ELASTIC CONSTANTS OF SODIUM IODIDE AT LOW TEMPERATURES by R. N. Claytor and B. J. Marshall (Rice Inst.); Phys. Rev., Vol. 120, pp. 332-334, Oct. 15, 1960

Measurements of specific heat from 2.4°K to 8°K and of elastic constants from 4.2°K to 300°K made on single crystals of sodium iodide are discussed. The Debye theta at 0°K, $\theta_{0\,k}$ as calculated from the specific heat data is $163 \pm 1^{\circ}$K. Values of the elastic constants at 4.2°K are $C_{11}=3.761$, $C_{12}=0.798$, and $C_{44}=0.781$ in units of 10^{11} dynes/cm^2. θ_0 calculated from the velocity of sound waves is $167 \pm 1.5^{\circ}$K. The present results are compared with the work of Morrison, et al.

6725 INFLUENCE OF F CENTERS ON THE LATTICE THERMAL CONDUCTIVITY IN LiF by R. O. Pohl (Cornell U.); Phys. Rev., Vol. 118, pp. 1499-1508, June 15, 1960

The influence of photochemically produced F centers in LiF on the thermal conductivity is investigated. The F centers decrease the thermal conductivity appreciably at low temperatures. Additive coloration of KCl has a similar effect. The experimental results are quite different from the results obtained in the case of the isotope effect in Ge. It is pointed out that Callaway's theory for the lattice thermal conductivity in the presence of point defects cannot explain the present observations satisfactorily. Two possible explanations are proposed.

MECHANICAL PROPERTIES

Plastic Deformation of Ge by Alloying - See 6748

Elastic Constants of Sodium Iodide at Low Temperatures - See 6724

6728 MAGNETO-ATTENUATION OF SOUND IN SEMIMETALS: LONGITUDINAL WAVES by M. J. Harrison (U. Chicago); Phys. Rev., Vol. 119, pp. 1260-1269, Aug. 15, 1960

The calculation of the magnetic field dependence of ultrasonic attenuation in a semimetal is discussed on a simple model of its band structure. The results are applied to the case where the electron and hole mean free paths are large compared to the wavelength of sound. A series of oscillations and a large peak in the attenuation as a function of magnetic field are derived. The oscillations are geometric resonances of the type previously derived for metals, and the large peak is associated with the presence of density waves in the electron-hole carrier gas. The theoretical results are discussed, compared with experimental data, and found to agree semiquantitatively with the latter.

SOLID STATE DEVICES

6729 IRE STANDARDS ON SOLID-STATE DEVICES: DEFINITIONS OF SEMICONDUCTOR TERMS, 1960; Proc. IRE, Vol. 48, pp. 1772-1775, Oct. 1960

Equipment for Encapsulating Semiconductor Devices - See 6772

SEMICONDUCTOR DIODES - GENERAL

6730 A METHOD FOR THE RAPID EVALUATION OF SEMICONDUCTOR DEVICE RELIABILITY by B. T. Howard and G. A. Dodson (Bell Labs.); 1960 Electron Dev. Mtg.

A rapid method for the evaluation of semiconductor device reliability was described. The stress level of the test is progressively increased until failure occurs in all the devices. This technique enables an approximate evaluation to be obtained in a time of one week with about fifty devices. The technique may be utilized to predict the long term, operating reliability of devices by the development of an acceleration curve of failure as a function of the stresses used. This acceleration curve has been found to have the form $f(\bar{S}) = a\log t + b$, where $\bar{S}$, t, a and b are, respectively, the stress for 50% failure, the time, and two constants characteristic of the device. For the particular case of temperature as stress, the relationship is $t = A\exp(-E/k\bar{T})$, where $\bar{T}$ is the temperature for 50% failure and E is an activation energy. The technique has also been utilized to study the statistics and mechanisms of failures and has shown that the distribution of failure times is log-normal rather than exponential. A general discussion of the problems of highly accelerated reliability evaluation was given and experimental results on both diodes and transistors were presented.

6731 NEGATIVE RESISTANCE IN SEMICONDUCTOR DEVICES by R. E. Burgess (U. Brit. Columbia); Can. J. Phys., Vol. 38, pp. 369-375, Mar. 1960

Negative resistance can appear in the static and high-frequency characteristics of devices in which the current is determined by both voltage and temperature. The properties of the a-c impedance arising from the interaction of thermal and non-thermal effects are discussed and criteria for the appearance of negative resistance over certain ranges of frequency are derived. The application of this analysis to devices which do and which do not exhibit isothermal negative resistance is considered. A current-temperature relation depending on two activation energies is shown to provide a quantitative model for interpreting the observed turnover behavior of germanium diodes.

POINT CONTACT DIODES

6732 GALLIUM ARSENIDE MICROWAVE DIODE AT X BAND by M. Herndon and A. C. Macpherson (U.S. Naval Res. Lab.); Proc. IRE, Vol. 48, p. 945 (L), May 1960

Measurements made at X band on five of the GaAs diodes used by Jenny [see 1895] are discussed. A typical diode as received exhibited conversion loss L of 7 db and noise temperature ratio t of 3 times. The diodes were then rebuilt by resetting the whisker on the crystal in order to maximize the short-circuit rectified current produced by the local oscillator. The best diode had an L of 5.6 db and a t of 1.14 times. It is concluded that it is possible to fabricate GaAs diodes which compare favorably in L and t at X band with Si and Ge diodes and which are less bias sensitive than Ge diodes.

JUNCTION DIODES

6733 AN EVALUATION OF THE P-N-P-N NEGATIVE RESISTANCE DIODE by H. I. Honor (Air Force Cambridge Res. Ctr.); U. S. Gov. Res. Rep., Vol. 34, p. 147 (A), Aug. 19, 1960 PB 146 446

The operation of the three junction diode is analyzed and interpreted in terms of two contiguous transistors. It is seen that avalanche breakdown and the sum of the forward alphas determine the switching characteristics. The properties of four diode types are presented and compared. A piecewise-linear equivalent circuit is developed and some simple circuit applications are analyzed.

6734 A VAPOR-GROWN VARIABLE CAPACITANCE DIODE by R. L. Anderson and M. J. O'Rourke (IBM); IBM J. Res. and Dev., Vol. 4, pp. 264-268, July 1960

Vapor-grown Ge p-n junctions which have a large fractional variation of capacitance with voltage are described. Capacitances which vary as the reciprocal of voltage over a considerable range have been observed. This capacitance variation corresponds to a net donor concentration which decreases from its value at the junction approximately as the reciprocal of distance from the junction. At a position corresponding roughly to the edge of the transition region at breakdown, the net donor concentration abruptly increases. This rapid variation of

capacitance with voltage and the low series resistance resulting from the discontinuity in doping level should result in high-frequency diodes, if the magnitude of the discontinuity can be increased sufficiently.

6735 TRANSIENT RESPONSE OF VARIABLE CAPACITANCE DIODES by D. Schulz (Hughes Aircraft); IRE Trans., Vol. CP-7, pp. 49-53, June 1960

A solution for the transient response of a reverse biased semiconductor diode to a step function (voltage) may be found by considering the junction essentially a voltage variable capacitance. The assumptions from which the analysis is made are given and found to be applicable in a wide variety of cases. Specific solutions are obtained for abrupt and linearly graded junctions, and experimental evidence which is in good agreement with the derived equations is presented.

6736 THE CHARACTERISTICS AND APPLICATIONS OF ZENER (VOLTAGE REFERENCE) DIODES by J. A. Chandler (Assoc. Electrical Ind.); Electronic Engrg., Vol. 32, pp. 78-86, Feb. 1960

The detailed characteristics of Zener diodes are presented and curves showing the variation of a-c and d-c slope resistance with both current and voltage, breakdown voltage variation with temperature, and the forward characteristics of the diodes are given. The general circuit of the simple stabilized supply is considered, with limitations due to the diode and circuit limits. Temperature compensation of the diodes is considered and results are shown. The stability of the output voltage with input and load variations is given in detail using the characteristics already mentioned. The two stage stabilizer is considered and a practical example of a high stability reference is given. The results show that a very high stability reference can be constructed using relatively simple circuits.

6737 ON THE NATURE OF THE MAXIMUM AND MINIMUM CURRENTS IN GERMANIUM TUNNEL DIODES by T. A. Longo (Sylvania); Bull. Am. Phys. Soc., Ser. II, Vol. 5, p. 160(A), Mar. 21, 1960

A study of the quantum mechanical tunneling effect in a wide variety of germanium narrow p-n junction systems was reported. Such junctions have been fabricated with indium alloying material containing varying amounts of gallium doping and with degenerate germanium doped with arsenic, phosphorus and combinations of these. The highest current ratios have been observed when using arsenic doped germanium; however, the highest current densities thus far attained (4000 amp/cm^2) have been observed when using the phosphorus plus arsenic doping. Negative and positive temperature dependences of the current maximum have been both observed. These would appear to reflect independently: (1) the temperature effect on the energy distribution of free carriers about the Fermi level in the carrier bands; (2) the temperature effect due to the sensitivity of the tunneling probability to the temperature dependent E_g. At liquid nitrogen temperature a structure is observed in the minimum current region of the current voltage characteristics obtained from junctions fabricated with germanium doped with phosphorus. This suggests a mechanism of tunneling from carrier band to carrier band via deep lying intermediate states. This hypothesis is supported with the results of irradiation with 7-Mev electrons. It is observed that the predominant effect irradiation is the increase of current minimum.

6738 TEMPERATURE DEPENDENCE OF CURRENT IN ESAK DIODES by R. A. Logan and A. G. Chynoweth (Bell Labs.); Bull. Am. Phys. Soc., Ser. II, Vol. 5, p. 160(A), Mar. 21, 1960

As the applied forward bias is increased in an Esaki diode, c observes first a current maximum, I_p, then a current minimur I_v, and finally the ordinary diode forward current. I_v is we in excess of the ordinary diode current as extrapolated from t portion of the curve at high forward bias. Measurement of I_p and I_v over the temperature range 10°-350°K in Si, Ge and InSb diodes were reported. The shape of the I_p vs T curves shows structure in the case of Si, but not for Ge or InSb. Thi is in agreement with similar measurements of the reverse curr flow where the current was shown to be due primarily to inter nal field emission across the indirect energy gap, E_I, in Si, and the direct gap, E_D, in Ge and InSb. The temperature va iation of I_p is determined by that of E_D for Ge and InSb; but for Si, in addition to the temperature variation of E_I there is contribution due to that of the phonon density, thus giving ris to the observed structure. No such phonon effects have been observed in I_v, even in the case of Si. This fact restricts the model which may be proposed for this excess current, and in particular, it appears to rule out one hypothesis for I_v, namel indirect transitions with photon emission.

6739 GALLIUM ARSENIDE TUNNEL DIODES by N. Holonyc Jr. and I. A. Lesk (GE); Proc. IRE, Vol. 48, pp. 1405-1409, Aug. 1960

The fabrication and properties of GaAs tunnel diodes are described. The material preparation is discussed and devices which have been fabricated consistently with peak to valley current ratios >15:1, with voltage swings in the range from 0.9 to 1.2, and with current densities from 2000 amp/cm^2 to over 10,000 amp/cm^2 (and with correspondingly low capacitances, e.g., as low as 0.2 μμf/ma and g/C figures of merit as high as 5×10^{10} sec^{-1} are described. The temperature behavior of typical units is presented. Applications particularly well suited to GaAs units are mentioned.

6740 SHOT NOISE IN TUNNEL DIODE AMPLIFIERS by J. J. Tiemann (GE Res. Labs.); Proc. IRE, Vol. 48, pp. 1418-1423, Aug. 1960

The contributions of Johnson noise and shot noise to the noise i a tunnel diode are analyzed according to a simple theoretical model. The current stream flowing across the junction in one direction is assumed to be uncorrelated with that flowing across the junction in the opposite direction, and both current streams are assumed to produce full shot noise. A simple parabolic bar structure is also assumed. There is qualitative, but not quantitative, agreement between the predictions of this model and th experiment. On the basis of some simplifying assumptions (whi are consistent with the experiment), the noise figure of a tunne diode amplifier is calculated. A simple graphical method of determining the approximate noise figure of a diode from its cu rent voltage characteristic is presented. It is found that the noise figure has a broad minimum centered about a point slight higher in bias than the bias value for maximum negative conduc ance.

Electron-Electron Scattering in N-P Tunneling - See 6700

Tunneling in InSb: Magnetic Field Effects - See 6701

6741 ANOMALOUS SURFACE CHANNELS ON SILICON P-N JUNCTIONS by R. Solomon (Hughes Semicon.); J. Appl. Phys., Vol. 31, pp. 1791-1799, Oct. 1960

The use of a chopped-light spot to explore the photoresponse of silicon p-n junction surfaces is discussed. Anomalous channel responses, extending in some cases to distances of 100 mils or more, have been observed on accumulation layer and intrinsic barrier surfaces. The phase shift of the induced a-c photocurrent is measured as a function of the distance of the light spot from the junction and phase shifts of more than 380° have been observed for the anomalous channels. Experimental evidence which shows that the excessive phase shift is due to multiple trapping of the injected carriers at surface interface states is presented. Additional evidence indicates that the anomalous channels are a result of an interaction of the fringing field with the slow surface states.

Excess Reverse Current due to Metal Precipitates - See 6754

6742 VISIBLE LIGHT EMISSION AND MICROPLASMA PHENOMENA IN SILICON P-N JUNCTION, I. by M. Kikuchi (Electrotech. Lab., Tokyo) and K. Tachikawa (Res. Lab., Tokyo); J. Phys. Soc. Japan, Vol. 15, pp. 835-848, May 1960

Experimental results on the visible light emission and microplasma phenomena in a silicon p-n junction are described. It has been found that the microplasma spot in the p-n junction can be located by scanning a small chopped light spot on the junction surface. Combining this method of location of the microplasma spot and observation by microscope, it is concluded that the light emitting spot does not necessarily coincide with the microplasma spot. Possibility of the effect of impurities on the light-emitting phenomena is discussed briefly in connection with recent experimental results on the visible light emission from a germanium p-n junction. A simple model of a p-n junction is proposed to explain the microplasma phenomenon.

6743 THEORY OF MICROPLASMAS IN SILICON JUNCTIONS by R. J. McIntyre (RCA Victor Res. Labs.); Bull. Am. Phys. Soc., Ser. II, Vol. 5, p. 375 (A), June 15, 1960

Avalanche breakdown in silicon junctions is known to occur at tiny localized regions in the junction. The initial breakdown occurs at just one spot and is characterized by a series of randomly occurring pulses of about 100 μa. A statistical theory to explain this instability has been derived in which the current is assumed to fluctuate about an average value I_0, at which the multiplication factor M is exactly unity. At any other instantaneous current I, the multiplication factor is $M = 1 + dM/dI\,(I-I_0)$ where dM/dI is negative and results from the effects of the spreading resistance, distributed space charge in the ionized region, and localized heating. Calculations show that, for a typical diode, $I_0 dM/dI \approx -10^{-2}$ so that large fluctuations can be expected. From the calculated probability distribution for the instantaneous current, both the breakdown and turn-off probabilities of the microplasma have been deduced. The results are found to agree both qualitatively and quantitatively with experiment.

6744 STATISTICAL FLUCTUATIONS OF DONORS AND ACCEPTORS IN P-N JUNCTIONS by W. Shockley (Shockley Transistor); Bull. Am. Phys. Soc., Ser. II, Vol. 5, p. 161 (A), Mar. 21, 1960

Reverse biased p-n junctions usually have localized regions of low avalanche breakdown voltage due to dislocations and other inhomogeneities but even a structurally perfect crystal will have statistical inhomogeneities if the donors and acceptors are distributed at random. For example, in an abrupt (p+)n junction with breakdown voltage V_B, field E_B, space-charge width W, donor concentration N_D, and dielectric constant K, the number of donor ions cooperatively producing the avalanche field in any small region is approximately $m = N_D W^3 = 4KV_B^2/qE_B \cong 50\,V_B^2$ for silicon. For a 10-v junction m = 5000 and rms deviation is 70 or 1.4% leading to a ±1.4% mean spread of breakdown voltage; there are about $6 \times 10^6\,mm^{-2}$ such regions so that a few relatively low breakdown spots are probable. In abrupt Esaki tunnel diode junctions, the number of cooperating ions in W^3 is $(2KV/q)^{3/2} N_D^{1/2} \cong 100$ for $N_D > 10^{19}\,cm^{-3}$. Significant fluctuations in lower band edge may result just outside the space charge layer and contribute to the current and voltage values at the current minimum.

6745 UNIFORM SILICON P-N JUNCTIONS. I. BROAD AREA BREAKDOWN by R. L. Batdorf, A. G. Chynoweth, G. C. Dacey and P. W. Foy (Bell Labs.); J. Appl. Phys., Vol. 31, pp. 1153-1160, July 1960

The preparation of small area silicon p-n junctions which are free from exposed edges and dislocations passing through the space-charge region is discussed. It is believed that the space-charge regions of these junctions more closely resemble plane parallel geometries than any studied similarly hitherto. The avalanche breakdown phenomena in these uniform junctions are shown to be drastically different from those occurring in junctions that contain many dislocations. A comparison is made between the uniform junctions and one that is similar except that it possesses two breakdown-inducing sites, probably dislocations. In the latter junction the reverse characteristic shows two slightly separated rapid increases in current which coincide, biaswise, with the formation of two isolated light-emitting microplasmas, the occurrence of characteristic microplasma noise, and two singularities in the charge-multiplication characteristics. The uniform junctions show no such phenomena at intermediate voltages, breakdown occurring at a voltage roughly twice that at which the microplasmas form and which was previously thought typical for the given material resistivity. The light emission pattern accompanying breakdown in the uniform junctions appears more diffuse (giving rise to the term macroplasma) than in nonuniform junctions where it normally appears as an array of intense local spots (microplasmas). It is concluded that microplasmas are not a necessary accompaniment of avalanche breakdown in silicon, but that they tend to occur where there are field or lattice inhomogeneities.

6746 UNIFORM SILICON P-N JUNCTIONS. II. IONIZATION RATES FOR ELECTRONS by A. G. Chynoweth (Bell Labs.); J. Appl. Phys., Vol. 31, pp. 1161-1165, July 1960

A study of charge multiplication as a function of reverse bias in a number of uniform silicon p-n junctions (junctions free from defects which promote local avalanche breakdown sites) is reported. From the multiplication characteristics new data have been derived for the field dependence of the ionization rate (α) for electrons. As previously found in junctions containing dislocations, α obeys the empirical relation $\alpha = a_\infty \exp(-b/E)$, where a_∞ and b are constants and E is the field. Thus, this law is not simply a consequence of distortions to the junction introduced by dislocations or other microplasma-inducing defects. The ionization rates and breakdown voltages for the uniform junctions can be made consistent with older data (for non-uniform junctions) if the junction fields, as determined from capacitance measurements, in the new junctions are multiplied by 0.65. The most obvious interpretation of this experimental fact is that breakdown is made relatively easier at defects because the field is actually higher by a factor of 1.55. Possible causes of such an enhancement are discussed together with alternative hypotheses for the different ionization rates.

6747 INTERNAL FIELD EMISSION AT NARROW P-N JUNCTIONS IN INDIUM ANTIMONIDE by A. G. Chynoweth and R. A. Logan (Bell Labs.); Phys. Rev., Vol. 118, pp. 1470-1473, June 15, 1960

An experimental study of the field and temperature dependence of internal field emission in narrow p-n junctions in indium antimonide is discussed. Relatively good agreement, both qualitative and quantitative, is obtained between the experimental results and the usual expression for the barrier transparency. From studies of Esaki characteristics at low temperatures and from the observed temperature dependence of the tunnelling current, it is confirmed that the tunnelling transitions do not involve phonons. Also, it is shown that the temperature dependence of the barrier transparency is determined by that of the energy gap at $k = 0$.

External Photoelectric Emission From Back-Based Si Junctions - See 6722

Shot and Thermal Noise at High Current Levels - See 6766

6748 PLASTIC DEFORMATION OF GERMANIUM BY ALLOYING by W. J. Feuerstein (Motorola); AIME Trans., Vol. 218, pp. 251-254, Apr. 1960

Plastic deformation of the germanium adjacent to the regrowth material after the alloying of single crystal germanium with tin is discussed. Of several solder alloys investigated, plastic deformation was observed only in the germanium samples in contact with a tin-doped regrowth material. Dislocations were observed to move on a viewed (111) plane following thermal cycling of tin-doped regrowth material on germanium.

6749 THE DIFFUSED SHOT-MELTING TECHNIQUE FOR MAKING GERMANIUM AND SILICON P-N JUNCTION DEVICES by I. A. Lesk (GE); J. Electrochem. Soc., Vol. 107, pp. 534-536, June 1960

The diffused shot-melting technique which involves the melting and resolidifying of a piece (conveniently obtained in the form of shot) of semiconductor on a wafer of the same material (having essentially the same melting point) to form a single crystal boundary region, and the subsequent diffusion of impurities across the interface, is described. Shot-melting may be done so quickly that the interface coincides with the original surface of the wafer. Impurity contents of the shot and wafer may be chosen so that a variety of p-n junction devices results after diffusion, and several junctions may be made on the same wafer by this process to form more complex structures. Although lifetime and resistivity changes generally occur, they can often be minimized by subsequent treatment such as alloy gettering or annealing. Simplicity and flexibility of diffused shot-melting have made it a convenient laboratory technique for making many semiconductor devices.

6750 ELECTRICAL PROPERTIES OF VAPOR-GROWN Ge JUNCTIONS by M. J. O'Rourke, J. C. Marinace, R. L. Anderson, and W. H. White (IBM); IBM J. Res. and Dev., Vol. 4, pp. 256-263, July 1960

A method of fabricating p-n junctions and p-n junction devices by a closed-cycle iodide vapor-growth process is described. The electrical characteristics of junctions made by alternately depositing p-type and n-type germanium onto a germanium substrate compare favorably with those fabricated by other means. Device arrays, such as diode matrices, and multijunction structures have been made by this process. If sufficient control can be achieved, devices having a wide range of impurity distributions and geometric configurations will be possible.

6751 IMPURITY REDISTRIBUTION AND JUNCTION FORMATION IN SILICON BY THERMAL OXIDATION by M. M. Atalla and E. Tannenbaum; Bell Sys. Tech. J., pp. 933-946, July 1960

In the process of growing an oxide on doped silicon, electrically active impurities near the silicon/silicon dioxide interface are redistributed according to the diffusion coefficients and the distribution coefficient of the impurity between the oxide and the semiconductor. An analysis of the phenomenon predicts that single-junction or two-junction material can be obtained by oxidation of the surface of a compensated silicon crystal. For parabolic growth of the oxide, the surface concentration is independent of time, and the junction depth, gradient and sheet resistivity vary with $t^{1/2}$. This has been demonstrated experimentally by oxidation of a compensated p-type silicon crystal doped with gallium and antimony.

Gallium Arsenide Tunnel Diodes - See 6739

6752 LOCATION OF P-N AND L-H JUNCTIONS IN SEMICONDUCTORS by P. A. Iles, and P. J. Coppen (Def. Res. Telecommun. Estab.); Brit. J. Appl. Phys., Vol. 11, pp. 177-184, May 1960

The properties of p-n and l-h junctions and the methods which have used these properties to locate the junctions are summar-

ized. Critical comments are made, criteria which must be considered when choosing a method are given, and some methods for the elements germanium and silicon are recommended. Some brief examples of useful additions to semiconductor knowledge which result from practical application of these methods are also given.

6753 ION DRIFT IN AN N-P JUNCTION by E.M. Pell (GE); J. Appl. Phys., Vol. 31, pp. 291-302, Feb. 1960

If a reverse bias is applied to an n-p junction at a sufficiently elevated temperature to give either the donor or the acceptor ions appreciable mobility, the ions will drift in the electric field of the junction to produce an intrinsic semiconductor region between the n and p regions. Such ion drift offers a simple and straightforward method for investigating diffusion constants, as well as chemical interactions within the host lattice which affect this diffusion. Preliminary results indicate its feasibility for measuring the diffusion constant of Li in Si to as low as 10^{-18} cm^2/sec and also for measuring the effect of Li-oxygen and Li-acceptor interactions in decreasing the diffusion rate. Intrinsic regions resulting from ion drift have been used to produce diodes with breakdown in excess of 4000 volts from low resistivity silicon. In addition, they can be used to extend the frequency range of devices by virtue of the decrease in junction capacitance associated with such an incorporated intrinsic region. Ion drift has also been used for the fabrication of analog transistors, an early unit having an input impedance of 6 megohms, a power gain of 17 db and a voltage gain of 4.

6754 METAL PRECIPITATES IN SILICON P-N JUNCTIONS by A. Goetzberger and W. Shockley (Clevite Trans.); J. Appl. Phys., Vol. 31, pp. 1821-1824, Oct. 1960

Excess reverse current below avalanche breakdown caused by metal precipitates in silicon junctions is discussed. The current, believed due to Zener tunneling at localized high-field points, varies as V^n where n is between 4 and 7. The removal or prevention of metal precipitates by "gettering" from metallic or glassy oxide surface layers has been investigated. The results indicate that Ni and Zn layers have a limited gettering effect and that glassy layers, especially those of boron and phosphorus, have the greatest gettering effect.

TRANSISTORS - GENERAL

6755 EVIDENCE FOR FAST DAMAGE ANNEALING PROCESSES IN SEMICONDUCTOR DEVICES by J. Rothstein (Edgerton, Germeshausen and Grier); Bull. Am. Phys. Soc., Ser. II, Vol. 5, pp. 197-198 (A), Mar. 21, 1960

The exposure of germanium transistors to Godiva II and Triga pulses and the monitoring of I_{co} and H_{fe} were reported. The I_{co} response was separated into sum of (a) a current pulse of the same shape as the radiation pulse, (b) a permanent change proportional to the integrated radiation pulse, and (c) a transient decay. Superpositions of (a) and (b) alone gave excellent agreement with the rising edge of the pulse and the beginning of the decay, or with the rising edge of the pulse and the final level, with different (b) amounts in the two cases. Decay times of approximately 0.1 (10) msec were found for (c) with Godiva (Triga), calculated as decay between the two cases of superposed (a) and (b). (a) is ascribed to gamma induced hole-electron pairs, (b) to integrated neutron damage, (c) to rapidly annealing neutron damage, electronic, surface, or isotope decay effects. Radiation pulse time constants were 0.04(5) msec for Godiva (Triga) and so were separable from device relaxation. The fast decay may be due to recombination of electrons and holes or of close vacancies and interstitials, the slow decay to vacancy-interstitial or surface relaxation, with isotope decay unlikely.

Microalloy Diffused-Base Transistor Resistant to Neutron Radiation Damage - See 6767

Evaluation of Transistor Reliability - See 6730

6756 TRANSIENT OPERATION OF TRANSISTOR WITH INDUCTIVE LOAD by H. C. Lin, A. R. Hlavacek, and B. H. White (CBS Electronics); IRE Trans., Vol. ED-7, pp. 174-178, July 1960

A transistor operating with an inductive load may develop a collector-emitter short circuit when the transistor is suddenly turned off. The secondary breakdown of the collector characteristics determines the susceptibility to this type of failure. The secondary breakdown is greatly influenced by the reverse base current. The reverse base bias voltage and impedance affect the reverse base current in a predictable manner. The failure mechanism can be explained in terms of the characteristics of a four-layer device. Transistor requirements and design considerations are examined. For safe operations, the secondary breakdown current should be greater than the maximum operating current. When the reverse base current is minimized, the transistor is also protected. Several circuits which prevent the flow of reverse base current are presented.

6757 THE DESIGN AND FABRICATION OF A VHF MEDIUM-POWER TRANSISTOR by D. R. Carley and S. W. Daskam (RCA); 1960 Electron Dev. Mtg.

The design criteria of a diffused base mesa transistor capable of power output of 15 w at 100 Mc and 5 w at 200 Mc was described. Efficiencies of approximately 75% have been achieved as a 100 Mc oscillator. Recent developments in the area of improving the reproductibility of the diffusion of impurities into silicon were reviewed. A method involving a "sealed box" for boron diffusion was outlined and the results of its use explained. Techniques for applying high conductance metal layers to the base and emitter areas were described. Aluminum thicknesses of approximately 70,000 A have been achieved by evaporation. Alternate methods of providing contact layers were discussed.

Very High Frequency Power Transistors - See 6917

15-Watt Microalloy Diffused-Base Transistor - See 6767

6758 A HIGH VOLTAGE, HIGH SPEED, THREE TERMINAL P-N-P-N SWITCH by W. G. Ansley and A. N. Baker (Bell Labs.); 1960 Electron Dev. Mtg.

The design of high voltage, high speed, three terminal silicon p-ν-p-n switches for high pulse current applications was discussed. The resistivity of the ν region and the minimum base widths are determined by the minimum breakover voltage requirement. The dependence of the delay and turn-on times and trigger requirements on the two base widths was then analyzed. It was pointed out that the breakover voltage, speed, and peak current requirement in combination with the desire for a low "on" drop necessitates stringent control of the resistivity of the ν material during processing. The emitter area and emitter contact sheet resistance are determined by the peak current requirement. Other design features of the device were also discussed. Representative values of the device parameters for various designs were given. In typical applications, the devices are capable of switching from 500 v to 50 a with turn-on times of 0.05 μsec.

6759 GERMANIUM P-N-JUNCTION-TUNNEL-JUNCTION COMBINATION DEVICES by I. A. Lesk and H. A. Jensen (GE); Solid-State Electronics, Vol. 1, pp. 183-187, July 1960

Germanium p_t-n-p transistors, with a tunnel-junction emitter and a normal-junction collector, made by a combination of diffusion and alloying processes are discussed. They exhibit a current gain of essentially zero at low emitter currents, jumping abruptly to a finite value at the tunnel-junction peak current. This effect was applied to control the characteristics of four region switches, for which p_t-n-p-n structures were used. The p_t-n-p-n triode can be made to have its switching current equal to the tunnel-junction peak current, and its hold current equal to the tunnel-junction valley current. A base current equal to the peak current may be used to turn the devices on. These structures can be made to have quite stable properties from -70°C to $+100^{\circ}$C, since germanium tunnel diodes show little change in characteristics over this temperature range.

6760 DESIGN CONSIDERATION FOR A GERMANIUM P-N-P-N SWITCHING DEVICE WITH THREE CONTACTS AND A "SANDWICH" STRUCTURE by G. Wertwijn (Int. Rectifier); IRE Trans., Vol. ED-7, pp. 132-141, July 1960

The current I_{off} through a germanium p-n-p-n switch in the OFF state is described as a simple function of the control current I_t in its third contact. The device is of a so-called "sandwich" structure, the third contact being the outer edge of the middle p layer. The voltages considered are sufficiently small so that avalanche multiplication can be neglected. An expression for I_{off} is derived in terms of I_t and a, b, and c, device parameters determined by the physical and geometrical structure. The conditions for switching into the ON state are given and the temperature dependence of the parameters is predicted. The experimental results are found to be in good agreement with the design theory.

6761 ON THE DETERMINATION OF THE EXTRINSIC EQUIVALENT CIRCUIT PARAMETERS OF DRIFT TRANSISTORS by M. B. Das (Imperial Coll., London); J. Electronics Control, Vol. 8, pp. 351-363, May 1960

Methods of determining the 'effective' extrinsic base resistance and collector capacitance of alloyed and diffused graded-base transistors are presented. The common base short-circuit output and input admittances are measured at frequencies much less than the cut-off frequency of the transistor and are particularly suitable for devices where the base contact is made very close to the emitter. Extrinsic base resistance measurements made in several types of graded base transistor by these and other methods are compared. The validity and accuracy of the approximate equivalent circuit representation of the extrinsic base properties by an 'effective' constant resistance are discussed.

6762 TRANSISTOR SCALING THEORY by W. E. Roach (Pacific Semicon.); 1960 IRE WESCON Conv. Rec., Part 3, pp. 65-71

Basic principles for the application of scaling theory to the problem of increasing the power capability of a certain class of high-frequency transistors are given. Effects of the scaling process on transistor characteristics and performance are predicted on a theoretical basis. Measured values for a range of sizes over a 2500 to 1 maximum collector-current range are compared with the theoretical values. It is concluded that the application of scaling principles represents a valid and useful approach to the problem of extending the power capability of high-frequency transistors.

6763 A MODIFICATION OF THE THEORY OF THE VARIATION OF JUNCTION TRANSISTOR CURRENT GAIN WITH OPERATING POINT AND FREQUENCY by A. W. Matz (Assoc. Transistors); A. T. E. J., Vol. 16, pp. 96-109, Jan.-July 1960

A modified solution of the continuity equation for minority carrier flow in junction transistors is discussed. The solution is obtained by adhering strictly to the space-charge neutrality approximation and applying alternative boundary conditions which differ from those usually taken principally in that a finite minority carrier density is permitted at the collector. An extension of the modified analysis to a-c conditions is given and a comparatively simple working formula for the intrinsic short-circuit a-c gain is determined as a function of operating point and frequency. The common-base cut-off frequency f_α is evaluated and the maximum in the variation of f_α with emitter current, which has been observed experimentally, is associated with reduced d-c emitter efficiency at high levels and is related to the corresponding fall-off in d-c alpha. Experimental results are presented to show that, for a transistor with given cut-off frequency, both the electrical and metallurgical base widths are smaller than is normally supposed. $\partial W/\partial Vc$, however, is larger than normally supposed as evidenced by measurements of punch-through voltage V_p. A theoretical explanation of both effects is given.

6764 ANALYTICAL STUDIES ON EFFECTS OF SURFACE RECOMBINATION ON THE CURRENT AMPLIFICATION FACTOR OF ALLOY JUNCTION AND SURFACE BARRIER TRANSISTORS by T. Sugano and H. Yanai (U. Tokyo); Proc. IRE, Vol. 48, pp. 1739-1749, Oct. 1960

Analytical formulas for the survival factor β of alloy junction and surface barrier transistors with various idealized geometries are derived by means of approximating methods. From these results, many useful design data such as the optimum radius ratio of the emitter electrode and the collector are obtained and the effect of curvature of the electrode surfaces is made clear. It is also pointed out that the survival factor can be expressed by four dimensionless quantities, thus establishing the principle of similitude among transistors having different surface recombination velocities and different geometrical dimensions of electrodes. The values of β calculated from these formulas are in good agreement with the experimental values previously obtained by Stripp and Moore from an analogy of three-dimensional electrolytic conductance.

6765 TRANSIENT BEHAVIOUR AND FUNDAMENTAL TRANSISTOR PARAMETERS by C. le Can (N. V. Philips); Electronic Applic., Vol. 20, No. 2, pp. 56-83, 1959-1960

The transient behavior of alloy junction transistors, both when switching on and switching off, is analyzed in detail. The approach employed permits a qualitative and in many cases a semi-quantitative interpretation of the transient behavior. Detailed discussion of the transient behavior is preceded by an analysis of the steady-state conditions. The consequences of voltage feed, current feed, and quasi-voltage feed are dealt with at some length. The relation of the transistor switching parameters to the more conventional parameters are discussed. The influence of transistor symmetry is investigated, and an electrical equivalent circuit for large-signal operation is given. An appendix dealing with junction diode "reverse recovery" is included.

6766 SHOT AND THERMAL NOISE IN GERMANIUM AND SILICON TRANSISTORS AT HIGH-LEVEL CURRENT INJECTIONS by B. Schneider and M. J. O. Strutt (Swiss Fed. Inst. Tech.); Proc. IRE, Vol. 48, pp. 1731-1739, Oct. 1960

An expression for noise figure at high current density in germanium and silicon alloy transistors in both the grounded base and grounded emitter configurations is derived. The derivation is based on a p-n junction equivalent circuit containing an inductance in addition to resistances and capacitances. Good agreement has been found between the calculated and experimental values of noise as a function of frequency.

6767 15-WATT MICROALLOY DIFFUSED-BASE TRANSISTOR by T. J. Miles and J. A. Sluss, Jr. (Philco); 1960 IRE Int. Conv. Rec., Part 3, pp. 3-9

The fabrication, characteristics, and applications of a germanium microalloy diffused-base power transistor with dissipation of 15 watts and f_t in the 25-50 mc range are discussed. The fabrication techniques employed yield base widths flat to two wavelengths of light. The device is more resistant to neutron radiation damage than previously investigated germanium alloy power transistors.

Design and Fabrication of a Diffused Base Mesa Transistor - See 6757

Diffused Shot-Melting Technique for Making Multi-Junction Devices - See 6749

Fabrication of Multi-Junction Structures by Vapor Deposition - See 6750

Triple Diffused Silicon Mesa Transistors - See 6917

6768 THE REGROWN-DIFFUSED TRANSISTOR by C. H. L. Goodman (GE Res. Labs., England); Solid-State Electronics, Vol. 1, pp. 188-193, July 1960

A new process for producing high-frequency n-p-n silicon transistors is described. The novel feature is the formation of a doubly doped region in contact with singly doped material by the direct melting of appropriately doped fragments on to the latter, followed by subsequent solidification. A diffusion cycle then enables the required transistor structure to be developed. The new technique is not limited to silicon and has a number of attractive features, among which are simplicity of apparatus, relatively high rate of production, and efficient utilization of material.

Two-Junction Formation in Si by Thermal Oxidation - See 6751

6769 A MASKING TECHNIQUE FOR VACUUM EVAPORATION by W. Rindner (Raytheon); Solid-State Electronics, Vol. 1, pp. 157-158, May 1960

A laboratory technique for producing a number of configurations of narrow, closely-spaced evaporated electrodes on semiconductor surfaces without the need for elaborate masks is described. The essential feature of the method is the use of a moveable wedge-shaped shield in contact with the surface to provide the separation between the electrodes. Extremely close contact between the wedge and the semiconductor is not required. The simultaneous evaporation of several electrodes is illustrated in two examples.

Evaporated High Conductance Metal Electrodes - See 6757

6770 ELECTRODE CONNECTIONS TO SEMICONDUCTIVE BODIES by G. Freedman (Raytheon); U. S. Pat. 2,948,836, Issued Aug. 9, 1960

A technique for making a strong mechanical contact to the thin base region of a grown junction transistor is described. An extremely small diameter wire, e.g., of tungsten, coated with a solder of the same impurity type as the base region, is stretched taut parallel to the base region. A current sufficient to cause the solder, but not the wire or the semiconductor, to melt is passed through the wire. Because neither the semiconductor nor the wire melts there is no spreading across the junctions. A strong mechanical contact results because of the large area of contact between the semiconductor and wire.

6771 SURFACE TREATMENT OF SILICON DEVICES by R. W. MacDonald (Bell Labs.); U.S. Pat. 2,948,642, Issued Aug. 9, 1960

Techniques for providing stable n- or p-type layers on the surfaces of silicon devices are described. The device is 1) immersed in xylene, benzene or alcohol, 2) rinsed in deionized water at about 100°C for about 15 minutes, 3) rinsed in hot concentrated HNO_3 for 15 minues, 4) washed in running deionized water for 30 minutes at room temperature, 5) treated in dry pure oxygen flowing at a rate of 40 liters per minute at 920°C for 30 minutes, 6) annealed for 10 minutes at 300°C, 7) treated with HF fumes for 2 minutes, 8) etched in a solution consisting of 6 parts concentrated nitric acid and one part concentrated HF by volume for approximately 3 seconds. Steps 2 through 6 (steps 9 to 13) are then repeated. The process results in an oxide layer free of impurities because the initial oxide layer containing impurities is removed by step 7. If the semiconductor has no more impurities than about 10^{-13} atoms / cm^3, steps 9 to 12 produce p-type surfaces. If prior to thermal oxidation (step 12) the same wafer is briefly exposed to hydrofluoric acid vapor, an n-type surface layer results.

JUNCTION TRANSISTORS (Cont'd)

6772 EQUIPMENT FOR THE ENCAPSULATION OF SEMICONDUCTOR DEVICES by R. D. Knight (SERL); J. Sci. Instr., Vol. 37, pp. 197-199, June 1960

A method for encapsulating semiconductor devices is described. A hydraulically operated ram carries the semiconductor device and its envelope, loosely assembled, into a Pyrex chamber. Here the two are separated while the envelope is outgassed by e.c.h. in vacuum. They are then brought together, in vacuum or in gas, and the residual heat in the envelope melts a ring of tin in the mount collar to make the final seal. During the process the device is warmed sufficiently to drive off any moisture. A novel three-port valve controls the gas and vacuum supplies to the chamber. The equipment has been designed with a view to ultimate automation.

6773 FORMATION AND PROPERTIES OF LOW-MELTING GLASSES IN THE TERNARY SYSTEMS As-Tl-S, As-Tl-Se, AND As-Se-S by S. S. Flaschen, A. D. Pearson, and W. R. Northover (Bell Labs.); J. Am. Ceram. Soc., Vol. 43, pp. 274-278, May 1960

Low melting glasses in the As-Tl-S, As-Tl-Se, and As-Se-S systems which can be used to hermetically seal semiconductor devices are described. The glasses are stable, covalent, chemically durable, and dielectric. They exhibit good wetting properties with respect to most metals, and the permeability of the seals formed as well as the volume permeability of the glasses themselves appears to be extremely low. Linear thermal expansion co-efficients of some compositions are high, but associated thermal cracking problems are minimized to some extent by the low softening temperatures. The glasses can be evaporated and directly condensed (in vacuo) to form continuous, grain-free glassy films.

SURFACE BARRIER TRANSISTORS

Effect of Surface Recombination on Amplification Factor - See 6764

ANALOG TRANSISTORS

Fabrication of Analog Transistors by Ion Drift - See 6753

FUNCTIONAL UNITS (INTEGRATED DEVICES)

6774 SOLID STATE MICROLOGIC ELEMENTS by L. Kattner, J. Last, and J. Nall (Fairchild Semicon.); 1960 IRE WESCON Conv. Rec., Part 3, p. 134(A)

A family of low power-high speed micrologic elements was discussed. The elements, which include flip-flops, gates, adders, shift registers, and buffers, are compatibly designed to form an interconnectable set to perform all logic function requirements in a typical digital computer. In their design and use, the emphasis is placed on the logical function to be performed rather than on the circuit details of the element. The elements, fabricated on single silicon substrates by extensions of conventional transistor fabrication techniques, are packaged in multiple lead TO-5 and TO-18 headers for convenience in handling and to assure high reliability. The elements are designed for operation at a speed of 10 Mc over a temperature range of -55°C to ±125°C, with an average power dissipation per element of 30 mw. Operational data, reliability considerations, and systems applications were discussed.

6775 SHIFT REGISTER TRANSISTOR by J. T. Wallmark (RCA); U.S. Gov. Res. Rep., Vol. 33, p. 183 (A), Feb. 12, 1960 PB 143 634

Integrated circuits, i.e., circuits constructed by forming active and passive components into one piece of solid material, are described. An integrated semiconductor shift register and a number of other semiconductor circuits utilizing unipolar transistors have been developed. The unipolar transistor, although inferior to the conventional bipolar transistor in high-frequency response and power capabilities, may offer advantages in noise and radiation tolerance under certain conditions.

6776 THEORY OF A MONOLITHIC NULL DEVICE AND SOME NOVEL CIRCUITS by W. M. Kaufman (Westinghouse Electric); Proc. IRE, Vol. 48, pp. 1540-1545, Sept. 1960

A new simple structure which performs the function of a twin-T network, i.e., a null output is produced at a single frequency, is discussed. This new structure has the advantage of being very small, simple to fabricate, and easy to use in conjunction with transistorized circuits. The theory of operation of the device, experimental verification of the theory, and some circuits containing the device are also discussed. The structure has been found useful to create a high-Q tuned amplifier, an oscillator, and a threshold transducer. The physical simplicity of the structure should result in a high degree of reliability and uniformity of response. The structure can be fabricated from semiconductor materials and is thus suited to "molecularized" or "integrated" solid state systems.

OTHER CONDUCTIVE DEVICES

6777 THE OSCILLISTOR - NEW TYPE OF SEMICONDUCTOR OSCILLATOR by R. D. Larrabee and M. C. Steele (RCA Labs.); J. Appl. Phys., Vol. 31, pp. 1519-1523, Sept. 1960

The oscillistor, a semiconductor oscillator which utilizes a new magneto-oscillatory effect observed in the electron-hole plasma in a semiconductor is described. The plasma can be produced by techniques such as contact injection and optical or thermal excitation of minority carriers. When the semiconductor is subjected to an electric field (through suitable contacts) and a magnetic field, current oscillations can be detected across a series load resistance. Experiments suggest that the oscillistor mechanism involves a magnetically induced interaction of the bulk plasma of electrons and holes with the exposed free surface areas of the specimen.

Crystal Type Resistors - See 6918

Varistors for Surge Protection of Silicon Rectifiers - See 6919

6778 A NEW SEMICONDUCTOR MICROWAVE MODULATOR by H. Jacobs, F. A. Brand, Jr., M. Benanti, and J. Meindl (USASRDL) and R. Benjamin (Monmouth Coll.); 1960 IRE Int. Conv. Rec., Part 3, pp. 155-164

A new semiconductor device for use as an amplitude modulator for microwave transmission is proposed. The principle of action depends upon the increase of absorption with an increase of conductivity caused by the injection of excess minority carriers. Experiments conducted at 9600 mc indicate little or no phase and frequency modulation. The mechanism of the modulation action is discussed as well as the device design.

6779 SOME DEVICE ASPECTS OF MULTIPLE MICROWAVE REFLECTIONS IN SEMICONDUCTORS by H. Jacobs, F. A. Brand, J. Meindl, M. Benanti (USASRDL), and R. Benjamin (Monmouth Coll.); 1960 IRE WESCON Conv. Rec., Part 3, pp. 42-48

The effects of absorption and multiple reflections within the medium on the transmission of microwave energy through a semiconductor such as high resistivity germanium are analyzed. The dependence of these properties on frequency, sample length, and conductivity has been determined analytically and experimentally verified. Variation of the conductivity by injected carriers results in changes in power transmitted. New devices such as an amplitude modulator with little or no change in phase, a phase shifter with no change in amplitude and other optical-electrical devices appear feasible.

PHOTODEVICES

6780 CONTACT GEOMETRY AND DETECTOR ORIENTATION CONSIDERATIONS IN MAXIMIZING PHOTOCURRENTS by Y. T. Sihvonen and D. R. Boyd (GM); Bull. Am. Phys. Soc., Ser. II, Vol. 5, p. 105 (A), Mar. 4, 1960

When photoconducting crystals are prepared for the purposes of detecting radiation, there is, in addition to the need for selecting suitable contact materials, the problem of arranging contact and crystal geometries relative to the radiation source so that optimum photocurrents will result. An analytical analysis undertaken to derive a general photoconductance equation for radiation incident onto a photoconductor incased between two materials serving as contacts was presented. This equation includes effects of all multiple reflections but does not incorporate scattering losses or interference effects. Specific cases were discussed to bring out pertinent ideas, including the desirability of having transparent contacts. Suitable transparent ohmic contacts to CdS yield photocurrents which are orders of magnitude greater than those obtained with end contacted specimens.

High Electric Fields in Shadow Regions on Photoconductors - See 6718

6781 NOISE IN InSb PHOTODIODES by B. R. Pagel (Texas Instr.); Bull. Am. Phys. Soc., Ser. II, Vol. 5, p. 186 (A), Mar. 21, 1960

Experimental investigations of the noise generation in seven InSb infrared photovoltaic solid-state diodes operated at 77°K were reported. The noise was measured with the photodiodes viewing only the infrared radiation of a black-body cavity at room temperature. The object of the experiment was to compare the total measured noise with the noise component generated by the background radiation. This latter component is associated with the random incidence of photons on the detector. It is calculated from the relation $\langle i^2 \rangle / \Delta f = 2qI_{PH}$ where I_{PH} is the photoinduced current which is measured directly by biasing the diode to zero potential. Measurements of the total noise generated in the photodiodes as a function of the bias current through the diodes showed that the noise is a minimum when the detector is biased to zero voltage. The noise character of the detectors when biased to zero voltage were then studied in detail by measuring the spectra to obtain the white noise level. The measurements showed that generally there was no excess noise at one kilocycle or above and that the white noise in InSb photodiodes is almost wholly attributable to the noise generated by the background infrared radiation. The measured values were of the order of only one decibel above the theoretical value.

6782 GaAs, A SENSITIVE PHOTODIODE FOR THE VISIBLE by G. Lucovsky and P. H. Cholet (Philco); J. Opt. Soc. Am., Vol. 50, pp. 979-983, Oct. 1960

Highly sensitive photodiodes formed in n-type GaAs by diffusion of Cd and Zn are discussed. The photodiodes display a peak monochromatic sensitivity of 6×10^{-13} w (cps) $^{-\frac{1}{2}}$ at 8500 A and have half-sensitivity points at 9100 and 5600 A. The dynamic impedance of these detectors is in the order of one meg and their time constant, which is determined by the dynamic impedance and junction capacity, is on the order of 1 msec. Noise measurements in the 200-1500-cps region show no evidence of any 1/f component. Preliminary experiments indicate that these photodiodes are equally sensitive when operated in the back-biased or photoconductive mode. The detectors operate at room temperature and do not require encapsulation. Several detectors have been successfully immersed behind sapphire optics. The optical transparency of GaAs in the 1- to 5-μ region enables the detector to be used in front of a suitable I. R. detector, eg., InAs, in "two-color" detection systems. The sensitivity of this detector is found to compare favorably with a commercial photomultiplier.

6783 PHOTOVOLTAIC EFFECT DERIVED FROM THE CARNOT CYCLE by A. Rose (RCA Labs.); J. Appl. Phys., Vol. 31, pp. 1640-1641, Sept. 1960

An expression for the maximum power derivable from any photovoltaic device is developed in terms of the incident light intensity measured in units of black body radiation. The expression shows the linear dependence of photovoltage on light intensity at low light levels, the logarithmic dependence at intermediate light levels and the saturation at high light levels. The analysis is used to resolve a paradox proposed by W. Shockley.

6784 PHOTOEFFECTS IN NONUNIFORMLY IRRADIATED P-N JUNCTIONS by G. Lucovsky (Philco); J. Appl. Phys., Vol. 31, pp. 1088-1095, June 1960

A theoretical basis for the interpretation of photoeffects observed in nonuniformly irradiated p-n junctions is presented. Differential equations describing the junction photovoltage are developed through an application of the continuity and diffusion equations. Solutions of the small-signal steady-state photoeffect equation indicate that the effects of nonuniform irradiation become increasingly important as the ratio of the lateral

to the transverse resistance increases. A parameter a, which is designated as the lateral-fall off parameter, is a measure of this resistance ratio. The lateral photovoltage resulting from nonuniform irradiation can be eliminated by reverse biasing the junction into saturation. Experimental curves in agreement with the predictions of the analysis are presented.

Photoemission in the Photovoltaic Response of Cu-CdS Cells - See 6721

6785 EFFICIENCY OF SOLAR ENERGY CONVERTERS by H. J. Queisser and W. Shockley (Shockley Transistor); Bull. Am. Phys. Soc., Ser. II, Vol. 5, p. 160(A), Mar. 21, 1960

Calculations for the theoretical efficiency of solar cells generally use empirical information on the current-voltage characteristic of p-n junctions. In order to find an upper theoretical limit, an ultimate efficiency has been calculated for the ideal case in which there is only the radiative recombination required by the principle of detailed balance between created hole-electron pairs and the cell is entirely surrounded by a blackbody of sun temperature. The fraction of this ultimate efficiency has been calculated for a real solar energy converter, where nonradiative recombination processes are more frequent than radiative ones by a factor ρ, estimated from respective lifetimes. The limited solid angle subtended by the sun and reflectivity have been taken into account. Maximum power output efficiency at matched loads has been obtained with band gap, temperature, and ρ as parameters. The results were compared to experimental yields.

6786 CHARACTERISTICS OF A HIGH SOLAR CONVERSION EFFICIENCY GALLIUM ARSENIDE P-N JUNCTION by E. G. Bylander, A. J. Hodges, and J. A. Roberts (Texas Instr.); J. Opt. Soc. Am., Vol. 50, pp. 983-985, Oct. 1960

The characteristics of high efficiency gallium arsenide solar cells are discussed. Their open-circuit voltage is commonly greater than 0.8 v and the short-circuit current density collected is about one-half that calculated on the basis of absorbed photons. The temperature coefficient for maximum power operation is $-0.0036/^{\circ}C$. Both spectral emissivity and spectral response are reported.

6787 LIMITATIONS AND POSSIBILITIES FOR IMPROVEMENT OF PHOTOVOLTAIC SOLAR ENERGY CONVERTERS. PART I: CONSIDERATIONS FOR EARTH'S SURFACE OPERATION by M. Wolf (Hoffman Electronics); Proc. IRE, Vol. 48, pp. 1246-1263, July 1960

Seven factors limiting the performance of photovoltaic solar energy converters are listed and explained. Various possibilities for the improvement of technology determined limitations in the silicon solar cell are investigated. Suitable materials other than silicon are considered, and new methods of approach, such as the multilayer and the multiple transition solar cell, are discussed. Both of these methods yield theoretically large improvements, but realization depends on further advances in compound semiconductor technology and in knowledge about localized centers in the forbidden gap. Limit conversion efficiencies of 38.2 per cent for a 3-layer cell and of 51 per cent for a 3-transition cell, compared to 23.6 per cent for a single p-n junction, single transition cell, are obtained. The possible merits of the application of the graded energy gap to photovoltaic energy converters are also discussed, and potential improvement in collection efficiency is found for certain cases.

6788 GRAIN-BOUNDARY PHOTORESPONSE by W. W. Lindemann and R. K. Mueller (Gen'l Mills); J. Appl. Phys., Vol. 31, pp. 1746-1751, Oct. 1960

Grain-boundary photodetector sensitivity measurements which indicate an expected minimum detectable power of better than 10^{-14}w are discussed. Major factors governing the sensitivity are the minority carrier lifetime and the distance of the boundary from the irradiated surface. Spectral measurements show an added absorption edge response at about 1.67μ and 1.72μ. This added response could be caused by deep-lying acceptor levels or by excitons with a long lifetime. Experimental evidence points to direct absorption at the grain boundary as the most likely reason for the absorption edge irregularities.

6789 TIME DISCRIMINATION IN SOLID-STATE INFRARED QUANTUM COUNTERS by J.V. Jelley (Harvard U.); J.Appl. Phys. Vol. 31, pp. 1145-1146, July 1960

Various considerations in the practical realization of the infrared solid-state quantum counter recently proposed by Bloembergen are discussed. It is suggested that a high degree of discrimination between the quantum to be counted and the optical pumping flux could be attained by a time-sequence switching system; it is estimated that an isolation of ~160 db might be required. The proposal demands that at least one of the levels in the crystal have a long lifetime, and a simple expression for the overall efficiency of the detector in this case is derived. An additional gain in efficiency and isolation would result if "double pumping" were used, with detection in the ultraviolet. In conclusion a suggested layout of components incorporating the switching scheme is presented.

THERMISTORS

Positive Temperature Coefficient Thermistors with Switching Characteristics - See 6920

MAGNETIC DEVICES

6790 STEPPED TRANSFORMERS FOR PARTIALLY FILLED TRANSMISSION LINES by D. J. Sullivan and D. A. Parkes (Sperry Microwave Electronics); IRE Trans., Vol. MTT-8, pp. 212-217, Mar. 1960

In recent years partially filled transmission lines have been used to improve the characteristics of various ferrite and garnet devices. A generalized outline for determining the approximate effective guide wavelength and characteristic impedance of two types of (dielectric-loaded) partially filled transmission line is presented. The results are used to determine the geometries required for the design of optimum stepped transmission line transformers. The stepped transitions are designed to yield a Tchebycheff type response for any given bandwidth. The measured results for stepped transitions in partially

filled coaxial line and partially filled double ridge waveguide are presented. The data is found to approximate the theory closely.

6791 MAGNETICALLY TUNABLE MICROWAVE FILTERS EMPLOYING SINGLE CRYSTAL GARNET RESONATORS by P.S. Carter, Jr. (Stanford Res. Inst.); 1960 IRE Int. Conv. Rec., Part 3, pp. 130-135

Two new types of magnetically tunable microwave filters which employ small (approximately 0.050 inch diameter) single crystal yttrium-iron-garnet spheres for the resonant elements are described. These are narrow-band filters, i.e., about 0.2 - percent bandwidth, and are tuned over a broad band of frequencies by means of a varying d-c magnetic field. One filter employs a single garnet resonator and is magnetically tuned over a frequency range from 7 to 11.2 kmc. The other is a double-tuned filter employing two garnet resonators and has been tuned over a frequency range from 8 to about 14 kmc. Measured insertion losses and response curves for both experimental filters are presented.

6792 WALKER MODES IN LARGE FERRITE SAMPLES by B. A. Auld (Stanford U.); J. Appl. Phys., Vol. 31, pp. 1642-1647, Sept. 1960

The modes of resonance for a ferrite strip and a ferrite post resonator between conducting planes are found by taking appropriate combinations of uniform plane-wave solutions. It is shown that magnetostatic resonances (Walker modes) may exist even when the resonator dimensions are arbitrarily large, provided the mode indices satisfy certain restrictions.

Properties of Gallium Iron Oxide Single Crystal Resonators - See 6681

Broadband Coaxial Isolators - See 6921

6793 STUDY OF MICROWAVE FERRITE DUPLEXERS by L. Levey and L. M. Silber (Brooklyn Polytech. Inst.); U. S. Gov. Res. Rep., Vol. 34, p. 156 (A), Aug. 19, 1960 PB 146 792

The development of a microwave circulator in which the ferrite element is in the form of a hollow tube of rectangular cross-section is discussed. This ferrite geometry lends itself to fast switching applications. The requisite properties of ferrite materials for optimum operation of a switching circulator and the development and shaping of suitable materials are considered. The switching performance of a prototype circulator is described.

6794 A Y-JUNCTION STRIP-LINE CIRCULATOR by U. Milano, J. H. Saunders, and L. Davis, Jr. (Raytheon); IRE Trans., Vol. MTT-8, pp. 346-351, May 1960

The theoretical approach to the three-port symmetrical circulator is reviewed and presented in a form valid for the most general waveguide case. A strip-line Y-junction circulator is described and the performance of different units in the band 800-1600 mc is illustrated. The new type of device described offers, for the low-frequency region of the microwave spectrum, advantages of simple design, light weight, and great compactness with respect to the classical types. When operated with a permanent magnet it gives, in a bandwidth of about 4 per cent, isolation greater than 20 db, insertion loss $\leq$ 0.4 db, and input VSWR $\leq$ 1.20.

6795 EFFECT OF PREVIOUS HISTORY ON SWITCHING RATE IN FERRITES by R. W. McKay and K. C. Smith (U. Toronto); J. Appl. Phys., Suppl. to Vol. 31, No. 5, pp. 133S-134S, May 1960

Existing theories of switching of square-loop ferrites indicate that the rate of switching is a function of the present state of magnetization and of the applied field. Experiments which show that the switching rate is also dependent on previous history are described. Two cases have been studied. In the first case, the ferrite was partially switched to a predetermined extent by a pulse of variable amplitude and then the switching cycle was completed by a pulse of fixed amplitude. In the second, the ferrite was brought to the remanent state by a pulse of variable amplitude before the switching cycle. Changes as great as two to one in switching rate were produced by variations of previous treatment.

6796 FAST SWITCHING BY DOMAIN WALLS IN FERRITES by W. Wiechec and C. M. Kelley (Stanford Res. Inst.); J. Appl. Phys., Suppl. to Vol. 31, No. 5, pp. 131S-132S, May 1960

Experimental evidence indicates that small grain size is associated with faster domain wall switching in ferrite cores. It has been shown by H. Amar that small grain size contributed an additional energy to the wall energy density σ_ω. Incorporation of this energy into the power equation $H \cdot (dM/dt) = \lambda H_e^2$ reveals that the loss coefficient decreases more than σ_ω increases, and, therefore, faster switching results. A qualitative explanation for faster switching by domain walls in magnetic materials is given. The significant variables in the switching coefficient equation are "d", T_c, K, and α. Experimental data show that the switching coefficient is lowered by decreasing values of the first three variables. Considerably faster switching is predicted when similar cores with grain sizes less than 1 μ are used.

6797 MAGNETIC FIELDS OF TWISTORS REPRESENTED BY CONFOCAL HOLLOW PROLATE SPHEROIDS by H. Chang (IBM) and A. G. Milnes (Carnegie Inst. Tech.); IRE Trans., Vol. EC-9, pp. 199-207, June 1960

The demagnetizing field in a twistor bit is analyzed in order to make it useful as a storage element. The analysis is based on the geometrical model of a confocal hollow prolate spheroid and the magnetic characterization of the material by $\bar{B} = \mu_0(H + M)$ where $\bar{M}$ is the intrinsic magnetization, constant in magnitude, but oriented by the external field. Demagnetizing factors for confocal hollow prolate spheroids are plotted against length-to-diameter ratio and wall thickness. Expressions for field intensities outside a twistor bit are given. Analogies between twistors and thin films are examined.

6798 MINIATURE MEMORY PLANES FOR EXTREME ENVIRONMENTAL CONDITIONS by R. Straley, A. Heuer, B. Kane, and G. Tkach (Indiana Genl.); J. Appl. Phys., Supp. to Vol. 31, No. 5, pp. 126S-128S, May 1960

Ferrite memory planes which are highly compact and can operate over the temperature range -55 to +125°C are described. Small size results from the use of a "continuous wire" method of inserting drive lines through memory planes and then folding the planes. This method eliminates the conventional frames and all solder connections between planes, increases reliability, and facilitates assembly of stacked memory planes. A typical folded stack of memory planes occupies as little as 2% of the vol-

ume of its conventional counterpart. The new miniature memory stacks perform as well as conventional units. The development of ferrite memory cores operable at ambients as high as 85°C, 100°C, and 125°C (together with the greatly reduced volume of the memory stack) allows operation under extreme environmental conditions with a minimum of space and power requirements. The folded memory planes are packaged with a heating element and control circuit which maintain the temperature of the cores at the maximum ambient. A tested prototype of twelve 16 x 16 memory planes, along with the heating element and control circuit, measures 2 in x 2-1/2 in x 2-1/2 in and has been successfully operated in the temperature range -55° to +125°C. Ferrite cores of both the "fast" relatively high drive and relatively "slow" lower drive type have been perfected. They are Mg-Mn ferrites with possible minor additions of other bivalent oxides.

6799 NEW MULTI-APERTURE MAGNETIC LOGIC ELEMENT by D. R. Bennion (Stanford Res. Inst.); J. Appl. Phys., Suppl. to Vol. 31, No. 5, pp. 129S-130S, May 1960

A new magnetic multi-aperture device (MAD) having general logic capability is described. This device can be used for either direct or complementary transfer of binary information, depending only on a simple change in wiring. AND and OR logic functions can be performed in the interconnecting circuitry, which consists only of conducting wire. Significant operating tolerances have been exhibited by the new element, which is simpler in structure and associated wiring than previous MADs having the same logic capability.

6800 MAGNETIC ANALOGS OF RELAY CONTACT NETWORKS FOR LOGIC by D. B. Armstrong, T. H. Crowley, U. F. Gianola, and E. E. Newhall (Bell Labs.); IRE Trans., Vol. EC-9, pp. 30-35, Mar. 1960

Two techniques for designing multi-aperture magnetic structures capable of realizing any specific logic function are described. The structures are made from rectangular hysteresis loop material. The designs are derived from the corresponding relay contact network by replacing each current carrying conductor in the relay circuit with its analog in the magnetic circuit, a flux-carrying conductor; replacing the emf with a pulsed mmf; and replacing each back contact with a saturable portion of the magnetic circuit in the topological equivalent of the contact network. A flux reversal through a saturated portion may then be blocked by means of an inhibiting current applied to a suitable winding, the current representing a logical input variable. Thus flux may be "steered" through the magnetic circuit in a manner analogous to the steering of current through the contact network. For planar structures the first technique may be used to obtain the analog of series-parallel and bridge type circuits; the second technique is suitable only for the analogs of series-parallel circuits. It is pointed out that the analog of a relay tree can be used as a standard structure suitable for realizing any Boolean function. Representative examples of both designs are shown, and experimental data are given.

6801 FERRITE FILMS -- NEW LOGIC AND STORAGE DEVICES by J. M. Brownlow, W. L. Shevel, Jr., and O. A. Gutwin (IBM); J. Appl. Phys., Suppl. to Vol. 31, No. 5, pp. 121S-122S, May 1960

The fabrication of magnetic devices for storage and switching applications in digital computers in the form of open flux path elements is described. The geometry employed is that of a planar film with thicknesses in the range of 5 to 50 μ and other dimensions in the fractional inch range. These elements have the advantages of a ferrite composition and of open flux paths without many of the disadvantages present in similar metallic devices. For use in storage systems, these devices possess excellent squareness characteristics and have coincident selection times comparable with ferrite-toroidal devices. Properties of these devices are given in terms of switching curves, low-frequency hysteresis loops, and one to zero-signal ratios. Other aspects that are discussed include disturb sensitivity of storage elements, heating effects due to high pulse repetition frequency and mechanical properties. For each of these, comparison is made with other types of magnetic elements such as toroids and metallic films. Applications are discussed in terms of drive requirements, packing densities, and switching times.

Preparation and Properties of Thin Ferromagnetic Films - See 6655

6802 OPERATION OF MAGNETIC FILM PARAMETRONS IN THE 100- TO 500- MC REGIONS by A. V. Pohm, A.A. Read, R. M. Stewart, Jr., and R. F. Schauer (Iowa State U. Sci. Tech.); J. Appl. Phys., Suppl. to Vol. 31, No. 5, pp. 119S-120S, May 1960

The behavior of thin magnetic films of Permalloy when used as time variable inductors is analyzed in terms of a modified Landau-Lifshitz equation. These results show that parametrons using time variable magnetic film inductors can be made to operate at reasonable power levels with large gains per cycle at oscillating frequencies in the 100- to 500-Mc region. The fabrication of magnetic film parametrons with strip line techniques is described. Calculations indicate that units with dissipations in the 10 mw range are feasible with existing techniques for operation in the 100- to 500- Mc region. Methods for advantageously using capacitive coupling between parametron units are discussed. These methods utilize the two new subharmonic states of a magnetic film parametron created by a bias reversal.

6803 DEVELOPMENT OF HIGH-SPEED COINCIDENT CURRENT MEMORY CORES by R. Eichbaum (Ford Motor); J. Appl. Phys., Suppl. to Vol. 31, No. 5, pp. 117S-118S, May 1960

In present day large computers the memory cycle is on the order of 8 μsec, requiring memory cores to switch in 1.5 μsec with a full select drive of approximately 0.7 amp. Memory cores suitable for use in such a computer can be fabricated from a $MgO \cdot MnO \cdot Fe_2O_3$ ferrite material. Using the same ferrite material, memory cores which have a switching speed of 0.4 μsec with a full select drive of approximately 1.0 amp have been developed. The procedure used to fabricate these high-speed coincident current memory elements is described. The drive current is reduced to approximately 0.7 amp when partial substitutions of CaO and Cr_2O_3 are made for MgO and Fe_2O_3, respectively, in the $MgO \cdot MnO \cdot Fe_2O_3$ core composition.

6804 NEW APPROACH TO HIGH-SPEED STORAGE -- LOW FLUX DENSITY MATERIALS by W. L. Shevel, Jr. and H. Chang (IBM); J. Appl. Phys., Suppl. to Vol. 31, No. 5, pp. 125S-126S, May 1960

A new approach toward overcoming the factors currently limiting the frequencies at which storage devices may be switched

from one information state to another is presented. Ferrite elements for random access storage which require a fraction of a microsecond for a cycle have been developed. Thus the ferrite switching time establishes a maximum switching rate given by the inverse of the total switching time in a cycle. However, operation of elements such as these in a large capacity memory at rates limited only by switching times is usually prevented by: deterioration of magnetic properties due to heating effects, increase in selection line impedance, and long transmission delays. A series of ferrimagnetic oxides with properties such that the limits on minimum cycle time are appreciably extended have been developed. The most important of these properties is the saturation flux density. Over a range of composition, flux densities which extend from 100-500 gauss have been obtained. The lower flux density results in an appreciably lower energy dissipation in the magnetic structure and consequently in higher switching rates for a given temperature rise within the magnetic material. In addition, temperature dependence of those magnetic properties which determine storage applicability is more favorable than with the better known ferrites. Toroids which are suitable for random access memories have been fabricated with these materials. These elements have been operated successfully in free air at repetition frequencies in excess of 2 Mc. The improvements in array characteristics that result are discussed in terms of impedances and transmission delays.

6805 DIRECTIONAL PARAMAGNETIC AMPLIFIER DESIGN by M. W. P. Strandberg (MIT); Proc. IRE, Vol. 48, pp. 1307-1320, July 1960

The radio-frequency parameters and the quantum-mechanical parameters entering into the design of paramagnetic quantum-mechanical amplifiers are described and discussed. The physical and electrical limitations on such parameters as gain-bandwidth product, gain stability, and nonreciprocity are described analytically and with design curves. Two realizations of nonreciprocal amplifiers are described and discussed. In particular, operation of a nonreciprocal amplifier at 9 kmc is described. Explanations for the observed properties of previously reported amplifiers are given, and steps necessary to achieve high gain-bandwidth product and reciprocity with paramagnetic amplifiers are described.

6806 CHROMIUM-DOPED TITANIA AS A MASER MATERIAL by H. J. Gerritsen, S. E. Harrison, and H. R. Lewis (RCA Labs.); J. Appl. Phys., Vol. 31, pp. 1566-1571, Sept. 1960

A discussion of the paramagnetic properties of Cr^{3+} in TiO_2, with particular reference to its use in solid-state masers, is given. Energy level diagrams for magnetic fields in the (110), (1$\bar{1}$0), (001), and (100) planes are included.

DIELECTRIC DEVICES

6807 PRINTED ALUMINUM CAPACITORS by F. Huber and W. Haas (Philco); Proc. IRE, Vol. 48, p. 1482 (L), Aug. 1960

The fabrication and properties of solid aluminum electrolytic capacitors are discussed. Pure aluminum is evaporated onto a substrate and oxidized anodically 10 to 20 minutes at room temperature. The oxidized film is cleaned with distilled water and counter electrodes are applied by evaporation of aluminum. Data on capacitors formed by several voltages are presented. For example, a capacitor formed to 20 v exhibits a capacity of 0.31 μf/cm^2, a leakage current of 0.005 μa/cm^2 at 2/3 of the forming voltage, and a dissipation factor of 0.050. As the forming voltage decreases, there is a larger scatter in the values of capacity and the dissipation factor increases. A working voltage of about 90 percent of the forming voltage is suggested. In several respects the aluminum capacitors are more easily fabricated than tantalum capacitors.

Solid Electrolyte Tantalum Capacitors - See 6922

SUPERCONDUCTIVE DEVICES

6808 AN IMPROVED FILM CRYOTRON AND ITS APPLICATION TO DIGITAL COMPUTERS by V. L. Newhouse, J. W. Bremer, and H. H. Edwards (GE); Proc. IRE, Vol. 48, pp. 1395-1404, Aug. 1960

A crossed film cryotron deposited on an insulated superconductor is described and analyzed. It has a time constant of less than one μsec and is approximately 100 times faster than the original crossed film cryotron. The d-c dissipation is less than five μw and the active area of each element is approximately 5×10^{-4} cm^2. These cryotrons and all their interconnecting circuitry can be deposited at one and the same time in a few simple steps. A cryotron storage circuit and a shift register based upon a principle unique to superconductors are described. The shift register is deposited in an area corresponding to 18,000 active elements per square foot. With this component density, a computer or memory containing more than one million elements can be operated in a one-cubic-foot container using a one-watt output liquid helium refrigerator.

6809 THIN FILM CRYOTRONS. PART I - PROPERTIES OF THIN SUPERCONDUCTING FILMS by C. R. Smallman (A. D. Little); Proc. IRE, Vol. 48, pp. 1562-1568, Sept. 1960

The characteristics of evaporated superconductive films as they apply to cryotrons are described. Their current-carrying capacity has been found to be proportional to width and proportional to thickness when the film is thinner than twice the penetration depth. Thermal effects caused by poor heat transfer to the bath distort the data, and the use of quartz substrates and low duty cycle pulse measurements help to reduce this distortion. The function of a superconductive reflector or ground plane under a film is discussed. The current-carrying capacity of such a film is increased because of effective cancellation of the normal component of magnetic field.

6810 THIN FILM CRYOTRONS. PART II - CRYOTRON CHARACTERISTICS AND CIRCUIT APPLICATIONS by A. E. Slade (A. D. Little); Proc. IRE, Vol. 48, pp. 1569-1576, Sept. 1960

The characteristics of the thin-film cryotron are described. The superconducting to normal transition in a tin gate 0.125 inch wide and 3×10^{-5} cm thick is controlled by current in a single lead control, 0.006 inch wide, which crosses the gate. Silicon

monoxide is used for insulation. The switching time of a cryotron circuit is dependent upon the inductance and resistance of the circuit. Therefore, it is important to reduce the inductance by using a superconductive ground plane and by reducing the length of all inter-connecting leads. Nonlocking flip-flops have been constructed, and a ring of five flip-flops have operated with a delay per stage of $\frac{1}{2}$ μsec.

6811 THIN FILM CRYOTRONS. PART III - AN ANALYSIS OF CRYOTRON RING OSCILLATORS by M. L. Cohen (A. D. Little); Proc. IRE, Vol. 48, pp. 1576-1582, Sept. 1960

A circuit analysis of cryotron ring oscillators which have been constructed to permit a study of the dynamic behavior of film cryotrons in circuits is presented. The analysis is concerned with the frequency-L/R time constant and circuit resistance-gate resistance relationships. Two analyses, based on different ideal characteristics, are made. The first treats each stage as a linear amplifier, and the second treats each stage as a switching circuit. Although the two analyses start with rather different assumed ideal characteristics, the results agree in many respects.

6812 SUPERCONDUCTING CONTACTS by J. I. Pankove (RCA Labs.); IRE Trans., Vol. ED-7, pp. 137-141, July 1960

The microscopic size of the contact between two crossed superconducting wires offers a practical way to make a class of superconducting devices which are operated at high speed by very small currents. The critical current through the contact can be modulated by a current flowing along one or both of the crossed superconductors. Several device possibilities are presented.

6813 THE "PERSISTOR" — A SUPERCONDUCTING MEMORY ELEMENT by E. C. Crittenden, Jr. and J. N. Cooper (U. S. Naval Postgrad. School) and F. W. Schmidlin (Space Tech. Labs.); Proc. IRE, Vol. 48, pp. 1233-1246, July 1960

The basic components of a Persistor memory element are a superconducting inductor in parallel with a switch element which is normally superconducting, but which becomes resistive when the current exceeds a critical value. When a suitable current pulse is applied to a Persistor memory element, a persistent circulating current is stored. A second pulse in the same direction as the first makes no change, but a pulse in the opposite direction reverses the circulating current and produces a voltage across the element. By mutual inductance coupling to two or more driving circuits, these memory elements can be made to operate in matrices similar to those employed with ferromagnetic cores. Persistor memory elements utilizing lead inductors and thin tin or indium films have performed typical memory unit functions for pulses of 15-μsec duration and a repetition rate of 15 mc. Performance at higher speeds is possible. The limiting speed is determined by the thickness of the thin film switch element and can be made as fast as is useful for the other parts of the associated circuits. The elements are well suited to compact printed circuit production with densities of a million per cubic foot possible.

6814 RECENT DEVELOPMENTS IN SEMICONDUCTOR STRAIN TRANSDUCERS by W. P. Mason, J. J. Forst and L. M. Tornillo (Bell Labs.); ISA 1960 Fall Instr. Automation Conf.

It was shown that some of the defects of lightly doped semiconductor strain gauges can be removed by going to considerably higher doping levels than have previously been employed. Measurements in the range from 5×10^{18} to 10^{20} boron atoms per cc in silicon result in a somewhat reduced gauge factor but one which is more constant with temperature and with strain. It was shown that there is a nonlinearity inherent in lightly doped semiconductor strain gauges. While various circuits can be used to take advantage of this effect and alleviate its deleterious effe the higher linearity of highly doped material is a decided advantage. Fluctuation noise is also less for a highly doped material and strains in the order of 3×10^{-10} have been measured by using such gauges. [Fall Instrument-Automation Conference and Exhibit, New York City, New York, September 26-30, 196

6815 EFFECT OF INITIAL STRESS IN VIBRATING QUARTZ PLATES by A. D. Ballato and R. Bechmann (USASRDL); Proc. IRE, Vol. 48, pp. 261-262 (L), Feb. 1960

Measurements of the frequency changes which occur when a compressional stress is applied to the edge of vibrating circular or square quartz plates of various orientations are discussed a the experimental apparatus is described.

6816 EXCITATION OF PIEZOELECTRIC PLATES BY USE OF PARALLEL FIELD WITH PARTICULAR REFERENCE TO THICKNESS MODES OF QUARTZ by R. Bechmann (USASRDL); Proc IRE, Vol. 48, pp. 1278-1280, July 1960

The parallel field excitation of piezoelectric plates, particularly of plates vibrating in thickness modes, and their resulting piezoelectric stress constants in general and of various quartz cuts are considered. Quartz AT-cut crystals excited by a parallel field are of practical interest for high precision frequency control and the data of the equivalent electric circuit of a 1000-kc AT quartz oscillator excited by a parallel field are given.

SOLID STATE DEVICE MEASUREMENTS

6817 TRACING TUNNEL DIODE CURVES by H. G. Dill and M. R. MacPherson (Hughes); Electronics, Vol. 33, pp. 62-64, Aug. 5, 1960

A tunnel diode curve tracer which traces the V-I curve of a tunnel diode including the negative resistance region on a conventional oscilloscope is described. A special low inductance

diode holder block using slabs of germanium for the circuit resistances and thin layers of mica between brass blocks with a silicone oil film for the capacitors is shown. The sine wave sweep circuit output is fed through a clamping circuit in order to limit the peak amplitude applied to the tunnel diode and eliminate retrace characteristics due to overheating. The test unit will accommodate the micro-miniature diode package as well as the TO-18 type, and with the power supply used will display currents to 600 ma.

200 Ampere Dynamic Test Set for a Full Wave Rectifier - See 6923

Transistor Curve Tracer for 200 Ampere Collector Curves - See 6924

6818 MEASUREMENT OF SWITCHING TRANSISTOR PARAMETERS by R. C. Johnston and R. L. Burke (Lincoln Lab.); Semicon. Prod., pp. 43-46, Feb. 1960

A system of transistor test sets which combines speed in loading with accuracy in both the d-c and high-frequency tests is described. The transistors are loaded into a ten-socket cartridge which is then inserted in sequence into the tests. Circuit diagrams for eleven test sets are given and the mechanical design of the cartridge and test sets is illustrated.

Transistor Thermal Test Set - See 6925

BASIC SOLID STATE DEVICE CIRCUITS

GENERAL

6819 TRANSFER FUNCTION SYNTHESIS OF ACTIVE RC NETWORKS by E. S. Kuh (U. California); IRE Trans., Vol. CT-7, pp. 3-7, Special Suppl., Aug. 1960; 1960 IRE Int. Conv. Rec., Part 2, pp. 134-138

A general method for synthesizing voltage transfer functions with complex poles and zeros using RC elements and a practical transistor amplifier is described. The method allows specified source and load resistances. The over-all network has a common ground and is economical in terms of the number of elements.

6820 APPLICATION OF SYNTHESIS TECHNIQUES TO ELECTRONIC CIRCUIT DESIGN by F. H. Blecher (Bell Labs.); IRE Trans., Vol. CT-7, pp. 79-91, Special Suppl., Aug. 1960; 1960 IRE Int. Conv. Rec., Part 2, pp. 210-222

Four very useful RC-active network synthesis techniques developed during the past decade are reviewed and compared from the points of view of generality and sensitivity. It is pointed out that at frequencies below about 30 kc, RC-active networks are competitive with other methods of filter design. Two of the synthesis techniques are used to realize a transistorized twelfth-order Tchebycheff parameter bandpass filter centered at 18 kc.

Monolithic Semiconductor Twin-T Network - See 6776

6821 THIN FILM CIRCUIT TECHNIQUES by J. J. Bohrer (Int. Resistance); IRE Trans., Vol. CP-7, pp. 37-44, June 1960

The techniques used in producing thin film circuits are discussed. Conductive, resistive, and insulating films are evaporated separately onto glass substrates to form resistors, capacitors and interconnections. Active elements, transistors and diodes, are mounted in holes drilled through the substrates. Studies aimed at developing thin film active elements are briefly discussed. Several possible methods of interconnection are presented.

Silicon Rectifier Surge Protector - See 6919

6822 COMPLEMENTARY TRANSISTOR CIRCUITS by F. Oakes and C. Thompson (Ferguson Radio); Electronic Engrg., pp. 438-440, July 1960

A number of circuits useful for pulse and digital applications which use complementary transistors are described. Several of these have no vacuum tube circuit equivalent, and provide faster operation or greater flexibility than could be obtained with only one single operating polarity.

AMPLIFIERS

6823 NOISE IN NEGATIVE-RESISTANCE AMPLIFIERS by P. Penfield, Jr. (MIT); IRE Trans., Vol. CT-7, pp. 166-170, June 1960

Negative-resistance amplifiers that consist of a noisy negative resistance imbedded in a lossless three-terminal-pair linear network to make a two-port amplifier are analyzed. It is shown that Haus and Adler's noise measure M_e is not constrained to lie between two eigenvalues of a noise matrix, as is the case for bona fide two-port amplifiers. Instead, it is always equal to its optimum value, and is independent of the (lossless) imbedding network used. As a corollary of this, the noise figure of such an amplifier fails to equal its optimum value only insofar as the exchangeable gain is not high. The single value of noise measure may be computed from any simple lossless circuit at hand, or else from the exchangeable noise power of the noisy negative resistance.

6824 A LOW-DRIFT TRANSISTOR CHOPPER-TYPE D.C. AMPLIFIER WITH HIGH GAIN AND LARGE DYNAMIC RANGE

by I. C. Hutcheon and D. Summers (George Kent); Proc. IEE, Vol. 107B, pp. 451-465, Sept. 1960

A transistor chopper-type d-c amplifier for use in the field of process measurement and control is described. The amplifier has a voltage drift below ±10 μv and a current drift below $\pm 4 \times 10^{-9}$ amp. Since the forward gain in the steady state is about 10 kv/μa and 15 volts/μv, the full output swing of 0 to 5 volts is provided by an input signal little greater than the drift. The application of sufficient overall negative d-c feedback therefore enables input signals of 0-10 mv or 0-4 μa to provide full output with an accuracy of ±0.1%. The low drift is obtained by operating the transistor chopper at 200 cps, stabilizing its temperature within $\pm 2^{\circ}C$, and providing suitably stable waveforms to drive the transistor and compensate for its voltage offset.

6825 BROAD-BAND UHF DISTRIBUTED AMPLIFIERS USING BAND-PASS FILTER TECHNIQUES by F. C. Thompson (HRB-Singer); IRE Trans., Vol. CT-7, pp. 8-12, Special Suppl., Aug. 1960; 1960 IRE Int. Conv. Rec., Part 2, pp. 139-148

The basic principles of distributed amplification as applied to the uhf band-pass amplifier are described. The modifying factors of major importance are evaluated and techniques for optimizing amplifier performance capabilities in the uhf region are discussed. Measured performance characteristics of several amplifiers are presented in order to show the practical capabilities of band-pass amplifiers in the uhf region. In addition, performance data for a transistorized distributed amplifier having useful gain to 700 Mc are presented.

6826 SEMI-CONDUCTOR SIGNAL CONVEYING CIRCUITS by L. E. Barton (RCA); U. S. Pat. 2,924,778, Issued Feb. 9, 1960

A double-ended balanced driving source for a Class B junction transistor push-pull amplifier which can be resistance coupled to the push-pull output stage is described. Germanium diodes in the base circuits of the output transistors alternately cut off the transistors during application of the signal voltage, eliminating the coupling transformer. Additional gain can be obtained by using junction transistors in place of the germanium diodes.

6827 LOW-NOISE PARAMETRIC AMPLIFIER by R. C. Knechtli and R. D. Weglein (Hughes Aircraft); Proc. IRE, Vol. 48, pp. 1218-1226, July 1960

A reformulation of the theory of the parametric amplifier permitting the prediction of noise temperature and pump power in terms of the physical parameters of the nonlinear element and circuit is presented. The results of this analysis are supported by careful experiments at S-band using a gold-bonded germanium semiconductor diode. These results are: 1) performance of a parametric amplifier using semiconductor diodes with respect to noise temperature and pump power can be accurately predicted, once the diode and circuit parameters have been measured, 2) the ultimate limitation on noise temperature depends simply on the product of the diode cutoff frequency and the normalized capacitance swing, and 3) the derived figure of merit for the diode can serve as a basis for optimum design of the semiconductor parameters.

6828 GAIN INCONSISTENCIES IN LOW-FREQUENCY REACTANCE PARAMETRIC UP-CONVERTERS by A. K. Kamal and A. J. Holub (Purdue U.); Proc. IRE, Vol. 48, pp. 1784-1785 (L), Oct. 1960

An explanation for the difference between calculated and actual gain in parametric amplifiers and methods of improving amplifier performance are presented. A lossless parametric diode is represented in ABCD matrix form and the conditions for match at the input are developed. Three possible remedies are suggested to obtain the required conditions. A measured gain of 1.97 vs a calculated gain of 2.02 has been obtained.

6829 NOISE CONSIDERATION OF THE VARIABLE CAPACITANCE PARAMETRIC AMPLIFIER by M. Uenohara (Bell Labs.); Proc. IRE, Vol. 48, pp. 169-179, Feb. 1960

A model of the variable capacitance diode in which the spreading resistance is considered as the source of amplifier noise is described. Gain and noise figure calculations are made for this model and experimental results obtained at 5.84 kMc while pumping at 11.7 kMc are presented for gallium arsenide, silicon and germanium diodes. The quantity $1/\omega C_0 R_s$ is defined as a "quality factor" where R_s is the spreading resistance and C_0 is the static capacitance at zero bias point. Minimum noise figure, optimum load admittance, optimum pumping factor are computed in terms of the parameter $\omega C_0 R_s$. The essential differences between single- and double-sideband reception are discussed. Over a range of sufficiently large values of the parameter $\omega C_0 R_s$, there is a reasonable correlation of the theory with the measurements performed on most of the diodes. In the range of relatively small values of $\omega C_0 R_s$, the model proves inadequate to describe some diodes properly and suggests the need for introducing extra noise sources. These noise sources are also discussed. Of the experimental data obtained thus far, the best result has been with a gallium arsenide diode which yields a 0.9 db double-sideband noise figure and, equivalently, 3.9 db for single-sideband operation with 16 db gain and 25 Mc of single-sideband frequency bandwidth.

6830 PARAMETRIC DIODE FIGURE OF MERIT AND OPTIMIZATION by K. E. Mortenson (GE Res. Lab.); J. Appl. Phys., Vol. 31, pp. 1207-1212, July 1960

The noise figure and gain expressions for the diode parametric amplifier are presented and discussed. From these relationships, a new diode figure of merit is defined as follows: $f_D = a_n / 4\pi a_0^2 C_0 R_D$, where a_n is the normalized Fourier coefficient of the time dependent (pumped) capacitance; C_0, the diode capacitance at the operating bias point; and R_D, the equivalent series diode resistance. It is shown that this figure of merit is directly applicable in comparing diodes of various types as well as in optimizing their respective design for low-noise amplifier use. Further, it is indicated how this figure of merit can be directly employed by the circuit designer to predict an amplifiers' noise figure performance including the effects of choice of bias, pump swing, and signal and idle frequency for a given diode. A complete evaluation of the proposed figure of merit is made for the abrupt junction diode by expressing f_D in terms of device design parameters and examining as a function of bias and base doping. It is concluded, if no constraints are considered, that the maximum value of f_D is obtained for a bias approximately equal to half the breakdown voltage with full pump swing and that f_D (max) increases with decreasing base doping from 10^{18} to 3.10^{15} atoms/cc. It is further concluded that the maximum possible value of a_1/a_0^2 for the inverse square root of voltage capacitance law is approximately 0.557 such that the greatest value f_D (max) can attain is 20% of f_c, the diode cutoff frequency. Some possible limitations on this evaluation are discussed including the effects of diode deviation from the model, pump power or diode dissipation restrictions, nonsinusoidal pumping waveform, and ambient temperatur

6831 THE HELIX PARAMETRIC AMPLIFIER — A WIDE-BAND MINIATURE SOLID-STATE MICROWAVE AMPLIFIER by C. L. Cuccia and K. K. N. Chang (RCA); 1960 Electron Dev. Mtg.

A new type of parametric amplifier which uses a helix as a slow wave distributed interaction structure and has variable capacitance solid state diodes distributively coupled to the helix was discussed. The applied signal and the pump signal are applied to the input of the helix; interaction occurs successively with the diodes and provides parametric amplification which results in the development of the amplified applied signal at the output of the helix. The helix parametric amplifier has an insertion loss of approximately 30 db between the input and the output of the helix before application of the pump signal. When a pump signal at fixed frequency is applied, the helix parametric amplifier provides wide band operation. A miniaturized-package helix parametric amplifier which weighs less than 6 ounces and provides a gain of 15 db across a 10 percent bandwidth in high L-band with a pump having a frequency at less than twice input signal frequency was described. The noise figure of the amplifier is from 5 to 6 db. Maximum gain is stable over a wide range of pump power.

6832 THEORY OF SINGLE-RESONANCE PARAMETRIC AMPLIFIERS by S. T. Fisher (Philco); Proc. IRE, Vol. 48, pp. 1227-1232, July 1960

A parametric amplifier that supports a resonance at the idler frequency only is capable of unlimited gain when operated either as a straight-through amplifier or as a lower-sideband up-converter. In the latter case, the idler frequency becomes the output frequency. The analysis of the single-resonance parametric amplifier consists of determining the stability criteria and power gains associated with a nonlinear capacitance that is incorporated in a network producing a resonance at the idler frequency but not at the signal frequency. The admittance matrix of the network is first established; and then from this matrix the input admittances and the power-gain expressions for straight-through amplification and lower-sideband up-conversion are derived. The single-resonance parametric amplifier, as contrasted with one which is tuned at both the signal frequency and the idler frequency, is, in principle, easy to adjust because there is only one resonance. For this reason, the feasibility of continuously tunable parametric receivers becomes immediately evident.

6833 A COMPACT TUNNEL-DIODE AMPLIFIER FOR ULTRA-HIGH FREQUENCIES by G. Schaffner (Motorola); 1960 IRE WESCON Conv. Rec., Part 2, pp. 86-93

A compact tunnel-diode amplifier for operation between 405 and 460 Mc is described. Used in conjunction with an equally compact UHF isolator, an unusually small, low-noise, and stable amplifier system is achieved. The design of the amplifier, including the effect of coupling on noise figure and stability, is described. Special attention focused on the biasing circuit prevents low-frequency oscillation in the bias leads. The amplifier achieves a 15-db gain, a 12-Mc bandwidth, and a noise figure of 5.5 db across the band. With the isolator, system gain changes less than 3 db with antenna VSWR variations of from 1.0 to 1.8 db. Possible applications for the amplifier are discussed.

6834 A SENSITIVE TRANSISTOR RECORDING-PEN AMPLIFIER by K. G. Beauchamp (UKAEA); Electronic Engrg., pp. 444-445, July 1960

It is shown that if a recording pen movement is connected in a bridge circuit in which two arms of the bridge consist of transistor elements, then a high sensitivity can result. With this arrangement a constant current is drawn from the supply source. Since this need not exceed the maximum pen driving current, low transistor power dissipation and low temperature drift result

6835 A DOUBLE-DELAY-LINE LINEAR AMPLIFIER EMPLOYING TRANSISTORS. I. by F.S. Goulding, R.W. Nicholson, and J.B. Waugh (Atomic Energy of Canada); Nuc. Instr. Methods, Vol. 8, pp. 272-281, Sept. 1960

A transistor amplifier designed mainly for precise scintillation counter spectroscopy is described. Techniques such as double-delay-line pulse shaping and considerable negative feedback result in excellent linearity, gain stability and overload behavior at high counting rates. An input charge of 2×10^{-13} coulombs develops a ± 4v output pulse into a 100Ω matched cable which feeds the Chalk River kicksorter. With 1μsec pulse shaping lines the input equivalent rms noise is 4000 ion pairs. Lower noise may be achieved by using shorter lines. The amplifier rise-time is 0.2 μsec (10 to 90%). Use of plug-in printed circuit boards increases the versatility of the amplifier and simplifies the adjustment procedures.

OSCILLATORS

6836 AUTOMATIC FREQUENCY CONTROL WITH REACTANCE TRANSISTORS by Y. Fujimura and N. Mii (Japan Broadcasting); Electronics, Vol. 33, pp. 97-99, Sept. 30, 1960

Automatic frequency control by regulating the dc bias of a reactance transistor (shunted across the oscillator tank circuit) with a modulating voltage from an oscillator is discussed. Synchronism is maintained over a frequency range of ±1.5 kc (f_o = 31.5 kc) with pull-in frequency range ± 0.7 kc. Mislocking caused by noise interference is reduced from that obtained with tube circuits. Stability is good over the range from -10°C to + 45°C.

6837 TRANSISTOR LC OSCILLATOR CIRCUITS GIVING MODERATE VALUES OF OUTPUT POWER by K. Holford (Mullard Res. Labs.); Mullard Tech. Commun., Vol. 5, pp. 60-70, Feb. 1960

A simple procedure for the design of single-ended, grounded-emitter LC oscillators working at frequencies up to about $f_1/10$ is described. The maximum frequency of operation of these circuits depends on the base resistance of the type of transistor used. Emphasis is placed on interchangeability of transistors of the same type. Design charts and formulas which enable the efficiency and the amplitude of oscillation to be predicted with an accuracy of a few per cent are given. The output power obtainable with these circuits is limited to about 100mw at the higher frequencies, the actual value again depending on the base resistance of the transistor. At lower frequencies, however, several times more output power is attainable. A practical circuit which will provide an output power of 90mw at 50 kc with OC72 transistors is given.

6838 INSURING STABILITY IN TIME DELAY MULTIVIBRATORS by P. E. Harris (Syracuse U.); Electronics, Vol. 33, p.

73, Apr. 8, 1960

The modification of a conventional transistor multivibrator circuit so that its performance is independent of transistor selection and its delay-stability does not vary appreciably with transistor temperature, trigger amplitude, or power supply fluctuations is described. The most significant modification is the isolation of a timing network during the timing interval.

SWITCHING CIRCUITS

6839 WAVE SHAPING CIRCUIT by R. L. Ellsworth (U. S. A.); U. S. Pat. 2,923,840, Issued Feb. 2, 1960

A junction transistor regenerative wave shaping circuit which provides two different output voltage levels depending on whether the input signal level is above or below a critical switching level is described. Variable biasing permits adjustment of switching sensitivity and selection of the quiescent output level. A semiconductor zener diode limits input signal amplitude and selects polarity. Feedback semiconductor diodes prevent saturation and minimize transistor differences and temperature changes. The device is useful in frequency counting circuits and can provide uniform output voltage pulses in response to a wide range in amplitude of input signal.

6840 TURN-OFF CIRCUITS FOR CONTROLLED RECTIFIERS by D. V. Jones (GE); Electronics, Vol. 33, pp. 52-55, Aug. 5, 1960

Several types of silicon controlled rectifier trigger and turn-off circuits are discussed in detail. Circuit problems dealing with high temperature, good stability and fast speed triggering operation are reviewed and solutions are given. A unijunction type inverter circuit using a commutator capacitor and a pulse transformer for better impedance matching is shown. A parallel inverter circuit designed to accommodate varying and reactive loads without creating high voltages under light loads or departing from square wave output under heavy loads is described.

Tunnel Diode Switching Circuits - See 6870

Transistor Isolating Switch - See 6851

6841 SWITCHING APPARATUS by N. H. Kramer and H. W. Mathers (IBM); U. S. Pat. 2,926,339, Issued Feb. 23, 1960

A junction transistor magnetic core switching circuit which reduces pulse power requirements and operates with short duration pulses is described. A reset and a regeneration winding are added to the core. A triggered transistor drives current through the reset winding. A capacitor, charged from the power source, discharges through the reset winding increasing current flow. Transformer action between the reset and regeneration windings increases transistor conduction, switching the core. The capacitor recharges during regeneration and turns off the transistor. The capacitor voltage reduces the carrier storage effect on transistor turn off time, permitting higher frequency operation.

6842 ON THE RESOLVING TIME AND FLIPPING TIME OF MAGNETORESISTIVE FLIP-FLOPS by A. Aharoni and E. H. Frei (Weizmann Inst. Science); Proc. IRE, Vol. 48, pp. 1436-1448, Aug. 1960

The time constant of the exponential approach to the stable states is shown to be a fair approximation for the flipping time of the "bridge" magnetoresistive flip-flop. This time constant turns out to be at least of the order of milliseconds for the magnetoresistive materials known at present, which is too large. Similar time constants are used as an approximation for the resolving times of a general nonlinear network, in particular networks in which the nonlinear element is a magnetoresistor. It is shown that these time constants are the latent roots of a certain matrix whose elements can readily be calculated from the parameters of the network.

Cryotron Flip-Flops - See 6810

SIGNAL CONVERTERS

6843 A NONLINEAR CAPACITOR HARMONIC GENERATOR SUITABLE FOR SPACE-VEHICLE APPLICATIONS by P. M. Fitzgerald, T. H. Lee, M. S. Moy, E. J. Powers, and J. J. Younger (Lockheed); 1960 IRE WESCON Conv. Rec., Part 2, pp. 43-61

A small, compact, efficient, 9th harmonic generator which consists of two cascaded triplers is described. This device was designed to operate in the environment normally encountered during the launch of a satellite and its subsequent sustained orbital flight. The results of environmental tests of shock, vibration, acceleration, and temperature are presented. In addition, the results of an analysis made of two basic harmonic generation circuits are presented. Curves of conversion efficiency as a function of the harmonic generation circuit parameters are given for each circuit (harmonic numbers two through ten inclusive). This is an extension of Chang's work and allows one to take into account the effect of lossy nonlinear elements on conversion efficiency.

Gain Inconsistencies in Low-Frequency Reactance Parametric Up-Converters - See 6828

OTHER SOLID STATE DEVICE CIRCUITS

Synthesis of a Transistorized Tchebycheff Parameter Bandpass Filter - See 6820

6844 A TRANSISTORIZED GALVANOMETER CURRENT LIMITER by P. L. Clemens and R. L. Ledford (Arnold Engrg.); U.S. Gov. Res. Rep., Vol. 34, p. 149 (A), Aug. 19, 1960 PB 146 763

The design, operating characteristics, and typical applications of a newly developed, transistorized, galvanometer current limiter are described. The limiter, which provides continuously variable adjustment of maximum permissible galvanometer current, has only a small effect on other characteristics of the instrumentation system within which it is used. Use of the limiter permits a decrease of system scale factor and results in greater resolution of diminutive data areas. Although intended for use with oscillograph galvanometers, the current limiter is also applicable to other galvanometers and to meter movements.

Transistorized FM and TV Limiter - See 6862

6845 SEMICONDUCTOR CLAMP HANDLES MILLIVOLT SIGNALS by A. J. Koll, E. Bleckner, and O. C. Srygley (Aero Geo Astro); Electronics, Vol. 33, pp. 64-65, Aug. 26, 1960

A diode bridge type detector-sampling circuit used to clamp pulse waveforms in the millivolt region to any d-c level is described. The bridge circuit, consisting of 2 conventional silicon diodes and 2 Zener type diodes, is used to overcome the barrier potential limitation of semiconductor devices to detect low level d-c signals. The input signal fed through an emitter follower drives one arm of the bridge while a gating pulse through a blocking oscillator is applied to the adjacent arms. The clamped d-c output signal appears across a storage capacitor connected to the remaining arm. Input levels ranging from 10 mV to 9 volts were clamped with good linearity. The readout circuit should have an input impedance of at least ten megohms.

Transistorized Microchopper - See 6926

6846 TRANSISTORIZED TIMING CIRCUIT by F. W. Chesson and L. J. A. van Lieshout (Consolidated Electronics Ind.); U. S. Pat. 2,923,863, Issued Feb. 2, 1960

A switch-activated time delay circuit, using junction transistors, which provides a delay between switch actuation and operation of a relay is described. The delay interval is determined by an r-c time constant circuit. A dummy load maintains uniform current drain when the relay coil does not draw current. The heat dissipated in the dummy load maintains a relatively constant temperature to provide stable operation of the transistors.

6847 TIME DELAY CIRCUITS by C. A. Booker, Jr. (Westinghouse); U. S. Pat. 2,924,724, Issued Feb. 9, 1960

A junction transistor time delay circuit which provides both an undelayed and a delayed output signal is described. Semiconductor diodes are used for coupling with signal transmission delayed until diode breakdown. The charge time of a capacitor connected between emitter and collector determines the delay time by selecting the breakdown point. The delayed output signal has a very rapid transition from zero to full level.

6848 HIGHLY ACCURATE PHANTASTRON DELAY CIRCUIT by S. R. Parris and D. A. Staar (Burroughs); Electronics, Vol. 33, pp. 72-74, Oct. 21, 1960

A junction transistor circuit which provides a delay of 220 μsec ± 1% with less than a μsec variation over 25 - 55°C is described. An input emitter follower increases the open-loop current gain and provides increased accuracy and linearity since the base input current is small compared to the capacitor charging current. An R-C network furnishes a secondary feedback path which shapes the HF response of the amplifier for stable closed-loop operation. A charging transistor returns the phantastron rapidly to the quiescent state after each cycle, reducing the charging time to 5 - 10 μsec. An output buffer allows the phantastron to drive its load without affecting timing accuracy. A silicon sensitor provides thermal stabilization by supplying a temperature dependent voltage reference level.

APPLICATIONS OF SOLID STATE DEVICES

GENERAL (MEDICAL, AERONAUTICAL, etc.)

6849 A TRANSISTORIZED, IMPLANTABLE CARDIAC PACEMAKER by W. Greatbatch, W. M. Chardack, and A. A. Gage, (U. Buffalo); 1960 IRE Int. Conv. Rec., Part 9, pp. 107-115

A transistorized and implantable pacemaker for the long term correction of complete heart block is described. The unit is miniaturized and self-contained and its internal battery supply insures five years of continuous operation. Physical and electrical features and requirements of the pacemaker and of the electrode are discussed and experimental data are presented.

6850 A PHYSIOLOGICAL STIMULATOR USING JUNCTION TRANSISTORS by W. T. Catton and L. Molyneux (U. Durham); Electronic Engrg., pp. 301-303, May 1960

A new physiological stimulator circuit using junction transistors and involving no alterations in the front-panel control arrangements of an earlier model is reported. The circuit provides a better pulse shape and a lower output impedance, with the added advantage of a lower supply battery voltage. The facilities provided are as for the earlier model; output voltage variable from 0 to 25 v; frequency variable from 2 to 100/sec; and constant pulse-width of about 1 msec.

6851 TRANSISTOR SWITCH STIMULUS ISOLATOR by H. Fein (U. Utah); Rev. Sci. Instr., Vol. 31, pp. 1070-1072, Oct. 1960

An instrument providing rectangular pulses separated from ground by less than 20 pf capacity and essentially infinite resistance is described. The transistor switch provides pulses at low output impedance, from a floating battery, of 0 to 80 v in amplitude and variable in duration by the width of a triggering stimulus from a conventional stimulator or pulse generator. The device is of particular use in biological experiments where isolation of a stimulating pulse from ground is required.

6852 WIDEBAND F-M RECEIVER FOR REMOTE AIRCRAFT CONTROL by T. L. Fischer (Babcock Radio Engrg.); Electronics,

Vol. 33, pp. 85-87, Sept. 30, 1960

A transistorized 406 - 549 Mc FM receiver which provides a demodulated audio output is described. Use of capacitance-tuned quarter-wave sections in the preselector provides a flat, coupled bandpass of approximately 2 Mc with a VSWR at the input terminals of better than 1.5:1 and overall insertion loss as low as 1 db with image and spurious response rejection greater than 60 db. Local oscillator frequency is stable within 0.005% with frequency change by plug-in units. Overall IF gain is 100 db. The audio amplifier provides 38 db power gain with frequency response flat within 3 db from 5 kc to 80 kc.

6853 MINIATURIZED AUTOPILOT SYSTEM FOR MISSILES by J. H. Porter (RCA); Electronics, Vol. 33, pp. 60-64, Oct. 21, 1960

A missile autopilot system, using micromodular construction and magnetic shift registers, which weighs 13 lbs and occupies 0.238 cubic foot is described. The programmer generates 19 discrete pulses at predetermined times. These times are resolvable to one second intervals and are flexible within a 2,000 second period. Magnetic shift registers consisting of ring connected elements provide timed switching outputs. Prior to lift-off, all elements contain logic ZERO's; at lift-off, logic ONE's are inserted in the first element of each ring and are shifted each second. Location of the ONE in each ring indicates elapsed time. Maximum torquing rate is 2.5 degrees per second. At changeover, the pitch and yaw gyros are made available for guidance control.

Harmonic Generator for a Satellite - See 6843

Motor Speed Controls for Satellite Tape Recorders - See 6898

RADIO

6854 SINGLE OC26 IN CAR-RADIO OUTPUT STAGES by J. F. Pawling (Mullard); Mullard Tech. Commun., Vol. 5, pp. 74-78, Feb. 1960

Two car radio output stages, one for an OC26 output transistor driven by a vacuum tube, the other for an OC26 driven by a transistor (the OC71) are described. The output power for the tube-driver circuit is 3.3w into the primary of the output transformer, at about 10% total-harmonic distortion. For the transistor-driver circuit, the corresponding output power is 3w at about 3% total-harmonic distortion.

6855 THE APPLICATION OF SEMICONDUCTORS IN AN 860 MC RADIO RECEIVER by L. G. Schimpf (Bell Labs.); IRE Trans., Vol. VC-9, pp. 33-37, May 1960

An all solid state, f-m radio receiver which operates at 860 mc is described. The receiver, which utilizes transistors and variable reactance diodes as the active elements, is of the double conversion type with i-f frequencies at 63 and 10.7 mc. The first local oscillator chain uses four stages to generate a signal at 923 mc. The crystal controlled oscillator and two frequency doublers use diffused base transistors. The output of the second doubler, at a frequency of approximately 300 mc, is then tripled in a circuit employing a varactor diode in order to obtain the desired local oscillator signal. The receiver has a 6 db bandwidth of 30 kc. If the output is equalized for a phase modulated signal, 10 db of noise quieting is obtained with a 0.8 μv input signal.

6856 PARASITIC OSCILLATIONS IN I.F. STAGES AND FREQUENCY CHANGERS OF A.M. RECEIVERS by P. Bikker, A. Cense, A. N. van Dijkum, and J. Rongen (N. V. Philips); Electronic Applic., Vol. 20, No. 2, pp. 41-55, 1959-1960

The cause of parasitic oscillations occasionally experienced in i-f amplifiers and frequency changers in a-m receivers employing alloy-diffused or drift transistors is briefly explained and a large number of experiments undertaken to determine the influence of various circuit parameters on the incidence of the oscillations are discussed. The design and operational conditions which can make the stages completely stable without appreciable sacrifice of the stage gain are indicated.

6857 A NEW CONCEPT IN TRANSISTOR CONVERTERS by L. Plus and R. A. Santilli (RCA); 1960 IRE Int. Conv. Rec., Part 7, p. 194 (A)

A method of obtaining an improved a-g-c characteristic in transistorized broadcast-band receivers was described. The improvement is made possible by the use of a new device developed specifically for this application. The device may be used in any transistorized broadcast-band receiver, but it is particularly advantageous when an r-f stage is not used. Several typical circuits using this new device are presented, and their a-g-c characteristics are compared with the a-g-c obtainable with conventional techniques.

6858 SQUELCH CIRCUIT by A. Goldman (Tele-Dynamics); U. S. Pat. 2,926,241, Issued Feb. 23, 1960

A junction transistor universal squelch circuit with a positive "snap" squelching operation which does not change the amplifier biasing arrangement is described. A Schmitt circuit connected across an amplifier provides either a high or low impedance, with squelching action when a low impedance is presented. Transistor operation is controlled by AGC voltage. A limiting semiconductor diode prevents overloading by large AGC voltages. Squelching action is produced when signal strength is below a preset threshold level. Thermistors provide temperature compensation. The device is useful where erratic performance must be avoided.

TELEVISION

6859 UNIQUE DESIGN CONSIDERATIONS FOR TRANSISTORIZED T. V. by L. Mattingly and A. Massman (Motorola); IRE Trans., Vol. BTR-6, pp. 40-44, July 1960

Design considerations involved in the development of a 19" 114° transistorized portable T.V. receiver are given. The operating characteristics of the receiver are discussed and some of the design problems which are unique in nature are described in detail.

TELEVISION (Cont'd)

6860 THE VIDEO PROCESSING CIRCUITS OF AN ALL TRANSISTOR TELEVISION RECEIVER by C. D. Simmons and C. R. Gray (Philco); IRE Trans., Vol. BTR-6, pp. 25-32, May 1960

The circuits which process the detected video signal and extract from it the various sub-signals required by a television receiver are described. The transistor requirements for these circuits are discussed and recommended transistors and circuits are shown. Performance data and design considerations are included to enable the circuit designer to choose the particular features which are applicable for his requirements.

6861 TRANSISTORIZED VERTICAL SCAN SYSTEM FOR MAGNETIC DEFLECTION by F. L. Abboud (Sylvania); IRE Trans., Vol. BTR-6, pp. 33-38, May 1960

A transistorized vertical deflection system that will scan a 90-degree, 14-inch picture tube at 14kv accelerating voltage is described. This system consists of two transistors in a common-emitter multivibrator to form a vertical oscillator, one transistor as a driver, and one output transistor. The system is supplied with power from a 12-volt d-c source. To prevent decentering of the raster, due to the d-c component of current in the deflection coils, the output stage is coupled to these coils by means of an isolation transformer. Feedback networks are introduced to correct for the non-linear characteristics of the transistors, and to predistort the input waveform to the output transistor in order to compensate for the non-linearity of the transformer.

6862 TRANSISTORIZED FM AND TV LIMITER DESIGN AND PERFORMANCE by C. R. Gray and T. C. Lawson (Philco); IRE Trans., Vol. BTR-6, pp. 10-14, July 1960

Recent experiments which demonstrate the feasibility of using transistor limiters at 4.5 and 10.7mc are reported. The circuits are fully described and the limiting performance is discussed in detail. These circuits include provisions for eliminating non-linear feedback effects between the collector and base of the transistor. They are fully capable of meeting the design requirements of conventional vacuum tube limiters and as such permit the design of transistorized equipment which is fully competitive with vacuum tube equipment in this respect.

6863 DESIGNING TRANSISTORIZED TELEVISION CAMERAS by D. G. Carreon (Blonder-Tongue Electronics); Electronics, Vol. 33, pp. 72-75, Sept. 9, 1960

A transistorized TV camera that overcomes low-frequency noise difficulties and blocking oscillator frequency instability is described. Noise is reduced by transistor selection and adjustment of the interstage RC time constants. Thermistors are used to compensate for blocking oscillator frequency drift. Response is flat from 15kc to 8Mc with a peak introduced at 7.5Mc to produce partial aperture correction and to minimize HF noise. Automatic video gain control over the entire video band is achieved by using the nonlinear dynamic impedance characteristics of semiconductor diodes. Power consumption is reduced by 90% and size and weight by two-thirds over a vacuum tube version.

6864 DEFLECTION CIRCUIT by D. A. Paynter (GE); U. S. Pat. 2,924,744, Issued Feb. 9, 1960

A circuit using a single junction transistor to regulate current flow through a deflection yoke is described. Yoke current is supplied by regular transistor action during half the deflection cycle. The yoke and associated circuitry, resonant at a frequency which has a half cycle duration equal to or less than the blanking period, breaks into oscillation at transistor cutoff. The oscillation-induced polarity reversal across the transistor output terminals causes current reversal through the yoke and the collector to base diode portion of the transistor shifting the electron beam from one extreme deflection point to the other. The current through the transistor provides damping action returning the beam to the center of deflection at a uniform rate.

TELEPHONY

Telephone Transmission by Infrared - See 6927

6865 A NEW MEASURING SET FOR MESSAGE CIRCUIT NOISE by W. T. Cochran and D. A. Lewinski (Bell Labs.); Bell Sys. Tech. J., pp. 911-931, July 1960

A new message circuit noise measuring set is described. The instrument is an easily portable, visual-indicating and direct-reading device with which rapid and accurate noise measurements may be made. The set is fully transistorized and battery powered, small in size and light in weight. It can be used for bridging, terminating and noise-to-ground measurements with a variety of plug-in weighting networks, one of which is the new C-message weighting designed for the 500-type telephone set. The sensitivity of the set is such that it can detect -90 dbm. This value is chosen as the new reference for measurement and is defined as "zero dbm".

MICROWAVES

6866 HIGH POWER AT 1,000 MC USING SEMICONDUCTOR DEVICES by G. Luettgenau, M. V. Duffin, and P. H. Dirnbach (Pacific Semicon.); 1960 IRE WESCON Conv. Rec., Part 3, pp. 13-26

Devices and procedures used to develop a solid-state RF generator capable of delivering 1 watt at 1 kMc are described. Theoretical analyses and practical considerations with regard to the design of frequency multipliers are presented. A specific circuit fulfilling the above requirements is discussed and block and circuit diagrams are given.

Semiconductor Microwave Modulator - See 6778

OTHER COMMUNICATION TYPE APPLICATIONS

6867 A MINIATURE TRANSISTORIZED ECHO-SOUNDER by R. N. B. Gatehouse (Brookes and Gatehouse); Electronic Engrg.,

pp. 336-340, June 1960

The development and main design features of a very small and robust echo-sounder for use in depths from 2.5 ft to 32 fathoms are discussed. The instrument is suitable for such purposes as hydrographic surveys, for the laying of underwater pipelines, and the pilotage of yachts and small fishing vessels. The complete equipment weighs only 5 1/2 pounds, has a power consumption of 0.1 w and provides an accuracy of ±3 percent or 6 in, whichever is the greater.

Correlator for a Vocoder - See 6903

COMPUTERS, etc.

6868 THE DESIGN OF A GENERAL-PURPOSE MICROPROGRAM-CONTROLLED COMPUTER WITH ELEMENTARY STRUCTURE by T. W. Kampe (Librascope); IRE Trans. Vol. EC-9, pp. 208-213, June 1960

The design of a parallel digital computer utilizing a 20-μsec core memory and a diode storage microprogram unit is discussed. The machine is intended as an on-line controller and is organized for ease of maintenance. A word length of 19 bits provides 31 orders referring to memory locations. Fourteen bits are used for addressing, 12 for base address, one for index control, and one for indirect addressing. A 32nd order permits the address bits to be decoded to generate special functions which require no address. The logic of the machine is resistor-transistor; the arithmetic unit is a bus structure which permits many variants of order structure. In order to make logical decisions, a "general-purpose" logic unit has been incorporated so that the microcoder has as much freedom in this area as in the arithmetic unit.

6869 SYNTHESIZING MINIMAL STROKE AND DAGGER FUNCTIONS by J. Earle (Underwood); IRE Trans., Vol. CT-7, pp. 144-154, Special Suppl., Aug. 1960; 1960 IRE Int. Conv. Rec., Part 2, pp. 55-65

Methods for synthesizing and minimizing transistor circuitry which perform stroke and dagger functions are presented. The methods, developed using adaptions of function tables, theorems of Boolean algebra, and Karnaugh maps, are applicable to NOR circuits and all AND-Inverter, OR-Inverter type circuits performing these functions.

6870 TUNNEL DIODE DIGITAL CIRCUITRY by W. F. Chow (GE); IRE Trans., Vol. EC-9, pp. 295-301, Sept. 1960

Basic tunnel diode logic circuits, including the monostable and the bistable analog-threshold gates and the "Goto-pair," which uses the principle of majority decision, are discussed. These circuits are studied to determine the requirement on tunnel diodes and other component tolerances. Relations between the "fan-in" and the "fan-out" numbers and the component tolerances are derived. The results indicate that the "Goto-pair" is somewhat superior to the analog-threshold gates with respect to circuit reliability. A tunnel diode flip-flop stage which has advantages with respect to speed, ease of operation, and component tolerances is also described. Combination of these flip-flops in counter and shift-register configurations have been successfully operated. Several potential advantages over conventional transistor circuits are discussed.

6871 THE DESIGN OF DIODE-TRANSISTOR NOR CIRCUITS by D. P. Masher (Stanford Res. Inst.); IRE Trans., Vol. EC-9, pp. 15-24, Mar. 1960

Considerations leading to the adoption of diode-transistor NOR circuitry for a moderately fast data-processing system are outlined. The design of the basic circuit is treated in detail. Development of a unique set of compatible logic packages from the basic circuit is described. This set is unique in the sense that a single type of diode-transistor circuit is used to provide the great majority of logic and storage functions required in the system. This single circuit type, which functions as a NOR circuit, is embodied in two package types. One package provides a single gate with a fan-in of five. The other package provides two gates, each with a fan-in of two. The latter type may be externally connected to provide a set-reset flip-flop. Only two other package types are used. The first is a passive transfer circuit which greatly simplifies shift register logic, and the second is a delay package which is closely related to the basic NOR circuit.

6872 ESAKI DIODE HIGH-SPEED LOGICAL CIRCUITS by E. Goto, K. Murata, K. Nakazawa, K. Nakagawa, T. Moto-Oka, Y. Matsuoka, Y. Ishibashi, H. Ishida, T. Soma, and E. Wada (U. Tokyo); IRE Trans., Vol. EC-9, pp. 25-29, Mar. 1960

Logical circuits using Esaki diodes which are based on a principle similar to parametron (subharmonic oscillator element) circuits are described. Two diodes are used in series to form a basic element called a twin, and a binary digit is represented by the polarity of the potential induced at the middle point of the twin, which is controlled by the majority of input signals applied to the middle point. Unilateral transmission of information in circuits consisting of cascaded twins is achieved by dividing the twins into three groups and by energizing each group one after another in a cyclic manner. Experimental results with the clock frequency as high as 30 mc are reported. Also, a delay-line dynamic memory and a nondestructive memory in matrix form are discussed.

6873 ANALYSIS AND DESIGN OF THE TWIN-TUNNEL-DIODE LOGIC CIRCUIT by C. H. Alford, Jr. (Lockheed); 1960 IRE WESCON Conv. Rec., Part 2, pp. 94-101

The operation of the series tunnel-diode logic circuit [see abstract 1004] is described and an analysis technique which yields an evaluation of circuit performance in terms of supply voltage tolerance, diode parameter variations, circuit loading, and input-output branching is presented. Equations to represent portions of the diode characteristic are derived. Circuit equations are solved to yield an analytical expression for the output characteristic, which permits a worst-case analysis involving all circuit variables.

6874 TRANSISTOR CURRENT SWITCHING AND ROUTING TECHNIQUES by D. B. Jarvis, L. P. Morgan, and J. A. Weaver (Mullard Res. Labs.); IRE Trans., Vol. EC-9, pp. 302-308, Sept. 1960

A system of circuit logic in which transistors, particularly diffused base transistors, are operated well out of saturation in order to make the most of their speed is described. Logical information is contained in the presence or absence of a current which can be switched or routed by the gates described. Also described is the application of this system of logic to certain

specific computer problems, namely, a parallel adder with a carry propagation time of 40 mμsec over 6 stages, a shifting register capable of operating at 10 mc and a binary decoder with a maximum delay of 40 mμsec.

6875 TRANSISTOR-RESISTOR LOGICAL CIRCUITS by P. D. T. Hawker (Mullard); Mullard Tech. Commun., Vol. 5, pp. 174-181, Sept. 1960

The operation of a basic transistor-resistor logical circuit is described and design and performance equations are derived. The simplicity of this type of circuit leads to economy, reliability, and design-ability. By way of illustration, circuits using the switching transistors types OC41 and OC42 are designed. Modifications to the basic circuit which give greater stage gain or faster operation are included.

6876 STATISTICAL ANALYSIS OF TRANSISTOR-RESISTOR LOGIC NETWORKS by W.J. Dunnet and Y.-C. Ho (Sylvania); 1960 IRE Int. Conv. Rec., Part 2, pp. 11-40; IRE Trans, Vol. CT-7, Special Suppl., pp. 100-129, Aug. 1960

A general approach to the statistical investigation of properties of complex transistor switching networks, particularly TRL circuits which use resistive coupling between grounded emitter stages to perform the logical NOR function, is described. An important consideration in the design of TRL systems is the delay in propagation of signals through various levels of these circuits. A mathematical model of the delay which is a complicated function of circuit variables as well as of the intrinsic parameters of the transistors involved has been constructed and a computer program has been written to simulate the model on an IBM 709. By using measured statistical data of transistor parameters and randomly sampled circuit variables as input, a Monte Carlo analysis of the distribution of propagation delay has been carried out.

New Multi-Aperture Magnetic Logic Element - See 6799

Magnetic Analogs of Relay Contact Networks for Logic - See 6800

6877 USE OF A TRANSISTOR FOR SETTING A SQUARE LOOP MAGNETIC CORE by I. Krajewski (Int. Computers and Tabulators); Electronic Engrg., Vol. 32, pp. 509-511, Aug. 1960

After showing that most available transistors have to be regarded as voltage sources when setting cores, the basic circuit for setting a core is analyzed. This shows that, under given conditions, for fastest setting there is an optimum number of turns for the setting winding. An experimental verification of these results which shows good agreement with calculation is given. A practical circuit is briefly described together with calculations of the junction power dissipations within the transistor used.

Open Flux Path Ferrite Films for Logic and Storage - See 6801

6878 SOME APPLICATIONS OF MAGNETIC FILM PARAMETRONS AS LOGICAL DEVICES by R.F. Schauer, R.M. Stewart, Jr., A.V. Pohm, and A.A. Read (State U. of Iowa); IRE Trans., Vol. EC-9, pp. 315-320, Sept. 1960

High-frequency magnetic film parametrons which exhibit two- or three-state operation for a single bias condition are described. As a two-stable-state device, the magnetic film parametron can be used as a majority decision element in much the same way as the ferrite core parametron. Another useful logical two-state device is a threshold element, in which the input excitation must reach a minimum level to sustain oscillations. The magnetic film inductor, when suitably clocked, can be used as a gate to permit unilateral flow of information in a system. The gating action, controlled by the bias field, can result from the rectified output of a parametron. Proposed logical designs for a two-element binary adder, a binary shift counter, and a shift register are presented. The possibilities of three state operation are also explored in the logical design of a seven-element ternary full adder.

Operation of Magnetic Film Parametrons in the 100-500 Mc Region - See 6802

Solid State Micrologic Elements - See 6774

6879 HIGH SPEED SCALERS USING TUNNEL DIODES by P. Spiegel (Philco); Rev. Sci. Instr., Vol. 31, pp. 754-755, July 1960

A decade scaler circuit which utilizes the characteristic of series-connected tunnel diodes wherein voltage is a multi-valued function of current is described. The scaler has a double pulse resolution of less than 50 nsec and requires very little power. It may be microminiaturized and is potentially more economical and easier to fabricate than present scalers.

6880 A SILICON TRANSISTORIZED SCALING STAGE by L. B. Gardner (Litton Ind.); IRE Trans., Vol. I-9, pp. 55-59, June 1960

The design, packaging, and evaluation of a scaling stage which utilizes silicon transistors to achieve stable operation at temperatures in excess of 110°C are discussed. The relative advantages and disadvantages of operating the transistors in the saturated or nonsaturated region are discussed and several practical circuits of each type are given. From laboratory measurements it appears that for a nonsaturated fast flip-flop the output transient response is independent of the input transient response. An hypothesis for this phenomenon is given along with the description and conclusions of controlled experiments designed to test the hypothesis.

Cryotron Flip-Flop Ring - See 6810

Transistor Parallel Adder - See 6874

6881 PULSE STEERING CIRCUIT by R. R. Blair (Bell Labs.); U. S. Pat. 2,924,725, Issued Feb. 9, 1960

A junction transistor pulse steering circuit which permits operation of binary counters at the highest trigger pulse repetition frequency at which the counter amplifiers are capable of operating and which produces sharply defined output voltage waveshapes is described. Trigger pulses applied to transistor

gates steer switching voltages, produced by transistor amplifiers, alternately to the counter amplifiers. The cross coupling impedances of the counter amplifiers are resonant at approximately one-half the repetition frequency of the trigger pulses to be counted. This improves the output voltage waveform. Trigger pulses having a duration as long as the switch and gate turn off and turn on times can be tolerated without causing false operation of the counter.

6882 NOVEL ADDER-SUBTRACTER CIRCUIT UTILIZING TUNNEL DIODES by R. A. Kaenel (Bell Labs.); 1960 IRE WESCON Conv. Rec., Part 3, pp. 53-64

Two binary counter configurations which fully exploit the properties of a modified tunnel (Esaki) diode flip-flop are presented. A bipolar regenerative gate and a conventional flip-flop utilizing tunnel diodes are described and partially analyzed to complete the understanding of the new counters. Experimental results which demonstrate the feasibility and reliability of the circuit are given. The counter stages described combine memory, gate, and amplifier without impairing reliability. The economy inherent in this arrangement gives the designer latitude in adding regenerative amplifiers to improve reliability.

Parametron Binary Adder - See 6878

6883 A SMALL HIGH-SPEED TRANSISTOR AND FERRITE-CORE MEMORY SYSTEM by W. L. Shafer, Jr., W. N. Toy, and H. F. Priebe, Jr. (Bell Labs.); Commun. and Electronics, No. 46, pp. 763-769, Jan. 1960; Elect. Engrg., Vol. 79, pp. 212-217, Mar. 1960

The design and operation of a 400-bit ferrite core memory for use in a time-division electronic switching system is described. A cycling binary counter establishes sequential access to the twenty rows (twenty twenty-bit words) of the memory. The read-out is blocked except when opened by a strobe pulse during the read period, to prevent partial switching caused by noise from the vertical-write pulse. Synchronization is by external clock; the read cycle takes five microseconds per word, or 100 microseconds to cycle through the memory. Operation was checked for supply voltage and temperature variation, with favorable results reported.

6884 FLUXLOK - A NONDESTRUCTIVE, RANDOM-ACCESS ELECTRICALLY ALTERABLE, HIGH-SPEED MEMORY TECHNIQUE USING STANDARD FERRITE MEMORY CORES by R. M. Tillman (Burroughs Res. Ctr.); IRE Trans., EC-9, pp. 323-328, Sept. 1960

The Fluxlok memory technique which uses the principle of cross-field magnetization to achieve the nondestructive sensing of the information state of standard, readily available, ferrite memory cores in a simply wired memory plane is described. Bipolar output (ONE and ZERO) signals are obtained at the rate of rise of the READ pulse. The signals are unaffected by test temperatures of from -65°C to +100°C. Coincident current WRITE operation or an inherent orthogonal field WRITE may be used. A 2-Mc 64-word Fluxlok memory test vehicle is described.

6885 SUBMICROSECOND CORE MEMORIES USING MULTIPLE COINCIDENCE by H. P. Schlaeppi and I. P. V. Carter (IBM); IRE Trans., Vol. EC-9, pp. 192-198, June 1960

Memories which use toroidal ferrite cores with cycle times less than a microsecond and in which the selection ratio is increased by the use of biasing and the multiple coincidence principles of Minnick and Ashenhurst are described. It is shown that this mode of operation leads to important changes in the structure of the store; in particular, the classical core switch does not fulfill the new requirements. The "two-core switch" is then briefly described; it permits an elegant and economic solution of the problems arising at high selection ratios. Details of the design and operation of memories embodying these ideas are given; it is shown, for example, that standard core memory matrices can be used very efficiently at a selection ratio of 3:1 to achieve a cycle time of 2 microseconds. Further illustrations are given from a model of a 100x100 store operated at 4:1 and 7:1 selection ratios, and it is shown that a store of 10,000 8-bit characters with a cycle time of 0.25 microsecond is feasible.

Miniature Memory Planes for Extreme Environmental Conditions - See 6798

Development of High-Speed Coincident Current Memory Cores - See 6803

6886 MAGNETIC FILM MEMORIES, A SURVEY by A.V. Pohm (State U. of Iowa), and E. N. Mitchell (U. of N. Dakota); IRE Trans., Vol. EC-9, pp. 308-314, Sept. 1960

An analysis of the modes of magnetization reversal and rotation in thin ferromagnetic films is presented. The ways in which the various modes can be employed for destructive and non-destructive memories are discussed and their performance limitations are considered. Existing film memory efforts are partially surveyed and the material and system problems are examined. Possible future developments are also discussed.

6887 MAKING REPRODUCIBLE MAGNETIC-FILM MEMORIES by E. M. Bradley (Int. Computers and Tabulators); Electronics, Vol. 33, pp. 78-81, Sept. 9, 1960

A magnetic film memory capable of storing 1,250 bits in a 4" x 3" sheet is discussed. The unit exhibits a reduction of the stray mutual inductance between the sense and drive lines by a factor of 1000 over ferrite core memories and a read-write cycle time less than a μsec. Memory units can be connected together for increased storage capacities. A 4"x 3" film of Gyralloy 1000 A thick, is deposited on a 7"x 3" aluminum plate by vacuum evaporation and the sense line separated from the plate with an insulator less than 0.0005" thick. A prototype memory store made from two coated aluminum plates stores 2500 bits organized into 50 words.

6888 A VACUUM EVAPORATED RANDOM ACCESS MEMORY by K. D. Broadbent (American Systems); Proc. IRE, Vol. 48, pp. 1728-1731, Oct. 1960

A basic multiple-layer magnetic thin film structure which has special and desirable properties in coincident-signal switching applications such as those employed in binary random access memories is described. Its demonstrated advantages in this application include: 1) magnetic turnover times as low as 30 mμsec; 2) wide latitude in selection currents, with greater than twelve-fold variations giving no appreciable change in the compensated signal-to-noise ratio of the cell's output;

3) extremely small volume of, typically, 0.025 inch x 0.010 inch x 0.0007 inch per complete cell; and 4) automated, microminiaturized production and assembly based on vapor phase handling techniques.

Thin Ferromagnetic Film Memory - See 6655

Representation of the Magnetic Field of Twistors - See 6797

Cryotron Storage Circuit - See 6808

Persistor Memory Element - See 6813

6889 A NEW SEMICONDUCTOR MEMORY ELEMENT WITH NON-DESTRUCTIVE READ-OUT AND ELECTROSTATIC STORAGE by V. H. Grinich and D. Hilbiber (Fairchild Semicon.); 1960 IRE WESCON Conv. Rec., Part 3, pp. 34-41

A method of information storage which utilizes the stored charge in the depletion layers of a p-n-p-n structure is described. Presence of a large space charge indicates a "zero", and a smaller charge a "one". In the determination of the existing state of the device, advantage is taken of the fact that the point at which breakdown occurs in a p-n-p-n device is a function of the rate of rise of the applied voltage, dV/dT. If one assumes a device with all junctions initially discharged, a voltage pulse having an amplitude less than V_S, the switching voltage, and a sufficiently short rise time will cause the device to switch. If, however, the middle junctions were previously charged to some level less than V_S at a sufficiently slow rate, the application of the first pulse would not result in a breakdown. Therefore, by selection of a proper "interrogation" pulse, and monitoring the current through the device, one may readily determine the storage state. Since this method is electrostatic, the only input power to the device is that which supplies the charge lost due to stray leakages. A non-destructive read-out is obtained since "interrogation" does not alter the existing state. Instead, it acts to regenerate the state that already exists. Other advantages include a high signal to noise ratio and the feasibility of constructing micro-memory systems. Experimental results are discussed.

Tunnel Diode Shift Register - See 6870

6890 SHIFT REGISTER INTERSTAGE COUPLING CIRCUITRY by S. T. Meyers (Bell Labs.); U. S. Pat. 2,923,839, Issued Feb. 2, 1960

Simplification of the interstage coupling circuitry in transistor shift registers with the elimination of active circuit elements and a reduction in the number of components is described. Only four passive circuit elements (a capacitor, two semiconductor diodes, and a resistor) and a voltage divider are required to shift stages progressively. Shifting is accomplished by biasing the stage corresponding to the off stage of the preceding binary cell deeper into cut-off and removing the bias upon termination of the shift pulse.

Transistor Shift Register - See 6874

Shift Register Transistor - See 6775

6891 A THIN MAGNETIC FILM SHIFT REGISTER by K. D. Broadbent (Amer. Syst.); IRE Trans., Vol. EC-9, pp. 321-323, Sept. 1960

An initial application of the dynamics and interactions of domains within continuous magnetic thin film structures is made to a shift register in which binary information is stored and translated in and along a continuous evaporated thin magnetic film. These thin magnetic film shift registers are capable of storing information having a density of several hundred bits per square inch of vacuum evaporated structure and of translating this amount of information at bit rates in excess of a megacycle with powers of less than 10 watts.

Parametron Shift Register - See 6878

Cryotron Shift Register - See 6808

Cryotron Ring Oscillators - See 6811

6892 A REVIEW OF PANEL-TYPE DISPLAY DEVICES by J. J. Josephs (Lincoln Lab.); Proc. IRE, Vol. 48, pp. 1380-1395, Aug. 1960

The activities of various governmental, industrial, and academic institutions in the field of panel display devices are reviewed. These devices are thin sheets which can display luminescent information. Insofar as possible the present state of the art is indicated. The displays are grouped as: evacuated, solid, gas, liquid and mechanical. The solid-type displays employ the electroluminescent panel in conjunction with an xy matrix of electrodes. Recent progress in panels of the above type with memory are included as well as a brief discussion of solid-state image intensifiers. A brief discussion of switching devices, including solid-state switching devices, is included. Actual as well as possible applications of these devices are listed.

POWER

6893 THE DESIGN OF CONTROLLED RECTIFIERS USING TRIODE TRANSISTORS by E. E. Ward (U. Birmingham); Proc. IEE, Vol. 107B, pp. 473-480, Sept. 1960

Polyphase rectifiers in which the switching element is a complementary combination of a p-n-p and an n-p-n transistor are discussed. The stability conditions for the open and closed states of this switch are investigated graphically, leading to the calculation of the voltage drop when conducting. There is a sharp upper limit to the permissible current. Tests on a 3-phase controlled rectifier are described.

6894 DESIGNING TRANSISTORIZED VOLTAGE REGULATORS by E. Wilson (Texas Instr.); Electronics, Vol. 33, pp.

62-65, Sept. 23, 1960

A design technique which breaks series voltage regulators into functional blocks and presents design criteria for each block is discussed. Performance equations are developed and test circuitry described. Temperature compensation is obtained by utilizing the temperature coefficient of the reference voltage silicon diodes and a symmetrical emitter-coupled differential amplifier as the comparison element. A preregulator eliminates output variation caused by ripple current and reduces the regulator output resistance by as much as an order of magnitude. Load current interruption is obtained by using a predetermined overload current to cause diode breakdown and supply gate current to a control rectifier which conducts a high current, opening the fuse faster.

Zener Diode Stabilized Power Supply - See 6736

6895 TRANSISTOR INVERTER by B. H. Pinckaers (Minneapolis-Honeywell); U. S. Pat. 2,926,296, Issued Feb. 23, 1960

A junction transistor inverter, containing no moving parts, which converts a variable magnitude reversible polarity d-c signal to an a-c signal of variable magnitude and reversible phase is described. A constant amplitude a-c reference signal alternately gates a pair of transistors. The direction of unbalance of a d-c impedance bridge determines which transistor is driven. The output phase depends upon the direction of bridge unbalance. A usable output signal has been obtained with a 10 μvolt bridge unbalance.

6896 TRANSISTOR SATURATION CONTROL by J.L. Anderson (IBM); U.S. Pat. 2,947,880, Issued Aug. 2, 1960

A method which permits normal inverter circuit operation of n-p-n and p-n-p transistors to a point just short of saturation and which stabilizes operation at that point is described. The increased turn-off delay produced by saturation is avoided, permitting higher frequency operation. A source of potential opposite to the input signal potential is applied to the base when the collector potential reaches a desired level. Saturation is thus prevented by reducing the base to collector amplification factor.

6897 TRANSISTOR THREE-PHASE D.C. - A.C. INVERTER by W. L. Stephenson (Mullard Res. Labs.); Mullard Tech. Commun., Vol. 5, pp. 78-80, Feb. 1960

A method of operating transistors in a self-oscillating three-phase circuit is described. The transistors operate in a switching mode to give high-efficiency power conversion, the output waveform being a 2:1 square wave to provide a balanced system.

Controlled Rectifier Inverter Circuit - See 6840

CONTROL

6898 TRANSISTORIZED MOTOR SPEED CONTROLS FOR SATELLITE TAPE RECORDERS by M. B. Pickover (USASRDL); Proc. IRE, Vol. 48, pp. 725-728, Apr. 1960

Two circuits for controlling the speed of small a-c and d-c motors are described. Current design for a specific satellite application of an a-c transistorized power supply for low power synchronous motors is treated and the over-all system parameters which must be considered in the choice of a hysteresis synchronous motor, the motor's operating frequency, and its characteristics are discussed. The servo loop used to accomplish speed control in d-c motors, and the accuracy that may be obtained are discussed. Relative advantages and disadvantages of the d-c motor and a-c synchronous motor in the low-power output range are discussed. The system is designed to meet the environment of the satellite package. The emphasis is on a system requiring a minimum of power consumption and smallest possible size and weight, with no sacrifice of reliability of performance.

Delay Circuit for Relays - See 6846

INSTRUMENTATION

Sensitive Transistor Recording-Pen Amplifier - See 6834

6899 AN A-C TRANSISTOR MILLIVOLTMETER WITH A HIGH INPUT IMPEDANCE by R. R. Vierhout (R. C. University); Electronic Engrg., pp. 435-437, July 1960

After a preliminary explanation of the operation of feedback systems, a transistor millivoltmeter with an input impedance of 1 to 6 MΩ, a frequency range of 1 cps to 200 kc, and a full-scale deflection in the most sensitive range of 10 mv with an accuracy of 2 percent of full scale is described.

Galvanometer Current Limiter - See 6844

Double-Delay-Line Linear Amplifier for Precise Scintillation Counter Spectroscopy - See 6835

6900 A SIMPLE TRANSISTOR OSCILLATOR FOR THE OBSERVATION OF NUCLEAR MAGNETIC RESONANCE [in German] by R. Kosfeld (Technische Hochschule, Aachen); Z. Instrumentenk., Vol. 68, pp. 114-115, May 1960

A simple transistor—autodyne—detector for the observation of nuclear magnetic resonance is described. The stability and sensitivity are equal to those of similar assemblies using tubes. The setup and power supply, however, are of greater simplicity. The signal-to-noise ratio is better than 25 db.

6901 ANALYSIS OF A MAGNETIC RESONANCE SPECTROMETER by J. P. Goldsborough and M. Mandel (Stanford U.); Rev. Sci. Instr., Vol. 31, pp. 1044-1046, Oct. 1960

An electron paramagnetic resonance microwave bridge spectrometer is analyzed and expressions for the relation between the signal and the imaginary part of the magnetic susceptibility are given. From these the conditions for maximum signal are obtained. The analysis is also applicable to many other types of magnetic resonance spectrometers.

6902 ON MEASUREMENTS OF MICROWAVE $\bar{E}$ AND $\bar{H}$ FIELD DISTRIBUTIONS BY USING MODULATED SCATTERING METHODS by M.-K. Hu (Syracuse U.); IRE Trans., Vol. MTT-8, pp. 295-300, May 1960

The modulated scattering method of Justice, Rumsey, and Richmond for measuring $\bar{E}$ field distribution is extended to the measurement of $\bar{H}$ field distribution by using a loop scatterer formed by two junction diodes. This method has the particular advantage of eliminating the large and undesirable effect produced by the associated $\bar{E}$ field when measuring the $\bar{H}$ field. A scattering analysis of the modulated diode loop is presented. A similar analysis for the modulated diode scatterer used in measuring $\bar{E}$ is also presented. It is believed that the explanation based upon this analysis for the $\bar{E}$ measurement is more satisfactory than that given by Richmond.

6903 A CORRELATOR EMPLOYING HALL MULTIPLIERS APPLIED TO THE ANALYSIS OF VOCODER CONTROL SIGNALS by A. R. Billings and D. J. Lloyd (U. Bristol); Proc. IEE, Vol. 107 B, pp. 435-438, Sept. 1960

After an initial discussion of short-term correlation functions, the design and performance of an auto- and cross-correlator using Hall-effect multipliers are described. It is shown that these devices are well suited to act as the multiplying elements and as modulators in associated circuits, provided that one of the time functions to be multiplied has a narrow bandwidth. Examples of measured auto- and cross-correlation functions are given for sine waves and noise and for the control signals of a vocoder, from which interesting conclusions can be drawn about the redundancy of vocoder signals.

6904 TRANSISTORIZED COINCIDENCE CIRCUIT FOR π-E EXPERIMENT by R. H. Miller (U. Chicago); Rev. Sci. Instr., Vol. 31, pp. 1047-1051, Oct. 1960

A special purpose coincidence circuit with millimicrosecond resolution time which illustrates the simplicity that can be achieved with transistorized circuits is described. The circuit performs all the logical operations of three simultaneous experiments to measure the branching ratio to the electronic mode of pion decay. Performance data under operating conditions on the cyclotron are given.

6905 A TRANSISTORIZED FAST-SLOW COINCIDENCE AND PULSE AMPLITUDE SELECTING SYSTEM. II. by F.S. Goulding and R.A. McNaught (Atomic Energy of Canada); Nuc. Instr. Methods, Vol. 8, pp. 282-296, Sept. 1960

A system developed for fast-slow coincidence experiments in nuclear physics is described and the design of functional units including a low level discriminator, single or dual-channel analyzer, coincidence circuit and linear gate, is discussed. The system is designed to use the ±4v double-delay-line shaped pulses produced by the amplifier described in the previous paper [see abstract 6835] or equivalent pulses from other amplifiers. Operation with single phase pulses of similar amplitude is also possible but with reduced performance. Uncertainty of the discriminator threshold and the spurious pedestal and disturbances introduced by the linear gate are less than 10 mv under all normal operating conditions. The system utilizes functional units constructed on plug-in printed circuit boards and is arranged so that the experimenter can change interconnections quickly. A coincidence resolving time of 40 nsec is possible without utilizing fast amplifiers or coincidence circuits.

6906 A SINGLE TRANSISTOR RADIATION SURVEY METER by M. Birnbaum (Inst. Fizica Atomica, Rumania); Electronic Engrg., pp. 428-429, July 1960

A new type of portable radiation survey meter which employs a single transistor to provide the high voltage necessary for the G.M. counter and at the same time integrate the pulses to be measured is described.

6907 FRACTIONAL MILLIMICROSECOND ELECTRICAL STROBOSCOPE by W. M. Goodall and A. F. Dietrich (Bell Labs.); Proc. IRE, Vol. 48, pp. 1591-1594, Sept. 1960

A simple electrical stroboscope having a rise time of 6×10^{-11} seconds and a 6 db bandwidth of 5.5 kMc is described. Oscillograms showing 160 Mc square waves and 640 million pulses per second are given. These waveforms display rise times as fast as 2×10^{-10} seconds. Instrumentation includes a strobepulse generator, a coaxial gate using a gallium arsenide point-contact crystal, suitable wide-band coaxial attenuators, a low-pass integrating filter and a low-frequency oscilloscope.

6908 LARGE AREA GERMANIUM SURFACE-BARRIER COUNTERS by F. J. Walter, J. W. T. Dabbs and L. D. Roberts, (Oak Ridge Labs.); Rev. Sci. Instr., Vol. 31, pp. 756-762, July 1960

A solid state counter of good resolution, long term stability, and fast rise time which is suitable for heavy charged particles, e.g., alpha particles and fission fragments, is described. A simple theoretical model which describes the observed behavior of the counter very well is presented. The importance of germanium purity in connection with pulse height, rise time, and counter area is discussed. Counters with sensitive areas up to 5 cm^2 have been used successfully.

6909 NEW SEMICONDUCTOR NUCLEAR PARTICLE DETECTOR by R. L. Williams (RCA Victor Res. Labs.); Bull. Am. Phys. Soc., Ser. II, Vol. 5, p. 354(A), June 15, 1960

A nuclear particle detector of transistor configuration which uses high-resistivity silicon was described. The depletion layer of the collector junction can be extended to the emitter junction by the application of the appropriate bias. Base widths can be made sufficiently narrow to give current multiplication factors from 300 to 1500. An increase in signal to noise compared with that of a single p-n junction detector which is proportional to the square root of the multiplication factor is predicted. The device can be used as an alpha-particle detector and a large area photo-transistor. The variation of noise, signal level, and impedance with bias was reported.

6910 THE SOLID-STATE IONIZATION CHAMBER by S. S. Friedland (Solid State Radiations), J. W. Mayer, and J. S. Wiggins (Hughes Aircraft); IRE Trans., Vol. NS-7, pp. 181-185, June-Sept. 1960

The use of shallow diffused silicon p-n junction detectors as room-temperature particle spectrometers for protons, alpha particles, heavy ions, and fission fragments is discussed. By the use of high base resistivity devices operated at high reverse biases (>200 volts), the width of the sensitive volume has been extended beyond 0.5 mm, permitting linear response to protons up to 9 mev. Improved diffusion techniques have resulted in more shallow diffusion depths so that the "window effect" is reduced, extending the low energy response to below 200 kev for alpha particles. Use of low-noise amplifiers has permitted observation of half-widths of the pulse height-distribution equivalent to 18 kev.

6911 SILICON SURFACE-BARRIER NUCLEAR PARTICLE SPECTROMETER by J. L. Blankenship and C. J. Borkowski (Oak Ridge Natl. Lab.); IRE Trans., Vol. NS-7, pp. 190-195, June-Sept. 1960

The fabrication and evaluation of gold silicon surface-barrier counters which give good resolution at room temperature are discussed. Counters from 150 ohm-cm material have given 15-kev (~1/4 per cent) resolution for Cm^{244} (5.801 mev) and Am^{241} (5.477 mev) alpha particles. A large-area 1-cm^2 counter has given 0.7 per cent resolution for Po^{210} (5.30 mev) alpha particles. The detector has resolved alpha particle groups which previously had been unresolved with Frisch-grid pulse-ion chambers.

6912 AN ENCAPSULATED SILICON JUNCTION ALPHA-PARTICLE DETECTOR by P. P. Webb, R. L. Williams, and R. W. Jackson (RCA Victor Res. Labs.); IRE Trans., Vol. NS-7, pp. 199-201, June-Sept. 1960

The construction of a silicon diffused junction alpha detector in a form which allows complete encapsulation and protection of the junction edge, and which preserves a good geometry is described. The unit is inherently shielded from electrical pick-up, and is shielded from ambient light by a thin metallic film over the sensitive surface. A modified form of the same encapsulation has been used for large area units of 2 cm^2 suitable for contamination monitoring. Measurements of energy resolution and other characteristics for units of sensitive area 5 mm^2, 20 mm^2 and 200 mm^2 are reported.

6913 SILICON P-N JUNCTION RADIATION DETECTORS by G. L. Miller (Brookhaven Natl. Lab.), W. L. Brown, P. F. Donovan, and I. M. Mackintosh (Bell Labs.); IRE Trans., Vol. NS-7, pp. 185-189, June-Sept. 1960

Silicon p-n junction particle detectors fabricated by diffusing phosphorus to various depths between 0.1 and 2.0 μ into high resistivity p-type silicon are discussed. Diffusions have been carried out both by the "gaseous" and the "paint-on" process. The devices have ranged in area from 1 mm^2 to 1 cm^2, with the majority of detectors having an area of ~.2 cm^2. Using 5.5 mev α particles and a 5 x 5 mm device, the best line width that has been obtained is 20 kev. It has been found that the 1 cm^2 devices give line widths of ~50 kev. The effect of the thickness of the n layer forming the front surface of the junction has been investigated, and it has been shown that 0.1-μ diffusions give essentially "windowless" detectors. Other properties that have been examined are space charge generation of leakage current, charge collection efficiency as a function of bias and incident particle direction, and signal rise time.

6914 SILICON JUNCTIONS AS PARTICLE SPECTROMETERS by J. M. McKenzie and J. B. S. Waugh (Atomic Energy of Canada); IRE Trans., Vol. NS-7, pp. 195-199, June-Sept. 1960

The fabrication and characteristics of Au-Si surface barriers and silicon p-n junctions operated as particle spectrometers are discussed. The use of high resistivity material gives a depletion region wide enough to stop high-energy protons, α particles, and heavier ions. A resolution of 16 kev (width at half-maximum) for 6.04 mev α particles is obtained with a junction depletion layer sufficient to stop 10 mev α particles. With the depletion region very close to the surface, β particles in the range from 10 kev to several hundred kev are detectable. The pulse amplitude distribution from Co^{57} indicates the presence of the two well-known lines at 115 and 129 kev. An attempt has been made to correlate the observed performance with the semiconductor parameters and the diode static characteristics.

6915 USE OF SILICON P-N JUNCTION DETECTORS IN STUDIES OF NUCLEAR REACTIONS INDUCED BY HEAVY IONS by A. E. Larsh, G. E. Gordon and T. Sikkeland (U. California); Rev. Sci. Instr., Vol. 31, pp. 1114-1118, Oct. 1960

Experiments using silicon p-n junctions as detectors of fission fragments and elastically scattered heavy ions are described. The curve of pulse height versus energy for carbon particles is linear and passes through the origin. Points for Cf^{252} fission fragments and alpha particles fall on the curve determined by the carbon particle points. This implies that the energy required for electron-hole pair formation is the same for the three types of particles. No "ionization defect" is observed for the fission fragments. Some other possible uses for detectors of this type are suggested.

6916 TRANSISTORIZED RADIATION MONITORING EQUIPMENT by J. J. Henry (Union Carbide Nuclear); 1960 IRE Int. Conv. Rec., Part 9, pp. 28-33.

An all transistor radiation monitor developed to attain optimum accuracy and dependability in industrial applications is described. A cascode circuit linear amplifier, a linear base line pulse height discriminator, and a pulse width modulated, diode switched, constant current rate meter circuit are employed. These circuits provide good linearity, stability, paired pulse resolution of <2 μsec, and no discernible zero drift. The circuits are designed for low power consumption and are hermetically sealed in a small corrosion resistant case. Modular-plug-in construction is used to aid maintenance.

NEW PRODUCTS

6917 VERY HIGH FREQUENCY POWER TRANSISTORS (Pacific Semiconductors, Inc., 12955 Chadron Ave., Hawthorne, California)

The 2N1505 and 2N1506 n-p-n triple diffused silicon mesa very high frequency power transistors are announced. The 2N1506 has a typical output of 1 w with 12 db power gain at 70 Mc and 28 v operating voltage. At 200 Mc the output is typically 500 mw. Both types are especially suited for general VHF power applications where severe environmental conditions are encountered.

6918 CRYSTAL TYPE RESISTORS (Filmohm Corp., 48 W. 25th St., New York, N. Y.)

Crystal type resistors fabricated by the vacuum deposition of a metal film on the ceramic body of a 1N21 or 1N23 package are announced. Extremely stable and reliable resistors are produced by immediately sealing the evaporated film in an impervious protective coating. Crystal detector mounts, crystal mixers, etc. can be checked for mis-match by replacing the crystal with a resistor having a resistance equal to the crystal impedance. Crystal resistors with resistance values between 25 and 400 ohms and power rating of 1 w average in an ambient of 100°C can be supplied.

6919 SURGE PROTECTOR (Vickers Inc., 1815 Locust St., St. Louis 3, Mo.)

The Captivolt surge protector for protecting silicon power rectifiers against high surge voltages is announced. The protector is a non-linear resistance device in which resistance decreases almost logarithmically with increase in voltage. Since the protector is non-polarized, it suppresses surges of either polarity. Power consumption is less than 5 w under steady-state conditions. Nine standard sizes covering the peak inverse voltage range of 50 v to 600 v are available. The device can also be used to suppress high-voltage surges in many other applications.

6920 POSITIVE TEMPERATURE COEFFICIENT THERMISTORS WITH SWITCHING CHARACTERISTICS (Westinghouse Electric Corp., Semiconductor Dept., Youngwood, Pa.)

Positive temperature coefficient thermistors which exhibit abrupt increases in resistance with temperature within a predetermined temperature range are announced. The temperature coefficient of resistance increases rapidly at the switching temperature from essentially zero to + 10%/°C at temperatures above the switching temperature. The combination of switching characteristic and positive temperature coefficient makes these thermistors particularly useful in control and indicating circuits. Thermistors with switching temperatures of 105°C and 115°C are currently available.

6921 BROADBAND COAXIAL ISOLATORS (Raytheon Co., Special Microwave Device Operations, 130 Second Ave., Waltham 54, Mass.)

Two broadband coaxial isolators for use in the L and S bands are announced. The IcLM3 operates from 1250 to 1600Mc, and has a minimum isolation of 20 db, a VSWR of 1.25, and a maximum insertion loss of 1.0 db. The IcSM2 operates between 2000 and 4000 Mc and has a minimum isolation of 20 db, a maximum VSWR of 1.25, and a maximum insertion loss of 2.0 db. Both devices can handle peak power of 5 kw with an average power of 25 w.

6922 SOLID ELECTROLYTE TANTALUM CAPACITORS (Sprague Electric Co., 91 Marshall St., N. Adams, Mass.)

Type 160 D Tantalex capacitors are announced. Designed for use in hearing aid and ultra-miniature circuits, the units have capacitance ratings of 0.05 µf to 10 µf and d-c working voltages of 2 v to 15 v. The capacitors utilize a solid semiconductor as the electrolyte and can operate over the temperature range -55°C to 65°C.

6923 DYNAMIC TEST SET (Wallson Associates, Inc., 912 Westfield Ave., Elizabeth, New Jersey)

A new 200 ampere dynamic test set, Model 164, designed to evaluate the characteristics of four silicon rectifiers simultaneously in a full wave circuit is announced. The basic circuitry consists of two power supplies — a low voltage, high current supply for forward characteristics; and a high voltage, low current supply for reverse characteristics. Simulation of actual operating conditions is achieved by electronically switching these power supplies on alternate half cycles. Parameters are adjusted independently of each other. Test capacity of the test set is four rectifiers in the range of 5—200 amperes d-c average forward current. Peak reverse voltage is adjustable between 0 - 1500 v and any combination of forward current and reverse voltage within these ranges may be obtained. Fine adjustments at the lower voltages is achieved and appropriate meter scales can be simultaneously switched.

6924 HIGH CURRENT ADAPTER FOR TRANSISTOR CURVE TRACER (Tektronix, Inc., P.O. Box 500, Beaverton, Oregon)

The Type 175 transistor curve tracer high current adapter which provides 200 ampere collector displays, three ranges of collector supply, and 12 ampere base supply is announced. When used with the Tektronix Type 575 Transistor Curve Tracer, the adapter permits the observation and measurement of characteristic curves of both high power n-p-n and p-n-p transistors and diodes. The diode curves can be plotted to 100 amperes or more.

6925 TRANSISTOR THERMAL TEST SET (Rescon Electronics Corp., 151 Bear Hill Road, Waltham 54, Massachusetts)

An instrument for making several different types of thermal measurements in transistors and diodes while the devices are operating in a circuit is announced. Transistor junction temperature can be determined by means of a "Thermograph" which relates the measured case temperature to the junction temperature. The instrument can also be used for determining heat sink efficiencies, temperature rises, thermal environmental conditions, and "hot spot" locations. Temperatures over the range -75°C to + 205°C can be measured. Other temperature ranges are also available on special order.

6926 MICROCHOPPER (Solid State Electronics Co., 15321 Rayen St., Sepulveda, California)

The Microchopper, a transistorized modulator solidly encapsulated within a transistor enclosure, is announced. The unit can be used to alternately connect and disconnect a load from a signal source or as a synchronous demodulator to convert a-c signals to d-c. It is capable of linearly switching or chopping voltages over the range from a fraction of a millivolt to 10 volts at frequencies from d-c to a hundred kilocycles. The circuitry is stable and free from drift over a wide temperature range. The noise figure of the chopper is competitive with mechanical choppers for many applications and does not increase with use. The unit is particularly suited for applications in which it will be subjected to shock and vibration and those which require power conservation, miniaturization, and elimination of maintenance.

6927 INFRAPHONE (Infrared Industries, Inc., P.O. Box 42, Waltham 54, Mass.)

A lightweight portable solid state instrument which utilizes infrared radiation to transmit messages over several hundreds of yards is announced. Each instrument is both a transmitter (microphone, voice-to-infrared converter, infrared source and optics) and a receiver (optics, infrared-to-voice converter, amplifier and earphone) and employs a fully-transistorized printed circuit amplifier. The receiver uses an infrared-sensitive photoconductor. Communication can be achieved with the Infraphone within line-of-sight, indoors or out, day or night.

SUBJECT INDEX

A

Absorption:
- Centers in Rutile Single Crystals 6629
- in Superconducting Aluminum, Millimeter Wave 6695
- of Evaporated Germanium Films, Index of 6716

Acceptors and Donors in P-N Junctions, Statistical Fluctuations of 6744
Adder-Subtracter Circuit Using Tunnel Diodes 6882
Adders,
- Magnetic Film Parametron 6878
- Solid State 6774
- Transistor Parallel 6874

Adsorption of Gases on Bismuth Telluride Cleavage Surfaces 6659
Aircraft Control, Transistor Wideband F-M Receiver for Remote 6852
Alkali Halide Points and Filaments by Controlled Dissolution, Production of 6658
Alloying, Plastic Deformation of Germanium by 6748
Alloys,
- Preparation and Properties of AlSb-GaSb 6623
- Solid Solution in II-VI Telluride 6624
- Solubility Enhancement in GaP-Si 6621
- Time Delays in the Superconducting Transition of Lead-Indium 6697
- X-ray Diffraction Studies of GaSb-Ge 6622

Alloys:
- for Bonding Thermocouples into Ferrites and Controlled Valency Semiconductors 6668
- for Use as Electrodes, Hard Gallium 6668

Aluminum,
- Energy Gap of Superconducting 6695, 6696
- Millimeter Wave Absorption in Superconducting 6695
- Penetration Depth in Superconducting 6696
- Superconductivity in 6693

Aluminum:
- Antimonide, Energy Gap and Lattice Constant of 6623
- Capacitors, Printed 6807

Amplifiers,
- Functional Unit: High-Q Tuned 6776
- Negative-Resistance: Noise in 6823
- Parametric:
  - Figure of Merit and Optimization 6830
  - Gain Inconsistencies in 6828
  - Helix 6831
  - Low-Noise 6827
  - Noise Considerations for 6829
  - Theory of Single Resonance 6832
- Transistor:
  - Broadband UHF Distributed 6825
  - Car-Radio Output Stages 6854
  - Chopper Type DC 6824
  - Double-Delay-Line Linear 6835
  - Driving Source with Push-Pull 6826
  - Recording-Pen 6834
  - Transfer Function Synthesis of Active RC Networks Using 6819
- Tunnel Diode: UHF 6833

Analog Transistors by Ion Drift, Fabrication of 6753
Anisotropy in Thin Films, Mechanical Model for Uniaxial Magnetic 6702
Antiferromagnetic:
- Manganese Di-Fluoride, Microwave Faraday Rotation in 6709
- Nickel Oxide Crystals,
  - Crystallographic Measurements in 6707
  - Domain Walls in 6707

Antiferromagnetic-Paramagnetic Transition in $CoBr_2 \cdot 6H_2O$ 6708
Arsenic into Vapor Grown Germanium, Incorporation of 6641
Automatic Frequency Control with Reactance Transistors 6836
Autopilot System for Missiles, Magnetic Shift Register 6853
Avalanche Breakdown in Silicon Junctions 6743

B

Barium Titanate,
- Measurement of the Dielectric Constant and Loss Tangent of 6674
- Temperature Dependence of Domain Wall Motion in 6677

Bismuth Telluride, Adsorption of Gases on Cleavage Surfaces of 6659
Bismuth Telluride Cleavage Surfaces, Bonding Properties of 6659
Boron into Silicon, Diffusion of 6637
Boron Phosphide, Electroless Contacts to 6666
Breakdown, Effect of Statistical Fluctuations of Donors and Acceptors on 6744
Breakdown in Uniform Silicon P-N Junctions, Broad Area 6745
Buffers, Solid State 6774

C

Cadmium in:
- Silver Bromide, Diffusion of 6639
- Silver Bromide-Cadmium Bromide Solid Solutions, Diffusion of 6639

Cadmium Sulfide, Transparent Contacts to 6667, 6780
Cadmium Sulfide Photovoltaic Cells, Photoemission in 6721
Cadmium Sulfide-Electrolyte Interface, Photovoltaic Effects at 6720
Cadmium Telluride, Decay Times of X-ray Excited Carriers in 6684
Cadmium Telluride-Mercuric Telluride Alloys, Solid Solution in 6624
Cadmium Telluride-Zinc Telluride Alloys, Solid Solution in 6624
Cameras, Transistor Television 6863
Capacitors, Printed Aluminum 6807
Capacitors with Semiconductor Electrolyte, Tantalum 6922
Carbon from Silicon Carbide, Study of Amorphous 6645
Cardiac Pacemaker, Transistor 6849
Carrier Concentration in Semiconductors Containing Multiply-Ionized Impurities, Equilibrium 6682
Carriers in Semiconductors, Measurement of Decay Times of X-ray Excited 6684
Casting, Preparation of AlSb and GaSb Alloys by Progressive and Zone 6623
Ceramics, Measurement of the Dielectric Constant of Ferroelectric 6675
Ceramics Containing Nb or Ta, Properties of Lead Titanate 6678
Channels on Silicon P-N Junctions, Anomalous Surface 6741
Chlorine, Reaction of Silicon Carbide Single Crystals with 6645
Chopper, Transistor Micro- 6926
Chopper Type DC Amplifier, Transistor 6824
Chromium^{3+} in TiO_2 as a Maser Material 6806
Circuit Techniques, Thin Film 6821
Circulators,
- Microwave Ferrite 6793
- Y-Junction Strip-Line 6794

Clamp for Millivolt Signals, Diode Bridge 6845
$CoBr_2 \cdot 6H_2O$, Néel Temperature of 6708
Cobalt Oxide, Oxygen Surplus in Mono-crystals of 6642
Coercive Force on Imperfections, Dependence of 6703
Coincidence Circuits, Transistor 6904, 6905
Complementary Transistor Circuits 6822
Compounds,
- Crystal Structure of $PbNb_2O_6$-Type 6676
- Ferroelectric Curie Temperature of $PbNb_2O_6$-Type 6676

Computer:
- Applications, Complementary Transistor Circuits for 6822
- Logic, Magnetic Analogs of Relay Contact Networks 6800
- Logic and Storage Devices, Ferrite Film 6801
- Logic Circuits,
  - Diode-Transistor 6871
  - Transistor 6874
  - Transistor-Resistor 6875, 6876
  - Tunnel Diode 6870, 6872, 6873
- Logic Devices, Magnetic Film Parametrons as 6878
- Logic Element, Multi-Aperture Magnetic 6799
- Memories,
  - Cryotron 6808
  - Fluxlok Technique for Magnetic Core 6884
  - Low Flux Density Materials for 6804
  - Reproducible Magnetic Film 6887
  - Survey of Magnetic Film 6886
  - Thin Magnetic Film 6655
  - Vacuum Evaporated Random Access 6888
- Memories Using Multiple Coincidence, Magnetic Core 6885
- Memory:
  - Cores, High-Speed Coincident Current 6803
  - Element, Persistor 6813
  - Element with Non-Destructive Read-Out Semiconductor 6889
  - Planes for Extreme Environmental Conditions, Miniature 6798
  - System, Transistor and Ferrite-Core 6885
- Scaling Circuits 6879, 6880
- with Elementary Structure, General-Purpose Microprogram-Controlled 6868

Computers, Solid State Micrological Elements for Digital 6774
Concentration Profile of Diffused Layers, Calculation of 6635
Conductivity:
- in Neutron Irradiated Germanium, Electrical 6672
- of Contacts to Silicon Carbide, Transient 6688
- Pulses in Irradiated Zinc Sulfide 6688
- Types, Infrared Techniques for Determining 6634

Contact:
- Electrification of Semiconductors 6673
- Layers to Transistors, Evaporated 6757

Contacts, Superconducting 6812
Contacts:
- to Boron Phosphide, Electroless 6666
- to Cadmium Sulfide, Transparent 6667, 6780
- to Silicon Carbide, Electroless 6666
- to Silicon Carbide, Transient Conductivity of 6689

Control, Transistor Wideband F-M Receiver for Remote Aircraft 6852
Controlled:
- Rectifier Circuits 6840
- Rectifiers Using Triode Transistors, Design of 6893

Conversion Loss of Gallium Arsenide Microwave Diodes 6732
Copper:
- in Germanium, Calculation of the Heat of Solution of 6620
- in the Heat Treatment of Gallium Arsenide, Effect of 6669

Cores,
- Fluxlok Memory Technique Using Ferrite 6884
- High-Speed Coincident Current Memory 6803

Correlators Using Hall Effect Multipliers 6903
Corundum, Paramagnetic Resonance of Mn^{2+} in 6714
Counters,
- Large Area Germanium Surface-Barrier 6908
- Transistor Pulse Steering Circuit for Binary 6881

SUBJECT INDEX (continued)

Cryotron:
  Shift Register 6808
  Storage Circuit 6808
  Trigger Circuits 6810
Cryotrons,
  Crossed Film 6808
  Superconducting Contacts for 6812
  Thin Film 6809, 6810, 6811
Crystal:
  Structure of:
    Ferroelectric Lead Metatantalate 6679
    $PbNb_2O_6$-Type Compounds 6676
  Type Resistors 6918
Crystals,
  Growth of GaP-Si Single 6621
  Resistivity Variations in Germanium Single 6648
  Role of Twin Planes in the Rapid Dendritic Propagation of Germanium 6656
Crystals by the Czochralski Method, Liquid-Solid Interface During Growth of Silicon 6647
Current Limiter, Transistor Galvanometer 6844
Curve Tracer,
  High Current Adapter for a Transistor 6924
  Tunnel Diode 6817
Czochralski Method, Liquid-Solid Interface During Growth of Silicon Crystals by the 6647

D

Defects:
  in Indium Antimonide, Deformation Induced 6632
  Produced in Neutron Irradiated Germanium 6627
Deformation-Induced Defects in Indium Antimonide 6632
Delay Circuit, Transistor Phantastron 6848
Delay Circuit for Relays 6846
Dendrites,
  Growth of Gallium Arsenide 6657
  Orientation of Etch Pits on Germanium 6664
  Propagation Mechanism of Germanium 6656
Density Reduction in Neutron Irradiated Germanium 6627
Device Reliability, Method for Evaluating Semiconductor 6730
Devices,
  Equipment for Encapsulating Semiconductor 6772
  IRE Standards on Solid State 6729
  Negative Resistance in Semiconductor 6731
Diamagnetism of Graphite, Electron 6715
Dielectric:
  Constant of:
    Barium Titanate, Measurement of the 6674
    Ferroelectric Ceramics, Measurement of the 6675
  Polarization of Ferroelectric Solid Solutions Based on Sodium Niobate 6680
  Properties of:
    Ferroelectric Lead Metatantalate 6679
    Lead Titanate Ceramics Containing Nb or Ta 6678
Diffraction Microscopy, Observation of Dislocations in Silicon Carbide by X-ray 6631
Diffused:
  Layers, Calculation of the Properties of 6635
  Shot-Melting Technique for Making Junction Devices 6749
Diffusion:
  Constants by Ion Drift, Measurement of 6753
  in Silicon, Influence of Surface Phenomena on the Rate of Impurity 6636
  of Boron in Silicon 6637
  of Cadmium in Silver Bromide 6639
  of Cadmium in Silver Bromide-Cadmium Bromide Solid Solutions 6639
  of Copper in Germanium, Activation Energies for the 6620
  of Copper in Germanium, Dissociation Mechanism for the 6620
  of Impurities into Silicon 6757
  of Lithium in Silicon 6638
  Techniques for Applying Contacts to Cadmium Sulfide 6667
Diffusivity with Surface Concentration in Silicon, Variation of 6637
Diode:
  Bridge Clamp for Millivolt Signals 6845
  Curve Tracer, Tunnel 6817
  Loop Scatterer for Microwave Field Distribution Measurements 6902
  Matrices, Vapor Grown 6750
  Parametric Amplifiers, Low-Noise 6827
  -Transistor NOR Circuits 6871
Diodes,
  Conversion Loss of Gallium Arsenide Microwave 6732
  Equipment for Encapsulating 6772
  Junction:
    Anomalous Surface Channels on 6741
    Breakdown in Uniform 6746
    Broad Area Breakdown in 6745
    Diffused Shot-Melting Technique for Making 6749
    Effect of Tunneling on I-V Characteristics 6700
    Excess Reverse Current Due to Metal Precipitates 6754
    External Photo-electric Emission from Back Biased Silicon 6722
    Fabrication by Thermal Oxidation 6751
    High Voltage Breakdown 6753
    Internal Field Emission in Narrow Indium Antimonide 6747
    Ionization Rates for Electrons in 6746
    Light Emission from 6742, 6745
    Location of Junctions in 6752
    Low Breakdown Spots in 6744
    Microplasmas in 6742, 6743, 6745
    Negative Resistance 6733
    P-N-P-N 6733
    Plastic Deformation of Germanium by Alloying 6748
    Preparation of Uniform 6745
    Shot and Thermal Noise at High Current Levels 6766
    Statistical Fluctuations of Donors and Acceptors in 6744
    Transient Response of Variable Capacitance 6735
    Vapor Grown 6734, 6750
    Variable Capacitance 6734
    Zener 6736
  Low-Melting Glasses for Sealing 6773
  Thermal Test Set for 6925
  Thin Film Circuit Techniques Using 6821
  Tunnel:
    Gallium Arsenide 6739
    Indium Antimonide 6747
    Maximum and Minimum Current in Germanium 6737
    Shot Noise in 6740
    Temperature Dependence of Current in 6738
  Turnover Behavior of Germanium 6731
Dislocation:
  Climb in Plastically Deformed Indium Antimonide 6632
  Etch Pits in Germanium, Effect of Copper Precipitation on 6662
Dislocations in:
  Alloyed Germanium 6748
  Graphite Single Crystals 6633
  Silicon by Anomalous Transmission of X-rays, Observation of 6630
  Silicon Carbide by Diffraction Microscopy, Observation of 6631
  Surface Layers of Lithium Fluoride, Effects of Temperature on 6643
  Vapor Grown Germanium 6651
Display Devices, Review of Panel-Type 6892
Dissociation Mechanism for the Diffusion of Substitutional Copper in Germanium 6620
Domain Wall Motion in Barium Titanate, Temperature Dependence of 6677
Domain Walls in:
  Antiferromagnetic Nickel Oxide Crystals 6707
  Ferrites, Fast Switching by 6796
Donors and Acceptors in P-N Junctions, Statistical Fluctuations of 6744
Doping, Infrared Techniques for Determination of Local 6634
Drift:
  Mobility for Electrons and Holes, Evaluation of the Ratio of Hall Mobility to 6683
  Transistors, Equivalent Circuit Parameters of 6761
Duplexers, Study of Microwave Ferrite 6793

E

Echo-Sounder, Transistor Underwater 6867
Elastic Constants of Sodium Iodide at Low Temperatures 6724
Electrical Properties of Thin Indium Antimonide Layers 6654
Electrode Connection to a Semiconductor Body 6770
Electrodes,
  Evaporated High Conductance Metal 6757
  Hard Gallium Alloys for Use as 6668
Electrodes for Transistors, Simultaneous Evaporation of Several 6769
Electroless Plated Contacts to SiC and BP 6666
Electrolytic Aluminum Capacitors 6807
Electron-Electron Scattering in N-P Tunneling 6700
Electron Paramagnetic Resonance Spectrometer, Analysis of a 6901
Electrons:
  and Holes, Evaluation of the Ratio of Hall Mobility to Drift Mobility for 6683
  in Semiconductors, Measurement of Excess 6683
Emission from Back Biased Silicon Junctions, External Photoelectric 6722
Encapsulation of Semiconductor Devices, Equipment for the 6772
Energy Gap of Superconducting Aluminum 6695, 6696
Energy Gaps of AlSb, GaSb and AlSb-GaSb 6623
Enthalpy of Formation of III-V Compounds 6626
Epitaxial Vapor:
  Deposition, Surface Preparation for 6650
  Growth of Germanium, Introduction of Impurities During 6651
Equivalent Circuit:
  of P-N-P-N Junction Diodes 6733
  Parameters of Drift Transistors 6761
Etch Pits:
  in Germanium, Effect of Copper Precipitation on Dislocation 6662
  in Pyrolytic Graphite, Ion-Bombardment Produced 6663
  on Germanium Dendrites, Orientation of 6664
Etches on Fast Germanium Surface States, Effect of Chemical 6670
Etching:
  of Semiconductors, Role of Holes in the Electrolytic 6661
  on Surface Structure, Effect of 6644
  Rate of Silicon 6665
Evaporated High Conductance Metal Electrodes 6757
Extinction Coefficient of a Highly Doped Silicon Surface 6723

F

Failure of Transistors with Inductive Loads 6756
Faraday Rotation in Antiferromagnetic Manganese Di-Fluoride, Microwave 6709

Ferrite:
- Core and Transistor Memory System 6883
- Duplexers, Study of Microwave 6793
- Films for Logic and Storage, Open Flux Path 6801
- Memory Cores,
  - Fluxlok Memory Technique Using 6884
  - High-Speed Coincident Current 6803
- Memory Planes for Extreme Environmental Conditions, Miniature 6798
- Samples, Walker Modes in Large 6792

Ferrites,
- Alloys for Bonding Thermocouples into 6668
- Effect of Previous History on Switching Rate in 6795
- Fast Switching by Domain Walls in 6796

Ferroelectric:
- Ceramics, Measurement of the Dielectric Constant of 6675
- Curie Temperature of $PbNb_2O_6$-Type Compounds 6676
- Lead Metatantalate, Properties of 6679
- Properties of Lead Titanate Ceramics Containing Nb or Ta 6678
- Solid Solutions Based on Sodium Niobate, Properties of 6680

Ferromagnetic Resonance:
- at High Power Levels, Theory of 6710
- Experiments, Generation of Phonons in High Power 6706
- in Rare Earth Garnets 6705

Ferromagnetic Thin Films, Preparation and Properties of 6655

Field Emission at Narrow P-N Junctions in Indium Antimonide, Internal 6747

Filaments by Controlled Dissolution, Production of Alkali Halide 6658

Films,
- Computer Store Employing Thin Ferromagnetic 6655
- Evaporator for the Deposition of Radioactive Germanium 6652
- Growth of Single Crystal Si and Ge 6649
- Indices of Absorption and Refraction in Evaporated Germanium 6716
- Mechanical Model for Uniaxial Magnetic Anisotropy in Thin 6702
- Preparation and Properties of Thin Ferromagnetic 6655
- Time Delays in the Superconducting Transition of Lead 6697
- Vacuum Evaporated Silicon Single Crystal 6653

Filter, Synthesis of a Transistorized Twelfth-Order Tchebycheff Parameter Bandpass 6820

Filters Employing Single Crystal Garnet Resonators, Magnetically Tunable Microwave 6791

Fluctuations of Donors and Acceptors in P-N Junctions 6744

Fluxlok Memory Technique Using Ferrite Memory Cores 6884

Formation:
- of SiC, Free Energy and Heat of 6625
- of III-V Compounds, Enthalpy and Free Energy of 6626

Free Energy of Formation of SiC, Standard 6625

Frequency Counting Circuits, Transistor Wave Shaping Circuit for 6839

Functional Units,
- Shift Register Transistor 6775
- Solid State Micrologic 6774
- Twin-T Network 6776

G

Gallium Antimonide, Properties of 6623

Gallium Antimonide-Aluminum Antimonide Alloys, Preparation and Properties of 6623

Gallium Antimonide-Germanium Alloys, X-ray Diffraction Study of 6622

Gallium Arsenide,
- Heat Treatment of 6669
- Surface Damage in 6660

Gallium Arsenide:
- Dendrites, Growth and Properties of 6657
- Diodes, Noise Temperature Ratio of 6732
- Photodiodes for the Visible Region 6782
- Solar Converters 6786
- Tunnel Diodes 6739

Gallium Arsenide-Electrolyte Interface, Photovoltaic Effect at 6720

Gallium Iron Oxide Resonators, Piezoelectric and Magnetostrictive Properties of 6681

Gallium Phosphide-Silicon Alloys, Solubility Enhancement in 6621

Gallium Phosphide-Silicon Single Crystals, Growth of 6621

Galvanometer Current Limiter, Transistor 6844

Garnet Resonators, Magnetically Tunable Microwave Filters Employing Single Crystal 6791

Garnets, New Synthetic 6646

Gates, Solid State 6774

Germanium,
- Decay Times of X-ray Excited Carriers in 6684
- Effect of Copper Precipitation on Dislocation Etch Pits in 6662
- Effect of P-Type Occlusions on the Resistivity of Heavily Doped N-Type 6686
- Electrolytic Etching of 6661
- Heat of Solution of Copper in 6620
- Neutron Radiation Effects in 6627, 6672
- Properties of Vapor Grown 6640, 6641, 6651
- Thermal Diffusivity of 6726

Germanium:
- by Alloying, Plastic Deformation of 6748
- Dendrites, Orientation of Etch Pits on 6664
- Dendrites, Propagation Mechanism of 6656
- Films, Evaporator for the Deposition of Radioactive 6652
- Films, Growth of Single Crystal 6649
- Films, Indices of Absorption and Refraction in 6716
- Single Crystals by the Disproportionation of GeI_2, Growth of 6640, 6641, 6651
- Single Crystals, Resistivity Variations in 6648
- Surface States, Effect of Chemical Etches on Fast 6670
- Surfaces, Origin of First-Order Structure on Etched 6644

Germanium-Gallium Antimonide System, Metastable Solid Solutions in the 6622

Grain-Boundary Photoresponse 6788

Graphite,
- Band Structure of 6715
- Diamagnetism of 6715
- Ion-Bombardment Produced Etch Pits in Pyrolytic 6663

Graphite Single Crystals, Dislocations in 6633

Growth of:
- Gallium Arsenide Dendrites 6657
- GaP-Si Single Crystals 6621
- Germanium Single Crystals by the Disproportionation of GeI_2 6640, 6641, 6651
- Silicon Crystals by the Czochralski Method, Liquid-Solid Interface During 6647
- Single Crystal Si and Ge Films 6649

H

Hall:
- Effect:
  - Measurements on Semiconductors at Microwave Frequencies 6699
  - Multipliers, Correlators Using 6903
- Field, Frequency Dependence of the Complex 6699
- Generator with Large Ratio of Length to Width 6698
- Mobility:
  - in Neutron Irradiated Germanium 6672
  - to Drift Mobility for Electrons and Holes, Evaluation of the Ratio of 6683
- Voltage in an Inhomogeneous Magnetic Field 6698

Hamiltonian for the Paramagnetic Spectrum of Iron in Strontium Titanate 6712

Harmonic Generator for Space-Vehicle Applications, Nonlinear Capacitor 6843

Hearing Aid Capacitors 6922

Heat Treatment of Gallium Arsenide, Effect of Impurities in the 6669

Holes in Semiconductors, Measurement of Excess 6683

I

Imperfections, Dependence of the Coercive Force on 6703

Impurities, Carrier Properties in Semiconductors Containing Multiply-Ionized 6682

Impurities During Epitaxial Vapor Growth of Germanium, Introduction of 6651

Impurity Redistribution in Germanium by Thermal Oxidation 6751

Indium Antimonide,
- Dislocation Climb in Plastically Deformed 6632
- Magnetic Field Effects in Tunneling in 6701
- Production and Properties of Thin Layers of 6654
- Surface Damage in 6660

Indium Antimonide:
- P-N Junctions, Internal Field Emissions at Narrow 6747
- Photodiodes, Noise in 6781

Inductors, Operation of Thin Magnetic Film as Time Variable 6802

Infrared, Voice Communication by 6927

Infrared:
- Quantum Counters, Time Discrimination in Solid State 6789
- Techniques for Determining Conductivity Types 6634

Intermetallic Compounds, Electrolytic Etching of 6661

Intrinsic Regions by Ion Drift, Production of 6753

Inverter,
- Controlled Rectifier 6840
- Transistor 6895, 6896, 6897
- Unijunction 6840

Iodine in Vapor-Grown Germanium Single Crystals, Concentration of 6640

Ion Drift, Measurement of Diffusion Constants by 6753

Ion-Bombardment Produced Etch Pits in Pyrolytic Graphite 6663

Ionization:
- Chamber, Solid-State 6910
- Rates for Electrons in Uniform Silicon P-N Junctions 6746

Iron, Thermal Diffusivity of Armco 6726

Iron in:
- Rutile, Paramagnetic Resonance of 6713
- Strontium Titanate, Hamiltonian for the Paramagnetic Structure of 6712

Isolator, Transistor Switch Stimulus 6851

Isolators, Broadband Coaxial 6921

J

Junction Formation in Silicon by Thermal Oxidation 6751

Junctions,
Photoeffect in Nonuniformly Irradiated 6784
Photoelectric Emission from Treated Silicon P-N 6722
Photoemission in Undiffused Metal-Semiconductor 6721
Tunneling in Indium Antimonide 6701
Vapor-Grown P-N 6640
Junctions in Semiconductors, Location of 6752

L

Lattice:
Constants of AlSb, GaSb and AlSb-GaSb 6623
Dispersion Frequencies of Sodium Chloride and Potassium Chloride, Fundamental 6671
Vacancies in Neutron Irradiated Germanium 6627
Lead, Superconductivity in 6693
Lead Films, Time Delays in the Superconducting Transition of 6697
Lead-Indium Alloys, Time Delays in the Superconducting Transition of 6697
Lead Metatantalate, Properties of Ferroelectric 6679
Lead Metatantalate with Niobium, Barium, and Strontium, Solid Solutions of 6679
$PbNb_2O_6$-Type Compounds,
Crystal Structure of 6676
Ferroelectric Curie Temperature of 6676
Lead Titanate Ceramics Containing Nb or Ta, Properties of 6678
Light Emission from Silicon P-N Junctions 6742
Lithium Fluoride,
Effects of Temperature on Surface Layers of 6643
Influence of F-Centers on the Thermal Conductivity of 6725
Lithium in Silicon, Diffusion of 6638
Location of Junctions in Semiconductors 6752
Logic,
Magnetic Analogs of Relay Contact Networks for 6800
Open Flux Path Ferrite Films for 6801
Logic:
Circuits,
Diode-Transistor 6871
Transistor 6874
Transistor-Resistor 6875
Tunnel Diode 6870, 6872, 6873
Devices, Magnetic Film Parametrons as 6878
Element, Multi-Aperture Magnetic 6799
Elements, Solid State Micro- 6774
Network, Statistical Analysis of Transistor-Resistor 6876
Loss Tangent of Barium Titanate, Measurement of the 6674
Luminescent Display Devices, Review of Panel-Type 6892

M

Magnetic:
Analogs of Relay Contact Networks for Logic 6800
Anisotropy in Thin Films, Mechanical Model for Uniaxial 6702
Core:
Memories Using Multiple Coincidence 6885
Transistor Switching Circuit 6841
Cores,
High-Speed Coincident Current 6803
Use of a Transistor for Setting 6877
Field, Hall Voltage in an Inhomogeneous 6698
Field:
Dependence of Ultrasonic Attenuation in Semimetals 6728
Effects on Tunneling in Indium Antimonide 6701
of Twistors, Representation of the 6797
Film:
Memories,
Reproducible 6887
Survey of 6886
Memory, Thin 6655
Parametrons, Operation of 6802
Parametrons as Logical Devices 6878
Shift Register 6891
Logic Element, Multi-Aperture 6799
Materials for High-Speed Storage, Low Flux Density 6804
Properties of Graphite 6715
Resonance:
Observations, Transistor Oscillator for Nuclear 6900
Spectrometer, Analysis of a 6901
Shift Register Missile Autopilot System 6853
Structure of Manganese Nitride 6704
Magnetically Tunable Microwave Filters Employing Single Crystal Garnet Resonators 6791
Magnetocrystalline Anisotropy, Coercive Force in Materials which have High 6703
Magneto-Oscillatory Effect in the Electron-Hole Plasma in a Semiconductor 6777
Magnetoresistive Trigger Circuits, Resolving Time and Flipping Time of 6842
Magnetostatic Resonance Modes in Large Ferrite Samples 6792
Magnetostrictive Properties of Gallium Iron Oxide Single Crystal Resonators 6681
Manganese Di-Fluoride, Microwave Faraday Rotation in Antiferromagnetic 6709
Manganese Dioxide, Effect of Thorium Doping on Resistivity Variations in 6687
Manganese in Corundum, Paramagnetic Resonance of 6714
Manganese Nitride, Magnetic Structure of 6704
Manganese Oxide, Oxygen Surplus in Mono-Crystals of 6642
Masers, Design of Directional 6805
Masking Technique for Vacuum Evaporation 6769
Measurement of:
Decay Times of X-ray Excited Carriers in Semiconductors 6684
Diffused Layers, P-N Junction Method for the 6637
Diffusion Constants by Ion Drift 6753
Diode and Transistor Thermal Properties 6925
Excess Holes and Electrons in Semiconductors 6683
High Current:
Rectifier Parameters 6923
Transistor Characteristics 6924
Local Doping, Infrared 6634
Microwave Field Distributions 6902
Semiconductor:
Homogeneity, Infrared 6634
Type, Infrared 6634
Switching Transistor Parameters 6818
the Dielectric Constant and Loss Tangent of Barium Titanate 6674
the Dielectric Constant of Ferroelectric Ceramics 6675
the Equivalent Circuit Parameters of Drift Transistors 6761
the Hall Effect in Semiconductors at Microwave Frequencies 6699
Measuring Set for Telephone Message Circuit Noise 6865
Medical Applications of Transistors:
Cardiac Pacemaker 6849
Physiological Stimulators 6850
Stimulus Isolator 6851
Memories,
Reproducible Magnetic Film 6887
Survey of Magnetic Film 6885
Memories Using Multiple Coincidence, Magnetic Core 6885
Memory,
Thin Ferromagnetic Film 6655
Vacuum Evaporated Random Access 6888
Memory:
Cores, High-Speed Coincident Current 6803
Element, Persistor Superconducting 6813
Element with Non-Destructive Read-Out, Semiconductor 6889
Planes for Extreme Environmental Conditions, Miniature 6798
System, Transistor and Ferrite-Core 6883
Mercuric Telluride-Zinc Telluride Alloys, Solid Solution in 6624
Mercury, Superconductivity in 6693
Metal Precipitates, Excess Reverse Current in Junction Diodes Due to 6754
Micrologic Elements, Solid State 6774
Microplasma Phenomena in Silicon P-N Junctions 6742
Microplasmas in Silicon Junctions, Theory of 6743
Microwave:
Energy Through a Semiconductor, Effect of Absorption and Multiple Reflections on the Transmission of 6779
Ferrite Duplexers, Study of 6793
Field Distributions, Measurement of 6902
Filters Employing Single Crystal Garnet Resonators, Magnetically Tunable 6791
Generator, Semiconductor 6866
Modulators, Semiconductor 6778, 6779
Millivoltmeter with High Input Impedance, Transistor 6899
Missile Autopilot System, Magnetic Shift Register 6853
Mobility for Electrons and Holes, Evaluation of the Ratio of Hall Mobility to Drift 6683
Mobility in Neutron Irradiated Germanium, Hall 6672
Modulators,
Semiconductor Microwave 6778, 6779
Transistor 6926
Motor Speed Control for Satellite Tape Recorders 6898
Multi-Aperture Magnetic Logic Element 6799
Multivibrators, Time Delay Stability in Transistor 6838

N

Negative Resistance:
Amplifiers, Noise in 6823
Diodes, P-N-P-N 6733
in Semiconductor Devices 6731
Network Synthesis Using a Practical Transistor Amplifier 6819
Neutron:
Bombardment Damage in Germanium, Stability of 6672
Irradiated Germanium,
Defects Produced in 6627
Density Reduction in 6627
Electrical Conductivity in 6672
Hall Mobility in 6672
Lattice Vacancies in 6627
Radiation Damage, Resistance of Microalloy Diffused Base Transistor to 6767
Nickel Oxide, Oxygen Surplus in Mono-Crystals of 6642
Nickel Oxide Crystals,
Crystallographic Measurements in Antiferromagnetic 6707
Domain Walls in Antiferromagnetic 6707

SUBJECT INDEX (continued)

Noise:
at High Current Levels in Junction Diodes, Shot and Thermal 6766
Consideration for the Variable Capacitance Parametric Amplifier 6829
in Indium Antimonide Photodiodes 6781
in Negative-Resistance Amplifiers 6823
in Tunnel Diode Amplifiers, Shot 6740
Temperature Ratio of Gallium Arsenide Microwave Diodes 6732
Nuclear:
Coincidence Circuits, Transistor 6904, 6905
Magnetic Resonance Observations, Transistor Oscillator for 6900
Particle:
Counters, Large Area Germanium Surface-Barrier 6908
Detectors, Silicon Junction 6909, 6912, 6913, 6915
Spectrometers,
Silicon Junction 6910, 6914
Silicon Surface-Barrier 6911

O

Occlusions on the Resistivity of Heavily Doped N-Type Germanium, Effect of P-Type 6686
Ohmic Contact Method for Obtaining Sheet-Conductance Profile of Diffused Layers 6635
Optical Properties of Thin Indium Antimonide Layers 6654
Organic Semiconductors,
Preparation of 6690
Resistivity of 6690
Orientation of Etch Pits on Germanium Dendrites 6664
Oscillators,
Cryotron Ring 6811
Functional Unit 6776
Semiconductor Oscillistor 6777
Transistor:
Automatic Frequency Control 6836
LC 6837
Oscillistor 6777
Oxide Monocrystals, Modified Bunsen Method for Determination of Stoichiometric Deviations in 6642

P

Paramagnetic:
Amplifiers, Design of Directional 6805
Properties of Cr^{3+} in Titanium Dioxide 6806
Resonance, Passage Effects in 6711
Resonance of Mn^{2+} in Corundum 6714
Parametric Amplifiers,
Helix 6831
Low-Noise 6827
Noise Considerations for 6829
Theory of Single Resonance 6832
Parametric:
Diode Figure of Merit and Optimization 6830
Up-Converters, Gain Inconsistencies in Low-Frequency Reactance 6828
Parametron:
Binary Adder 6878
Shift Register 6878
Parametrons, Operation of Magnetic Film 6802
Parametrons as Logical Devices, Magnetic Film 6878
Penetration Depth in Superconducting Aluminum 6696
Persistor Superconducting Memory Element 6813
Phantastron Delay Circuit, Transistor 6848
Phonon-Assisted Transitions in Tunnel Currents 6701
Phonons in High Power Ferromagnetic Resonance Experiments, Generation of 6706
Photoconductivity in Potassium Chloride, F-Center 6717
Photoconductor Response, Contact Geometry and Detector Orientation Considerations in Maximizing 6780
Photoconductors, High Electric Fields in Shadow Regions on 6718
Photodetectors, Grain-Boundary 6788
Photodiodes, Noise in Indium Antimonide 6781
Photodiodes for the Visible Region, Gallium Arsenide 6782
Photoeffects in Nonuniformly Irradiated P-N Junctions 6784
Photoemission:
from Back Biased Silicon Junctions, External 6722
in the Photovoltaic Response of Cu-CdS Cells 6721
Photoresponse of Silicon P-N Junction Surfaces 6741
Photovoltaic:
Effect:
at a Gallium Arsenide - Electrolyte Interface 6720
from the Carnot Cycle, Derivation of the 6783
in Binary Compounds, Becquerel 6720
Response of Cu-CdS Cells, Photoemission in the 6721
Solar Energy Converters,
Efficiency of 6785
Gallium Arsenide 6786
Improvement of 6787
Phthalocyanine, Photoconductivity in Films of 6719
Physiological:
Stimulator, Transistor 6850
Stimulus Isolator, Transistor 6851
Piezoelectric:
Constants of Gallium Iron Oxide 6681
Plates by Use of Parallel Field, Excitation of 6816
Properties of Some Ferroelectric Solid Solutions Based on Sodium Niobate 6680
Plasma in a Semiconductor, Magneto-Oscillatory Effect in the Electron-Hole 6777
Plastic Deformation of Germanium by Alloying 6748
Plastically Deformed Indium Antimonide, Dislocation Climb in 6632
Points by Controlled Dissolution, Production of Alkali Halide 6658
Polygonization in Plastically Deformed Indium Antimonide 6632
Potassium Chloride,
F-Center Photoconductivity in 6717
Fundamental Lattice Dispersion Frequency of 6671
Power Supply, Zener Diode Stabilized 6736
Protector, Silicon Rectifier Surge 6919
Pulse Circuits,
Complementary Transistor 6822
Diode Clamp 6845
Pulse Steering Circuit for Binary Counters, Transistor 6881
Push-Pull Transistor Amplifiers, Driving Source for 6826
Pyrolytic Graphite, Ion-Bombardment Produced Etch Pits in 6663

Q

Quantum Counters, Time Discrimination in Solid State Infrared 6789
Quartz Plates, Effect of Initial Stress in Vibrating 6815
Quartz Plates by Use of Parallel Field, Excitation of 6816

R

Radiation:
Effects in Germanium Transistors 6755
Monitor, Transistor 6916
Produced:
Defects in Germanium 6627
Density Reduction in Germanium 6627
Vacancies in Sodium Chloride, Optical Detection of 6628
Survey Meter, Transistor 6906
Radio:
Circuits,
Transistor Car 6854
Transistor FM Limiter 6862
Receivers,
Improved A-G-C Characteristics in Transistor 6857
Parasitic Oscillation in Transistor AM 6856
Transistor FM 6855
Rare Earth Garnets, Ferromagnetic Resonance in 6703
Recombination Rate in Semiconductors Containing Multiply-Ionized Impurities 6682
Recording-Pen Amplifier, Transistor 6834
Rectifier Parameters, Measurement of High Current 6923
Rectifiers,
Surge Protector for Silicon Power 6919
Test Set for Silicon 6923
Rectifiers Using Triode Transistors, Design of Controlled 6893
Refraction:
in Evaporated Germanium Films, Index of 6716
of Highly-Doped Silicon Surfaces, Index of 6723
Relay Contact Networks for Logic, Magnetic Analogs of 6800
Relays, Delay Circuit for 6846
Reliability, Evaluation of Transistor 6730
Resistivity:
Measurements on Tunnel Diode Materials, Anomalous 6685
of Heavily Doped N-Type Germanium, Effect of P-Type Occlusions on the 6686
of Organic Semiconductors 6690
Variations in:
Germanium Single Crystals 6648
Manganese Dioxide, Effect of Thorium Doping on 6687
Resistors, Crystal Type 6918
Resonance:
Modes in Large Ferrite Samples 6792
of Fe^{3+} in Rutile 6713
Resonators,
Magnetically Tunable Microwave Filters Employing Single Crystal Garnet 6791
Properties of Gallium Iron Oxide Single Crystal 6681
Rutile, Paramagnetic Resonance of Fe^{3+} in 6713
Rutile:
as a Maser Material, Chrome-Doped 6806
Single Crystals, Absorption Centers in 6629

S

Sandwich Structure for a Germanium P-N-P-N Switch 6760
Satellite, Harmonic Generator for a 6843
Satellite Tape Recorders, Motor Speed Control for 6898
Scalers,
Transistor 6880
Tunnel Diode 6879
Scaling Theory, Transistor 6762
Scattering in N-P Tunneling, Electron-Electron 6700
Scintillation Counter Spectroscopy, Transistor Amplifier for 6835
Semiconductor:
Device Reliability, Method for Evaluating 6730
Devices,
Equipment for Encapsulating 6772
Low-Melting Glasses for Sealing 6773
Negative Resistance in 6731

Memory Element with Non-Destructive Readout 6889
Microwave:
Generator 6866
Modulators 6778, 6779
Strain Transducers 6814
Type, Infrared Techniques for Determination of 6634
Semiconductors,
Alloys for Bonding Thermocouples to 6668
Contact Electrification of 6673
Effect of Absorption and Multiple Reflections on the Transmission of Microwave Energy Through 6779
Electrodes for Controlled Valency 6668
Electrolytic Etching of 6661
Location of Junctions in 6752
Magneto-Oscillatory Effect in the Electron-Hole Plasma in 6777
Measurement of:
Decay Times of X-ray Excited Carriers in 6684
Excess Holes and Electrons in 6683
Preparation and Properties of Organic 6690
Semiconductors:
at Microwave Frequencies, Hall Effect Measurements on 6699
Containing Multiply-Ionized Impurities, Properties of 6682
Shift Registers,
Cryotron 6808
Parametron 6878
Solid State 6774
Thin Magnetic Film 6891
Transistor 6874
Tunnel Diode 6870
Shift Register:
Autopilot System for Missiles, Magnetic 6853
Interstage Coupling Circuitry 6890
Transistor 6775
Signalling Device Utilizing Infrared 6927
Silicon,
Diffusion of:
Boron into 6637
Impurities into 6757
Lithium in 6638
Electrolytic Etching of 6661
Epitaxial Vapor Deposition of 6650
Etching Rate of 6665
Extinction Coefficient of Highly Doped 6723
Influence of Surface Phenomena on the Rate of Impurity Diffusion in 6636
Observation of Dislocations in 6630
Silicon:
Crystals by the Czochralski Method, Liquid-Solid Interface During Growth of 6647
Devices, Surface Treatment of 6771
Films, Growth of Single Crystal 6649
Power Rectifiers, Surge Protector for 6919
Single Crystal Films, Vacuum Evaporated 6653
Surfaces, Index of Refraction of Highly Doped 6723
Silicon Carbide,
Dislocations in 6631
Electroless Contacts to 6666
Standard Free Energy and Heat of Formation of 6625
Study of Amorphous Carbon from 6645
Transient Conductivity of Contacts to 6689
Silicon Carbide Single Crystals with Chlorine, Reaction of 6645
Silicon-Gallium Phosphide Alloys, Solubility Enhancement in 6621
Silver Bromide, Diffusion of Cadmium in 6639
Silver Bromide-Cadmium Bromide Solid Solutions, Diffusion of Cadmium in 6639
Skin Depth in Superconducting Aluminum 6696
Sodium Chloride,
Fundamental Lattice Dispersion Frequency of 6671
Optical Detection of Radiation Produced Vacancies in 6628
Sodium Iodide,
Elastic Constants of 6724
Specific Heat of 6724
Sodium Niobate, Properties of some Ferroelectric Solid Solutions Based on 6680
Solar Energy Converters,
Efficiency of 6785
Gallium Arsenide 6786
Improvement of 6787
Solid Solution:
Ceramics Containing Nb or Ta, Lead Titanate 6678
in the GaSb-AlSb System 6623
in the GaSb-Ge Pseudo-Binary System 6622
Solid Solutions:
Based on Sodium Niobate, Properties of Ferroelectric 6680
in II-VI Tellurides 6624
of Lead Metatantalate with Niobium, Barium, and Strontium 6679
Solid State:
Devices, IRE Standards on 6729
Micrologic Elements 6774
Solubility Enhancement in GaP-Si Alloys 6621
Solution of Copper in Germanium, Calculation of the Heat of 6620
Space-Vehicle Applications, Nonlinear Capacitor Harmonic Generator for 6843
Specific Heat of Sodium Iodide 6724
Spectrometer, Analysis of an Electron Paramagnetic Resonance 6901
Spin Alignment in Superconductors 6694
Sputtering Techniques for Applying Contacts to Cadmium Sulphide 6667
Squelch Circuit, Transistor 6858
Stabilization of Time Delay Multivibrators 6838
Stabilizer, Zener Diode Voltage 6736
Stoichiometric Deviations in Oxide Monocrystals, Modified Bunsen Method for Determination of 6642
Stoichiometry of $PbNb_2O_6$-Type Compounds, Non- 6676
Storage,
Low Flux Density Materials for High-Speed Storage 6804
Open Flux Path Ferrite Films for 6801
Storage Circuits, Cryotron 6808
Strain Transducers, Semiconductor 6814
Stip-Line Circulator, Y-Junction 6794
Stroboscope, Fractional Millimicrosecond 6907
Strontium Titanate, Hamiltonian for the Paramagnetic Spectrum of Iron in 6712
Structure of Etched Germanium Surfaces 6644
Superconducting:
Aluminum,
Energy Gap of 6695, 6696
Millimeter Wave Absorption in 6695
Penetration Depth in 6696
Contacts 6812
Films, Properties of Thin 6809
Memory Element, Persistor 6813
Transition, Time Delays in the 6697
Superconductivity,
Gauge Invariant Formulation of the Bardeen-Cooper-Schrieffer Theory of 6691
Law of Corresponding States in 6693
Superconductivity in Aluminum, Lead, Mercury, and Tin 6693
Superconductors, Spin Alignment in 6694
Superconductors with Very Low Transition Temperatures 6692
Surface:
Barrier:
Counters, Large Area Germanium 6908
Counters for Nuclear Particles, Silicon 6911
Transistors, Effects of Surface Recombination on the Current Amplification Factor of 6764
Channels on Silicon P-N Junctions, Anomalous 6741
Concentration of Diffused Layers, Calculation of 6635
Damage in:
Gallium Arsenide 6660
Indium Antimonide 6660
Layers of Lithium Fluoride, Effects of Temperature on Dislocations in 6643
States, Effect of Chemical Etches on Fast Germanium 6670
Structure, Effect of Etching on 6644
Treatment of Silicon Devices 6771
Surfaces, Index of Refraction of Highly Doped Silicon 6723
Surfaces of Bismuth Telluride, Adsorption of Gases on Cleavage 6659
Surge Protector for Silicon Power Rectifiers 6919
Switches,
Four Layer Tunnel 6759
High Voltage, High Speed, P-N-P-N 6758
P-N-P-N Sandwich 6760
Transistor Isolating 6841
Switching:
Behavior of Alloyed Junction Transistors 6765
by Domain Walls in Ferrites, Fast 6796
Characteristics, Positive Temperature Coefficient Thermistors with 6920
Characteristics of P-N-P-N Diodes 6733
Circuits,
Controlled Rectifier 6840
Cryotron 6810
Transistor 6839
Transistor Magnetic Core 6841
Tunnel Diode 6870, 6882
Circulator, Microwave Ferrite 6793
Functions, Synthesis of Minimal Stroke and Dagger 6869
Networks, Statistical Analysis of Transistor-Resistor 6876
Rate in Ferrites, Effect of Previous History on 6795
Transistor Parameters, Measurement of 6818
Synthesis of RC Active Networks 6819, 6820

T

Tape Recorders, Motor Speed Control for Satellite 6898
Telephone:
Message Circuit Noise, Measuring Set for 6865
Transmission by Infrared 6927
Television:
Cameras, Transistor 6863
Deflection Circuits, Transistor 6861, 6864
Receivers,
Design Considerations for Transistor 6859
Limiters for Transistor 6862
Video Processing Circuits for Transistor 6860
Temperature Distribution in Materials with Positive Temperature Coefficients of Electrical Conductivity 6727
Thermal:
Conductivity of Lithium Fluoride, Influence of F-Centers on 6725
Diffusivity of:
Armco Iron 6726
Germanium 6726
Solids, Measurement of 6726
Oxidation, Impurity Redistribution and Junction Formation in Silicon by 6751
Test Set, Transistor and Diode 6925
Thermistors with Switching Characteristics, Positive Temperature Coefficient 6920

Thermocouples, Alloys for Bonding 6668
Thermodynamic Data for III-V Compounds 6626
Thin Film:
  Circuit Techniques 6821
  Memory, Vacuum Evaporated Random Access 6888
Thin Films,
  Analogies between Twistors and 6797
  Preparation and Properties of Ferromagnetic 6655
Thin Layers of Indium Antimonide, Preparation and Properties of 6654
Thorium Doping on Resistivity Variations in Manganese Dioxide, Effect of 6687
III-V Compounds,
  Thermodynamic Properties of 6626
  Vapor Pressures of 6626
Threshold Transducers, Functional Unit 6776
Time Delay Circuits, Transistor 6846, 6847
Tin,
  Superconductivity in 6693
  Time Delays in the Superconducting Transition of 6697
Titanium Dioxide, Paramagnetic Properties of Cr^{3+} in 6806
Transducers, Semiconductor Strain 6814
Transfer Function Synthesis of Active RC Networks 6819
Transformers for Partially Filled Transmission Lines, Stepped 6790
Transient:
  Behavior of Alloyed Junction Transistors 6765
  Operation of Transistors with Inductive Loads 6756
  Response of Variable Capacitance Diodes 6735
Transistor, Shift Register 6775
Transistor:
  AM Radio Receivers, Parasitic Oscillation in 6856
  Amplifier, Transfer Function Synthesis of Active RC Networks Using a 6819
  and Ferrite Core Memory System 6883
  Cardiac Pacemaker 6849
  Chopper Type DC Amplifier 6824
  Circuits, Complementary 6822
  Current Switching and Routing Techniques 6874
  Curve Tracer, High Current Adapter for 6924
  -Diode Logic Circuits 6871
  Distributed Amplifier 6825
  FM:
    and TV Limiter 6862
    Radio Receiver 6855
  for Setting Magnetic Cores, Use of a 6877
  Galvanometer Current Limiter 6844
  Inverter 6895, 6896, 6897
  Isolating Switch 6841
  LC Oscillator Circuits 6837
  -Like Nuclear Particle Detectors 6909
  Magnetic Core Switching Circuits 6841
  Measuring Set for Telephone Message Circuit Noise 6865
  Millivoltmeter with High Input Impedance 6899
  Motor Speed Controls for Satellite Tape Recorders 6898
  Multivibrators, Stability in Time Delay 6838
  Nuclear Coincidence Circuits 6904, 6905
  Oscillator for Nuclear Magnetic Resonance Observations 6900
  Parallel Adder 6874
  Parameters, Measurement of Switching 6818
  Phantastron Delay Circuit 6848
  Physiological Stimulator 6850
  Pulse Steering Circuit for Binary Counters 6881
  Push-Pull Amplifiers, Driving Source for 6826
  Radiation:
    Monitor 6916
    Survey Meter 6906
  Radio Receivers, Improved A-G-C Characteristics in 6857
  Recording-Pen Amplifier 6834
  Regenerative Wave Shaping Circuit 6839
  Reliability, Evaluation of 6730
  -Resistor Logic:
    Circuits 6875, 6876
    Network, Statistical Analysis of 6876
  Scalers 6880
  Scaling Theory 6762
  Shift Register Interstage Coupling Circuitry 6890
  Squelch Circuit 6858
  Switch Stimulus Isolator 6851
  Switching Circuits 6839
  Television:
    Cameras 6863
    Deflection Circuit 6864
    Receivers,
      Design Considerations for 6859
      Video Processing Circuits for 6860
  Thermal Test Set 6925
  Time Delay Circuit 6847
  Timing Circuit 6846
  Twelfth-Order Tchebycheff Parameter Bandpass Filter, Synthesis of 6820
  Underwater Echo-Sounder 6867
  Vertical Scan System for Television Magnetic Deflection 6861
  Voltage Regulators 6894
Transistors,
  Analog: Fabrication by Ion Drift 6753
  Automatic Frequency Control with Reactance 6836
  Design of Controlled Rectifiers Using Triode 6893
  Equipment for Encapsulating 6772
  Junction:
    Diffused:
      Base Mesa 6757
      Silicon Mesa 6917
      Shot-Melting Technique for Making 6749
    Effect of Radiation on 6755
    Effects of Surface Recombination on the Amplification Factor of 6764
    Electrode Connection to 6770
    Equivalent Circuit Parameters of Drift 6761
    Fabrication by:
      Regrowing-Diffusion 6768
      Thermal Oxidation 6751
    Failure Mechanism with Inductive Loads 6756
    Four Layer Tunnel 6759
    High Voltage, High Speed, P-N-P-N Switch 6758
    Increasing the Power Capability of High Frequency 6762
    Microalloy Diffused Base 6767
    Noise Figure at High Current Density in Alloyed Transistors 6766
    P-N-P-N Sandwich 6760
    Production of Stable N- or P-Type Layers on 6771
    Resistance to Neutron Radiation Damage 6767
    Transient Switching Behavior 6765
    Tunnel 6759
    Vapor Grown 6750
    Variation of Current Gain with Operating Point and Frequency 6763
    Very High Frequency:
      Medium Power 6757
      Power 6917
  Low-Melting Glasses for Sealing 6773
  Simultaneous Evaporation of Several Electrodes for 6769
  Surface Barrier: Effects of Surface Recombination on the Current Amplification Factor 6764
  Thermal Test Set for 6925
  Thin Film Circuit Techniques Using 6821
Transition Temperatures, Superconductors with Very Low 6692
Transmission Lines, Stepped Transformers for Partially Filled 6790
Trigger Circuits,
  Controlled Rectifier 6840
  Cryotron 6810
  Magnetoresistive 6842
  Solid State 6774
  Tunnel Diode 6870
Tunnel Currents, Magnetic Field Effects on 6701
Tunnel Diode:
  Adder-Subtracter Circuit 6882
  Amplifier for Ultra High Frequencies 6833
  Curve Tracer 6817
  Logic Circuits 6872, 6873
  Scalers 6879
  Shift Register 6870
  Switching Circuits 6870
Tunnel Diodes,
  Maximum and Minimum Currents in Germanium 6737
  Shot Noise in 6740
  Temperature Dependence of Current in 6738
Tunnel Junction Transistors 6759
Tunneling, Electron-Electron Scattering in N-P 6700
Tunneling in Indium Antimonide, Magnetic Field Effects in 6701
Twistors Represented by Confocal Hollow Prolate Spheroids, Magnetic Fields of 6797

U

Ultrasonic Attenuation in Semimetals, Magnetic Field Dependence of 6728

V

Vacancies in:
  Neutron Irradiated Germanium, Lattice 6627
  Sodium Chloride:
    Optical Detection of 6628
    Radiation-Created 6628
Vacuum Evaporation, Masking Technique for 6769
Vapor:
  Deposition of Silicon, Epitaxial 6650
  Grown:
    Germanium,
      Chemical Purity of 6651
      Dislocations in 6651
      Incorporation of Arsenic into 6641
    Germanium Junctions, Electrical Properties of 6750
    Germanium Single Crystals, Concentration of Iodine in 6640
    Si and Ge Single Crystal Films 6649
    Variable Capacitance Diode 6734
  Growth of Germanium Single Crystals, Closed-Cycle Process for the 6651
  Pressures of III-V Compounds 6626
Varactor:
  Diodes,
    Transient Response of 6735
    Vapor Grown 6734
  Harmonic Generator for Space-Vehicle Applications 6843
Vocoder, Correlator for a 6903
Voltage:
  Reference Diodes, Characteristics and Applications of 6736
  Regulators, Transistor 6894

W

Walker Modes in Large Ferrite Samples 6792

X

X-ray:
  Attenuation Coefficients for Germanium 6684
  Diffraction Study of GaSb-Ge Alloys 6622
  Excited Carriers in Semiconductors, Measurement of Decay Times of 6684

Y

Y-Junction Strip-Line Circulator 6794
Yttrium Iron Garnet, Ferromagnetic Resonance in 6705
Yttrium Iron Garnet Resonators, Single Crystal 6791

Z

Zener:
  Diode Stabilized Power Supply 6736
  Diodes, Characteristics and Applications of 6736
Zinc as a Differential Charge Compensator in GaP-Si Alloys 6621
Zinc Sulfide, Conductivity Pulses in Irradiated 6688
Zinc Telluride - Cadmium Telluride Alloys, Solid Solution in 6624
Zone Casting, Preparation of AlSb-GaSb Alloys by 6623

AUTHOR INDEX

Abboud, F. L. 6861
Abeles, B. 6726
Aharoni, A. 6703, 6842
Aisenberg, S. 6712
Alford, Jr., C. H. 6873
Alfrey, G. F. 6688
Allard, J. G. 6628
Amelinckx, S. 6631
Anderson, J. L. 6896
Anderson, P. W. 6694
Anderson, R. L. 6734, 6750
Ansley, W. G. 6758
Armstrong, D. B. 6800
Atalla, M. M. 6751
Auld, B. A. 6792
Authier, A. 6630

Bacon, R. 6633
Baker, A. N. 6758
Baker, W. E. 6640, 6641
Ballato, A. D. 6815
Barton, L. E. 6826
Batdorf, R. L. 6745
Bate, G. 6654
Beauchamp, K. G. 6834
Bechmann, R. 6815, 6816
Beers, D. S. 6726
Benanti, M. 6778, 6779
Benjamin, R. 6778, 6779
Bennion, D. R. 6799
Bikker, P. 6856
Billings, A. R. 6903
Biondi, M. A. 6695, 6696
Birnbaum, M. 6906
Blair, R. R. 6881
Blankenship, J. L. 6911
Blecher, F. H. 6820
Bleckner, E. 6845
Bohrer, J. J. 6821
Bonfiglioli, G. 6644
Booker, Jr., C. A. 6847
Borkowski, C. J. 6911
Bose, M. 6690
Boyd, D. R. 6667, 6780
Bradley, E. M. 6887
Brand, Jr., F. A. 6778, 6779
Bremer, J. W. 6808
Brenet, J. 6687
Broadbent, K. D. 6888, 6891
Brockus, C. G. 6675
Broom, R. F. 6697
Brown, W. L. 6913
Brownlow, J. M. 6801
Brunner, J. 6698
Bube, R. H. 6721
Buchman, W. W. 6727
Burgess, R. E. 6731
Burke, R. L. 6818
Bylander, E. G. 6786

Calvin, M. 6719
Carley, D. R. 6757
Carreon, D. G. 6863
Carter, D. L. 6713
Carter, I. P. V. 6885
Carter, Jr., P. S. 6791
Catton, W. T. 6850
Cense, A. 6856
Champlin, K. S. 6699
Chandler, J. A. 6736
Chang, H. 6797, 6804
Chang, K. K. N. 6831
Chardack, W. M. 6849
Chesson, F. W. 6846
Chevillot, J. -P. 6687
Cholet, P. H. 6782
Chow, W. F. 6870
Chynoweth, A. G. 6701, 6738, 6745, 6746, 6747
Claytor, R. N. 6724
Clemens, P. L. 6844
Cochran, W. T. 6865
Cody, G. D. 6726
Cohen, M. L. 6811
Compton, D. M. J. 6640 6641
Cooper, J. N. 6813
Coppen, P. J. 6752
Crittenden, Jr., E. C. 6813
Crowley, T. H. 6800
Cuccia, C. L. 6831
Czerlinsky, E. R. 6645

Dabbs, J. W. T. 6908
Dacey, G. C. 6745
Das, M. B. 6761
Daskam, S. W. 6757
Davis, Jr., L. 6794
De Gennes, P. G. 6705
Dietrich, A. F. 6907
Dikhoff, J. A. M. 6648
Dill, H. G. 6817
Dirnbach, P. H. 6866
Dodson, G. A. 6730
Donovan, P. F. 6913
D'Stefan, D. J. 6665
Duffin, M. V. 6866
Duga, J. J. 6632
Dunnet, W. J. 6876
Duwez, P. 6622

Earle, J. 6869
Edmond, J. T. 6669
Edwards, H. H. 6808
Edwards, W. D. 6647
Eichbaum, R. 6803
Ellsworth, R. L. 6839
Etzel, H. W. 6628
Euler, F. 6645

Fagen, E. A. 6689
Fein, H. 6851
Ferro, A. 6644
Feuerstein, W. J. 6748
Feuillade, G. 6636
Fischer, T. L. 6852
Fisher, S. T. 6832
Fitzgerald, P. M. 6843
Flaschen, S. S. 6773
Forst, J. J. 6814
Forstat, H. 6708
Foy, P. W. 6745
Frazer, B. C. 6704
Freedman, G. 6770
Frei, E. H. 6842
Friedland, S. S. 6910
Fujimura, Y. 6836

Gage, A. A. 6849
Gardner, L. B. 6880
Garfunkel, M. P. 6695, 6696
Gatehouse, R. N. B. 6867
Gatos, H. C. 6660
Gazza, G. E. 6663
Geller, S. 6646
Gerritsen, H. J. 6806
Gianola, U. F. 6800
Goering, H. L. 6623
Goetzberger, A. 6754
Goldman, A. 6858
Goldsborough, J. P. 6901
Goodall, W. M. 6907
Goodman, B. B. 6692
Goodman, C. H. L. 6768
Gordon, G. E. 6915
Goto, E. 6872
Goulding, F. S. 6835, 6905
Gray, C. R. 6860, 6862
Greatbatch, W. 6849
Grinich, V. H. 6889
Gutwin, O. A. 6801

Haas, W. 6807
Hale, A. P. 6653
Hall, Jr., J. F. 6723
Hamilton, D. R. 6656
Haneman, D. 6659
Hanlon, J. E. 6639
Hardtke, F. C. 6717
Harman, G. G. 6668
Harper, W. R. 6673
Harrick, N. J. 6634
Harris, P. E. 6838
Harrison, M. J. 6728
Harrison, S. E. 6806
Hass, M. 6671
Hawker, P. D. T. 6875
Hegyi, I. J. 6621
Henry, J. J. 6916
Herndon, M. 6732
Heuer, A. 6798
Hilbiber, D. 6889
Himes, R. C. 6623
Hlavacek, A. R. 6756
Ho, Y. -C. 6876
Hodges, A. J. 6786
Holford, K. 6837
Holmes, P. J. 6664
Holonyak, Jr., N. 6739
Holub, A. J. 6828
Honor, H. I. 6733
Howard, B. T. 6730
Hu, M. -K. 6902
Huber, F. 6807
Hutcheon, I. C. 6824

Iles, P. A. 6752
Ishibashi, Y. 6872
Ishida, H. 6872
Isupov, V. A. 6680

Jackson, R. W. 6912
Jacobs, H. 6778, 6779
James, B. D. 6653
Jarvis, D. B. 6874
Jelley, J. V. 6789
Jensen, H. A. 6759
Johnston, R. C. 6818
Jona, F. 6679
Jones, D. V. 6840
Josephs, J. J. 6892

Kaenel, R. A. 6882
Kamal, A. K. 6828
Kampe, T. W. 6868
Kane, B. 6798
Kane, E. O. 6700
Kattner, L. 6774
Kaufman, W. M. 6776
Kearns, D. R. 6719
Kelley, C. M. 6796
Kikuchi, M. 6742
Kirsch, J. 6652
Kittel, C. 6705
Klein, D. L. 6665
Klement, Jr., W. 6622
Knechtli, R. C. 6827
Knight, R. D. 6772
Koll, A. J. 6845
Kosfeld, R. 6900
Kosyakov, V. I. 6680
Krajewski, I. 6877
Kramer, N. H. 6841
Kuh, E. S. 6819
Kurtz, A. D. 6637
Labes, M. M. 6690
Lamorte, M. F. 6635
Larrabee, R. D. 6777
Larsh, A. E. 6915
Last, J. 6774
Lavine, M. C. 6660
Lawson, T. C. 6862
le Can, C. 6765
Ledford, R. L. 6844
Lee, T. H. 6843
Lesk, I. A. 6739, 6749, 6759
Levey, L. 6793
Lewinski, D. A. 6865
Lewis, H. R. 6806
Lin, H. C. 6756
Lindemann, W. W. 6788
Lloyd, D. J. 6903
Loebner, E. E. 6621
Logan, R. A. 6701, 6738, 6747
Longo, T. A. 6737
Low, W. 6714
Lucovsky, G. 6782, 6784
Luettgenau, G. 6866
Lukes, F. 6716
Lurio, A. 6674

MacDonald, R. W. 6771
Machlup, S. 6718
Mackintosh, I. M. 6913
Macpherson, A. C. 6732
MacPherson, M. R. 6817
Mandel, M. 6901
Marette, S. 6636
Margoninski, Y. 6670
Marinace, J. C. 6651, 6750
Maringer, R. E. 6632
Marshall, B. J. 6724
Masher, D. P. 6871
Mason, W. P. 6814
Massman, A. 6859
Mathers, H. W. 6841
Matsuoka, Y. 6872
Mattingly, L. 6859
Matz, A. W. 6763
Mayer, J. W. 6910
McClure, J. W. 6715
McIntyre, R. J. 6743
McKay, R. W. 6795
McKenzie, J. M. 6914
McNaught, R. A. 6905
McNulty, J. 6658
Meindl, J. 6778, 6779
Meyers, S. T. 6890
Mii, N. 6836
Milano, U. 6794
Miles, T. J. 6767
Miller, C. E. 6646
Miller, G. L. 6913
Miller, J. F. 6623
Miller, R. C. 6677
Miller, R. H. 6904
Milnes, A. G. 6797
Mitchell, E. N. 6886
Mojoni, A. 6644
Molyneux, L. 6850
Moore, A. C. 6655
Morgan, L. P. 6874
Mortenson, K. E. 6830
Moss, R. H. 6657
Moto-Oka, T. 6872
Moy, M. S. 6843
Mueller, R. K. 6788
Murata, K. 6872

Nakagawa, K. 6872
Nakazawa, K. 6872
Nall, J. 6774
Newhall, E. E. 6800
Newhouse, V. L. 6808
Nicholson, H. C. 6657
Nicholson, R. W. 6835
Nixon, J. D. 6718
Northover, W. R. 6773

Oakes, F. 6822
Oguey, H. J. 6702
Okaya, A. 6713
Oliphant, T. A. 6691
O'Rourke, M. J. 6734, 6750

Pagel, B. R. 6781
Pankove, J. I. 6812
Parkes, D. A. 6790
Parris, S. R. 6848
Pawling, J. F. 6854
Paynter, D. A. 6864
Pearson, A. D. 6773
Pell, E. M. 6638, 6753
Penfield, Jr., P. 6823
Pickover, M. B. 6898
Pinckaers, B. H. 6895
Plus, L. 6857
Pohl, R. O. 6725
Pohm, A. V. 6802, 6878, 6886
Porter, J. H. 6853
Portis, A. M. 6705, 6709
Powers, E. J. 6843
Priebe, Jr., H. F. 6883
Prussin, S. A. 6650

Queisser, H. J. 6785

Ray, B. 6624
Raybold, R. L. 6666
Read, A. A. 6802, 6878
Renner, T. 6626
Rhoderick, E. H. 6697
Rindner, W. 6769
Roach, W. E. 6762
Roberts, J. A. 6786
Roberts, L. D. 6908
Rongen, J. 6856
Rose, A. 6783
Rothstein, J. 6755
Rothstein, J. 6755
Russell, G. 6649

Sachse, H. B. 6642
Sandler, N. P. 6650
Santilli, R. A. 6857
Saunders, J. H. 6794
Saunders, N. H. 6682
Savage, A. 6677
Savage, H. 6662
Schaffner, G. 6833
Schauer, R. F. 6802, 6878
Schimpf, L. G. 6855
Schlaeppi, H. P. 6885
Schlömann, E. 6706, 6710
Schmidlin, F. W. 6813
Schneider, B. 6766
Schultz, J. M. 6643
Schulz, D. 6735
Scott, A. B. 6717
Sehr, R. 6690
Seidensticker, R. G. 6656
Selikson, B. 6685
Shafer, W. L. 6883
Sharpe, C. B. 6675
Shevel, Jr., W. L. 6801, 6804
Shirane, G. 6676, 6679, 6704
Shockley, W. 6744, 6754, 6785
Sihvonen, Y. T. 6667, 6780
Sikkeland, T. 6915
Silber, L. M. 6793
Silver, M. 6658
Simmons, C. D. 6860
Simon, R. E. 6722
Slack, G. A. 6707
Slade, A. E. 6810
Sluss, Jr., J. A. 6767
Smallman, C. R. 6809
Smiltens, J. 6625
Smith, K. C. 6795
Solomon, R. 6741
Soma, T. 6872
Spence, R. D. 6708
Spicer, W. E. 6722
Spiegel, P. 6879
Sprague, R. 6633
Srivastava, K. G. 6629
Srygley, O. C. 6845
Staar, D. A. 6848
Statz, H. 6712
Steele, M. C. 6777
Stein, H. J. 6672
Stephenson, W. L. 6897
Stern, E. 6674
Stevenson, A. 6650
Stewart, Jr., R. M. 6802, 6878
Straley, R. 6798
Strandberg, M. W. P. 6805
Strumane, G. 6631
Strutt, M. J. O. 6766
Subbarao, E. C. 6676, 6678, 6679
Sugano, T. 6764
Suhl, H. 6694
Sullivan, D. J. 6790
Summers, D. 6824
Suss, J. T. 6714
Swihart, J. C. 6693

Tachikawa, K. 6742
Takei, W. J. 6704
Tanenbaum, M. 6620
Tannenbaum, E. 6751
Tarpinian, A. 6663
Taylor, G. 6708
Taylor, K. N. R. 6654, 6688
Teaney, D. 6709
Thomas, D. E. 6701
Thompson, C. 6822
Thompson, F. C. 6825
Tiemann, J. J. 6740
Tillman, R. M. 6884
Tkach, G. 6798
Tobocman, W. 6691
Tollin, G. 6719
Tornillo, L. M. 6814
Toy, W. N. 6883
Treuting, R. G. 6646
Trumbore, F. A. 6686
Turner, D. R. 6661 6829

van der Does de Bye, J. A. W. 6684
van der Maesen, F. 6683
van Dijkum, A. N. 6856
van Dykum, A. N. 6856
van Lieshout, L. J. A. 6846
Vierhout, R. R. 6899

Wada, E. 6872
Wallmark, J. T. 6775
Walter, F. J. 6908
Ward, E. E. 6893
Warekois, E. P. 6660
Washburn, J. 6643
Waugh, J. B. S. 6835, 6914
Weaver, J. A. 6874
Webb, P. P. 6912
Webb, W. W. 6631
Weger, M. 6711
Weglein, R. D. 6827
Wertwijn, G. 6760
White, B. H. 6756
White, D. L. 6681
White, W. H. 6750
Widmer, H. 6652
Wiechec, W. 6796
Wiggins, J. S. 6910
Willens, R. H. 6622
Williams, R. L. 6720, 6721, 6909, 6912
Wilson, E. 6894
Witte, R. S. 6658
Wittels, M. C. 6627
Wolf, M. 6787
Woodley, R. E. 6717
Woolley, J. C. 6624

Yanai, H. 6764
Yee, R. 6637
Younger, J. J. 6843

in'for·ma'tion re·triev'al, *n.* **1.** rapid location of technical information on specific topics.

information retrieval system for the solid state:

SOLID STATE ABSTRACTS ON CARDS

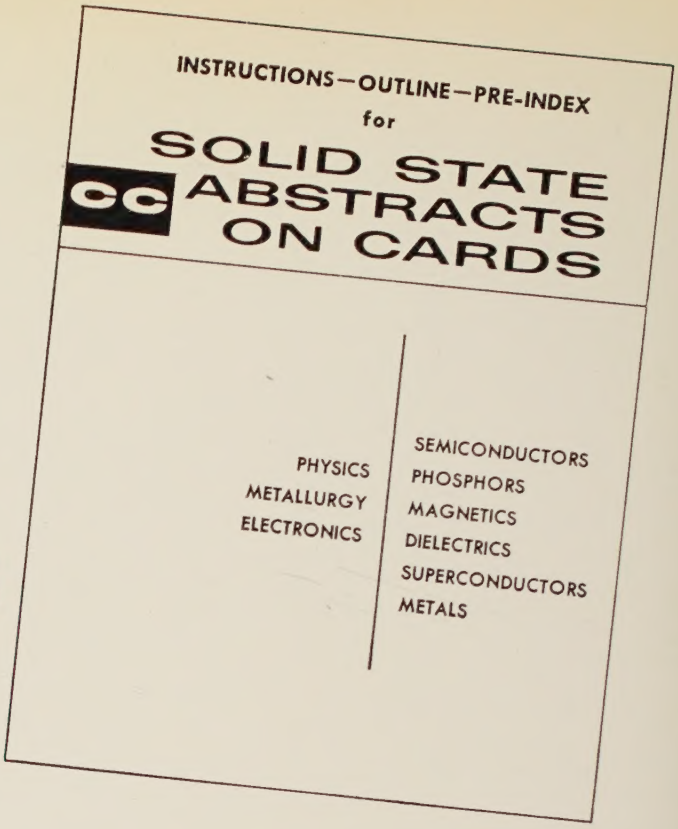

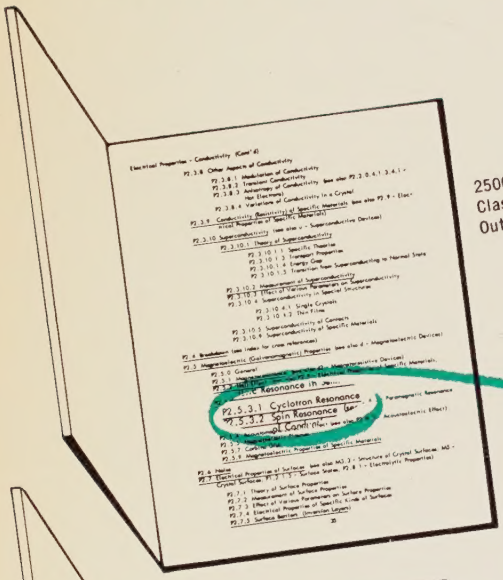

2500-Topic Classification Outline

Send for your free copy of our new 120 page book describing this unique system which is now being used in more than 300 solid state laboratories throughout the world.

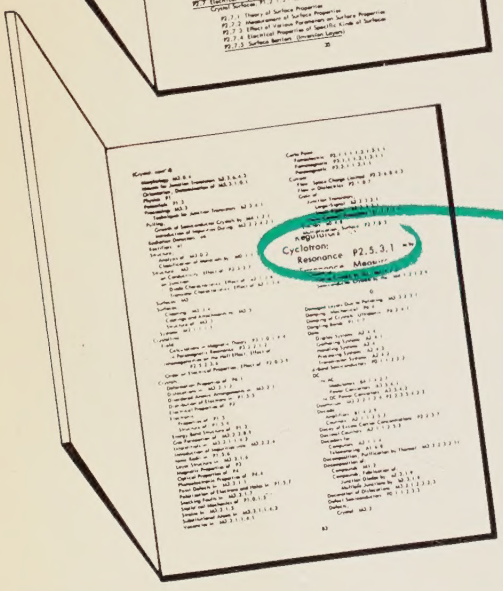

4000-Entry Alphabetical Pre-Index

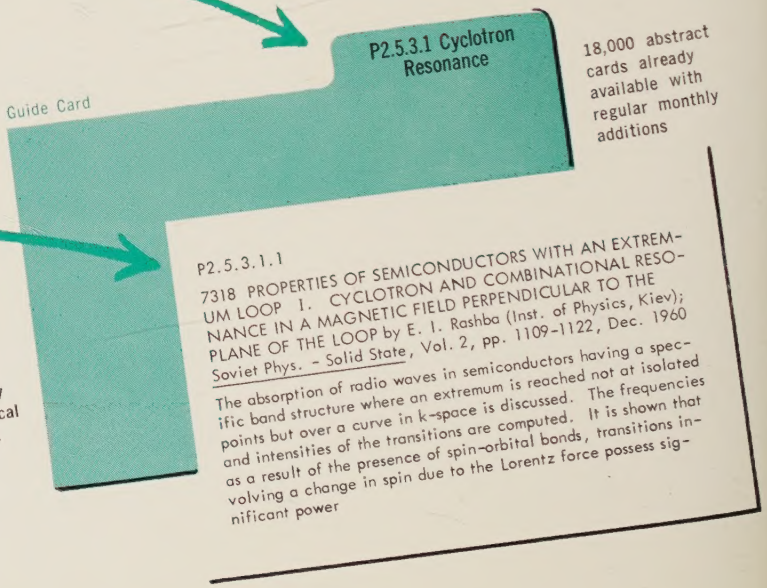
P2.5.3.1 Cyclotron Resonance
Guide Card
P2.5.3.1.1
7318 PROPERTIES OF SEMICONDUCTORS WITH AN EXTREMUM LOOP I. CYCLOTRON AND COMBINATIONAL RESONANCE IN A MAGNETIC FIELD PERPENDICULAR TO THE PLANE OF THE LOOP by E. I. Rashba (Inst. of Physics, Kiev); Soviet Phys. - Solid State, Vol. 2, pp. 1109-1122, Dec. 1960
The absorption of radio waves in semiconductors having a specific band structure where an extremum is reached not at isolated points but over a curve in k-space is discussed. The frequencies and intensities of the transitions are computed. It is shown that as a result of the presence of spin-orbital bonds, transitions involving a change in spin due to the Lorentz force possess significant power

18,000 abstract cards already available with regular monthly additions

CAMBRIDGE COMMUNICATIONS CORPORATION

236 MAIN STREET • CAMBRIDGE 42, MASSACHUSETTS • Tel. 491-0710